Actin cytoskeleton and endomembrane system dependent cell growth

Dissertation

zur

Erlangung des Doktorgrades (Dr. rer. nat.)

der

Mathematisch-Naturwissenschaftlichen Fakultät

der

Rheinischen Friedrich-Wilhelms-Universität Bonn

vorgelegt von

Boris Voigt

aus

Ersdorf

Bonn 2008

Angefertigt mit Genehmigung der Mathematisch-Naturwissenschaftlichen Fakultät der Rheinischen Friedrich-Wilhelms-Universität Bonn

1. Referent: Prof. Dr. Diedrik Menzel
2. Referent: PD Dr. Frantisek Baluska

Tag der Promotion: xx.xx.2008

Diese Dissertation ist auf dem Hochschulschriftenserver der ULB Bonn http://hss.ulb.uni-bonn.de/diss_online elektronisch publiziert.

Erscheinungsjahr: 2008

Table of Contents

List of figures

List of tables

Abbrevations

1. INTRODUCTION 1

1.1. The Actin Cytoskeleton 3

1.2. Endosomes and tip growth 5

1.3. The Syntaxin SYP121 7

1.4. *A. thaliana* Synaptotagmins 8

2. MATERIALS AND METHODS 10

2.1. Molecular Biology 10

2.1.1. Actin cytoskeleton vectors 10

2.1.2. FYVE labelled endosome vectors 11

2.1.3. Synaptotagmin vectors 11

2.2. Plant material, cultivation and transformation 13

2.3. Microscopy 14

2.4. Drug treatments and fluorescent dye staining 14

2.5. Histochemical ß-Glucoronidase (GUS) staining 15

3. RESULTS 16

3.1. Live cell imaging of the actin cytoskeleton in Arabidopsis 16

3.1.1. GFP-FABD2 allows *in vivo* visualization of F-actin in all cell types. 16

3.1.2. Comparison with other in vivo F-actin markers 20

3.1.3. Arabidopsis stably transformed with GFP-FABD2 show normal growth in response to light, darkness and gravity 22

3.2. PI(3)P marked endosomes 25

3.2.1. A tandem FYVE-construct recognizes plant endosomes 25

3.2.2. Motile endosomes are present in all root cells 26

3.2.3. Plant endosomes are present at sites of actin-driven polar growth 27

3.2.4. Motile F-actin patches in root hair tips 30

3.2.5. Actin polymerization propels endosomes 31

3.2.6. Brefeldin A, wortmannin, and jasplakinolide affect GFP-FYVE endosomes 34

3.3. Syntaxin SYP121 36

3.3.1. Intracellular localization of GFP-SYP121 in root cells 36

3.3.2. SYP121 accumulates in endosomal BFA-induced compartments and its tip-localization is F-actin dependent 38

3.3.3. SYP121 co-localizes partially with the endocytic tracer FM4-64 39

3.4. Synaptotagmin expression and localization 40

3.4.1. Expression pattern of synaptotagmins 40

3.4.2. Intracellular localization in *A. thaliana* and *N. tabacum* 45

3.4.3. Characterization of the SytA T-DNA line 50

4. DISCUSSION 55

4.1. The Actin Cytoskeleton 55

4.2. Endosomes and tip growth 58

4.3. The Syntaxin SYP121 62

4.4. *A. thaliana* Synaptotagmins 64

5. SUMMARY 70

REFERENCES 72

List of figures

Figure 1	*In vivo* visualization of F-actin using GFP-FABD2 in different cell types of Arabidopsis	17
Figure 2	In vivo visualization of F-actin using GFP-FABD2 in the transition and elongation zone of Arabidopsis roots	18
Figure 3	In vivo visualization of F-actin using GFP-FABD2 in all stages of root hair development	20
Figure 4	*In vivo* visualization of GFP-Fim1 labelled structures in different cells of Arabidopsis	21
Figure 5	GFP-plastin and GFP-mTn expressed in *M. truncatula* and *A. thaliana*	22
Figure 6	Plot of hypocotyl length of WT, GFP-FABD2 and GFP-mTn	23
Figure 7	Co-localization of DsRed-FYVE labelled endosomes	26
Figure 8	Localization of GFP-FYVE labelled endosomes in *M. truncatula* roots	27
Figure 9	GFP-FYVE in root hairs of *M. truncatula*	28
Figure 10	GFP-FYVE in root hairs of *A. thaliana*	29
Figure 11	GFP-ABD2 in root hairs of A. *thaliana* and *M. truncatula*	31
Figure 12	Time lapse imaging of GFP-FYVE in root hair tips	32
Figure 13	FYVE labelled endosomes with actin-myosin inhibitors	34
Figure 14	BFA, wortmannin and jasplakinolide effect on GFP-FYVE endosomes	35
Figure 15	Localization of GFP-SYP121 in *A. tahliana*	37
Figure 16	Imaging of BFA treated GFP-SYP121 root cells	38
Figure 17	GFP-SYP121 and FM4-64 co-localization	40
Figure 18	Exon/intron structure of the six synaptotagmin members	41
Figure 19	Expression pattern of synaptotagmin A-F	41
Figure 20	promoterSytA:GUS localization	42
Figure 21	promoterSytB:GUS localization	43
Figure 22	promoterSytC:GUS localization	44
Figure 23	promoterSytD:GUS and promoterSytF:GUS localization	45
Figure 24	SytA-GFP expression in stable transformed *A. thaliana*	46
Figure 25	synaptotagmin-GFP constructs expressed in *T. nicotiana* epidermal leave cells	48

Figure 26	SytA-GFP in tobacco leaves	50
Figure 27	WT and mSytA roots under salt stress	51
Figure 28	WT and mSytA roots labelled for live and dead cells after salt shock treatment	52
Figure 29	WT and mSytA seedlings after 3h growing on different concentrations of NaCl stained for live and dead cells.	54

List of tables

Table I	promoter:β-glucuronidase (GUS) fusion constructs	12
Table II	Synaptotagmin-GFP fusion constructs	12
Table III	Growth speed and curvature of WT, GFP-FABD2 and GFP-mTn seedlings	24
Table IV	Speed and rest times of GFP-FYVE	32

Abbrevations

A23187	Calcimycin A23187
aa	amino acid
AtFim1	*Arabidopsis thaliana* fimbrin 1
BDM	2,3-butanedione monoxime
BFA	brefeldin A
bp	base pair
CaMV	Cauliflower Mosaic Virus
CD	cytochalasin D
Col-0	*Arabidopsis thaliana* ecotype Columbia 0
DMSO	Dimethyl sulfoxide
DNA	desoxyribonucleic acid
DsRed	*Discosoma spec*. red fluorescent protein
EDTA	ethylenediamine tetraacetic acid
EGTA	ethylene glycol tetraacetic acid
ER	endoplasmatic reticulum
FABD2	fimbrin actin-binding domain 2
F-actin	filamentous actin
FDA	fluorescein diacetate
Fig	figure
FM4-64	N-(3-triethylammoniumpropyl)-4-(6-(4-(diethylamino)phenyl)hexatrienyl)pyridinium dibromide
GFP	green fluorescent protein
GUS	ß-Glucoronidase
kb	kilobases
lat B	latrunculin B
MS	Murashige and Skoog
mSytA	synaptotagmin A T-DNA mutant
mTn	mouse talin
ORF	open reading frame
PI(3)K	phosphatidylinositol 3-kinase
PI(3)P	phosphatidylinositol 3-phosphate

PM	plasma membrane
PtdIns(4,5)P_2	phosphatidylinositol-4,5-bisphosphate
RNA	ribonucleic acid
SNARE	soluble N-ethyl-maleimide sensitive factor attachment protein receptor
SytA	synaptotagmin A
Wort	wortmannin
WT	wild type

1. INTRODUCTION

Life on earth depends on the ability of plants to trap radiation energy and use it for the formation of chemical bondages in carbohydrates synthesized from carbondioxide and water. Plant growth, therefore, is the essential prerequisite for the production of biomass on earth. In present times, large scale agro-cultivation of crops is the basis for feeding the human world population. Furthermore, field crops are becoming increasingly important in the modern, industrial world as a source of renewable energy, which poses an alternative to the limited energy resources stored in fossile fuels. This fundamental importance of plants makes it desirable to better understand the intricacies of plant growth at the cellular and molecular level. Plant growth results from the three fundamental processes of (i) cell division, (ii) cell expansion, and (iii) cell differentiation. These processes are driven by the metabolic energy converted from light and they are tightly regulated by intracellular signalling networks, resulting in an optimized, highly adaptive growth behaviour to meet the challenges of an ever changing environment. Cell expansion not only causes an increase in the cell´s volume, but is a process which anticipates the subsequent steps of cell differentiation in that it executes the early steps of cellular polarization. The current thesis work addresses some issues in this important aspect of plant growth.

As the cell enlarges, either in a specific cell region or over the whole cell body, the surface area of the plasma membrane increases and at the same time the biopolymer network of the cell wall on the outside of the membrane yields. Subsequently new cell wall material is incorporated into the existing polymer framework to compensate for the thinning of the wall layer. It has been shown that new plasma membrane as well as cell wall components are delivered to and also recycled at the growing areas of the cell via vesicles (Cosgrove, 1999; Dhugga, 2005). Golgi derived secretory vesicles are the primary source of wall precursor materials (Dhugga, 2005). Recently, particular attention has been given to the role of the endosome-based recycling processes which are involved in rapidly shifting wall precursor materials from one area of the cell surface to another (Dhonukshe et al., 2006). The trafficking of secretory vesicles and endosomes is strongly dependent on the actin cytoskeleton with its many associated proteins (Ovecka et al., 2005). A great number of different proteins are responsible for sorting and fusion of vesicles and for the regulation of Ca^{2+} dependent exo- and endocytotic events. Some of these have been identified in plants (Tyrrell et al., 2007), however, the majority of them is yet unknown, awaiting identification

and characterization. Very recent data indicate that membrane recycling is also involved in the adaptation of growth processes to environmental, abiotic stimuli such as gravity and light and biotic challenges, such as microbial infections (Lipka et al., 2007). The current thesis is making a contribution to this area of plant research by addressing the following four issues:

1) Visualization and understanding the role of the actin cytoskeleton in endosomal dynamics. For the visualization of the actin cytoskeleton a new GFP fusion probe as fluorescent reporter of the plant actin cytoskeleton has been developed and it is demonstrated that this reporter has superior properties, which give it a clear advantage over other GFP-actin binding protein fusion probes (Kost et al., 1998).
2) Identification of a particular endosome fraction involved in tip growth, determined by their PI(3)P-containing character. To achieve this, we adapted a GFP-fusion construct containing the so called FYVE-domain, which has previously been developed from the mouse protein Hrs for the visualization of early endosomes in animal systems (Gillooly et al., 2000). With this modified endosome reporter we showed that endosomal motility in plants is actin dependent and tightly linked to tip growth in root hairs.
3) Identification and intracellular localization of SYT121, a member of the syntaxin family, which has a role in targeted vesicle fusion, in connection to plant-microbe interactions (Collins et al., 2003).
4) Molecular characterization and identification of synaptotagmins, a family of proteins known from animal neurons that are involved in vesicle fusion at target membranes (Chapman, 2002). In particular, the properties, intracellular localization and function of synaptotagmin A (SytA) is in the focus.

The study uses the small weed *Arabidopsis thaliana* as the major experimental model system, but other plants like *Medicago truncatula* and *Nicotiana tabacum* have also been used as well. Arabidopsis is an obvious choice as a model system as it has been outlined numerous times in the past. It continues to remain in the focus of plant biologists, because of the many advantages such as the fully sequenced genome, an almost complete expression chart of proteins, availability of mutant lines etc. (Swarbreck et al., 2007). Arabidopsis seeds germinate fast and are easy to handle, e.g. sterilize, sow and grow. Especially the roots and root hairs are very well suited for cell biological research. The roots of living seedlings are thin and can be adapted and maintained in slide chambers. Therefore, circumstances for

microscopic studies of living and undisturbed root and root hair cells are optimal. Root hairs are single, tubular cell extensions growing by tip-growth out of single epidermal cells, the trichoblasts. The mean diameter of a root hair is about 10 µm, the length is up to 1 mm or even more and they grow comparatively fast at a speed of about 1 µm/min. The main function of root hairs is to increase the surface area for efficient uptake of water and nutrients from the soil. Furthermore, they are believed to take part in the anchorage of the whole system to the soil and they serve as contact zones in plant-microbe interactions. Tip-growing root hairs are so well suited for cell-biological studies because they are easy to visualize in the microscope and drugs or other chemical probes are easy to apply. Because of the rapid speed of tip growth, root hairs are ideal objects for the study of polarized cell surface expansion. Additionally, root hairs are not essential for the survival of plants in petri-dish cultures, so experimental work with all types of root hair mutants even those showing severe phenotypes in their shape and development, is still possible.

1.1. THE ACTIN CYTOSKELETON

In vivo visualization of the actin cytoskeleton is critical due to the continuous and often rapid, dynamic reorganization of the actin filament network. Over a long time, concerns have been discussed as to whether chemical fixation sufficiently preserves the more dynamic actin filament populations in plant cells. At the time when the GFP-reporter technology was developed, expectations have been raised that the new technology may help to overcome this problem and, in fact, data obtained with the first fluorescent actin-reporter construct called GFP-mTn, which was made by fusing the actin binding portion of the mouse focal contact protein, talin, (Kost et al., 1998, 2000) have been encouraging. As a consequence the new construct is widely used in cytoskeleton research and since the fusion protein appeared to bind to plant F-actin as well many studies have been published using this probe especially on plant epidermal cells and their derivatives such as trichomes of wild-type and diverse mutants of *A. thaliana* (El-Din El-Assal et al., 2004; Jedd and Chua, 2002; Li et al., 2003; Mathur et al., 1999, 2002, 2003a,b).

However, as it has turned out, there is some constraint in the use of this construct for *in vivo* analysis of root hairs, root apex cells as well as of stelar cells localized deeper in plant organs. Ketelaar et al. (2004) showed that the expression of GFP-mTn in root hairs of *A. thaliana* caused severe defects in actin organization. These defects lead to either termination of growth, cell death and/or changes in cell shape. The GFP fusion protein binds extremely

strong to the actin filaments and appears to protect them against interactions with actin modulating proteins, like the plant actin depolymerizing factor, ADF (Ketelaar et al., 2004).

Stelar and root apex cells are of particular interest, because they are essential for polar auxin transport, which is mediated by the putative auxin efflux carriers of the PIN family (Friml et al., 2002a,b; Geldner et al., 2001; Grebe et al., 2002; Willemsen et al., 2003). Several authors have shown, that the correct placement and function of auxin efflux carriers depend on the intact actin cytoskeleton (Muday, 2000; Muday et al., 2000; Sun et al., 2004). The elucidation of other roles of F-actin in pericycle and stelar cells, including initiation of lateral roots are critically dependent on the exact *in vivo* visualization of dynamic arrays of F-actin. However, this has been difficult due to the fact that these cells are localized more deeply in the root body.

For these reasons, the development of an improved reporter for *in vivo* visualization of F-actin in plants was desirable and it was seen as essential for our understanding of how the actin cytoskeleton dynamically interacts with components of the polar auxin transport within the root stele and how the polarity of tip-growing cell types is established.

Using the Steedman's wax based immunolocalization technique, it was reported previously for maize root apices that young, developing stelar cells are extremely rich in F-actin and accomplish dramatic reorganization of their actin filament system in the transition zone, which is interpolated between the meristem and the zone of rapid cell elongation (Baluska et al., 1997b, 2000a). This reorganization of the actin cytoskeleton in cells of the transition zone encompasses dramatic accumulation of perinuclear F-actin elements, which then organize into prominent bundles extending towards the non-growing but F-actin rich end-poles, also termed polar cross walls (Baluska et al., 1997b, 2000a). Experimental depolymerization of F-actin with both cytochalasin D and latrunculin B prevented these cells from accomplishing cell elongation (Baluska et al., 2001a,b). Another yet controversial topic is the status of the actin cytoskeleton in root cap statocytes, which are regarded as the essential sensory cells of the primary root, accomplishing gravisensing within seconds after a change in the gravitational vector. Although F-actin is generally implicated in gravisensing, most attempts to visualize F-actin elements in these cells have failed so far. The only report of distinct F-actin in root cap statocytes was based on the application of phalloidin before/during fixation of samples (Collings et al., 2001), which might be the result of aberrant induction of actin polymerization.

Answering these questions requires the availability of transgenic seedlings stably transformed with a sensitive, plant F-actin specific GFP reporter constructs allowing *in vivo*

visualization of the actin cytoskeleton in all cells of the root apex. As the GFP-mTn construct did not allow visualization of F-actin in most cells of the meristem, transition zone and root cap statocytes, experiments have been initiated to design and test other GFP constructs, which might be better suited for *in vivo* visualization of plant F-actin. One of these constructs is GFP-FABD2, an N-terminal fusion of GFP to the C-terminal half of AtFim1 (aa 325-687), which includes the second actin-binding domain and the C-terminal end of *A. thaliana* fimbrin 1 (a generous gift from David McCurdy, University of Newcastle, Australia). The usfulness of this construct was recently demonstrated in a preliminary fashion in Arabidopsis roots (Ketelaar et al., 2004a) and it worked also quite well in tobacco protoplasts after subcloning into a different binary vector (Sheahan et al., 2004).

In this thesis, a full account is given of the properties of this construct in Arabidopsis roots and its versatility and usefulness is compared with other GFP-based actin reporter constructs. It will be shown, that in contrast to GFP-fusions with the complete sequence of AtFim1 (GFP-AtFim1, this thesis), the C-terminal fusion to the first actin-binding domain of human plastin (Timmers et al., 2002), and the N-terminal fusion to the actin-binding domain of mouse talin (GFP-mTn), the new construct (GFP-FABD2) reports a very detailed image of the filamentous actin cytoskeleton in virtually all cell types of the *A. thaliana* seedling. Also in contrast to the recent report by Wang et al. (2004), who have examined the usefulness of several other GFP-fusion variants to *A. thaliana* fimbrin1 as fluorescent reporters of the plant actin cytoskeleton, our construct gives a more detailed representation of the actin cytoskeleton in the root transition zone, in the apical meristem and in the root cap. Therfore, the GFP-FABD2 construct appears to be the best suited reporter for filamentous plant actin so far. The availability of a construct with these properties provides the unique opportunity to analyze the dynamic changes in the architecture of the root actin cytoskeleton *in vivo* in the course of organ development.

1.2. ENDOSOMES AND TIP GROWTH

In eukaryotic cells, endosomes are defined as pleiotropic tubulo-vesicular membrane compartments, which accumulate, modify and reroute internalized cargo (Gruenberg, 2001; Zerial and McBride, 2001). Classically, endosomes are involved in the maintenance of plasma membrane homeostasis, nutrient uptake, cellular defence responses, and the termination of signalling pathways through internalization and down-regulation of activated receptor-ligand complexes (Samaj et al., 2005). More recent evidence reveals that endosomes are involved in signalling, transcytosis and synaptic cell-to-cell communication (Sorkin and von Zastrow,

2002). Thus, endocytic compartments are highly dynamic and this activity is clearly linked with many important functions within eukaryotic cells (Gruenberg, 2001; Sorkin and von Zastrow, 2002; Zerial and McBride, 2001).

In both yeast and mammals, endosomes recruit FYVE-domain proteins due to high levels of phosphatidylinositol-3-phosphate (PI(3)P) in their membranes (Gillooly et al., 2000). This is mediated via specific recruitment of PI(3)-Kinases to these membranes by regulatory GTPases, such as Ypt51p and Rab5 (reviewed by Gruenberg, 2001; Zerial and McBride, 2001). While both FYVE-domain proteins and endosomal-localized Rab GTPases are conserved in plants, it is not known, whether these two sets of proteins are localized to the same compartment as demonstrated in other systems (Lawe et al., 2000). More recently, the importance of cytoskeletal elements in endosomal sorting and trafficking events has been highlighted. For instance, both sorting and trafficking of proteins has been shown to be dependent upon the ability of endosomes to associate with and move along cytoskeletal elements (reviewed by Gruenberg, 2001; Zerial and McBride, 2001). The current view, established largely from animal models, suggests that long-range intracellular movements of endocytic compartments are accomplished along microtubules, whereas the actin cytoskeleton is responsible for short-distance movements (Goode et al., 2000).

Important roles for endocytosis during polarized root hair expansion, which is restricted to the tips (apical domes) of these cells, have been postulated based on electron microscopic observations that plasma membrane associated clathrin-coated vesicles are preferentially enriched at the tips of root hairs (reviewed by Hepler et al., 2001). The apical domain preferentially recruits actin, together with actin-binding proteins such as ADF and profilin in order to initiate cell expansion (Baluska et al., 2000b; Baluska and Volkmann, 2002; Gilliland et al., 2002; Jiang et al., 1997; Miller et al., 1999; Nishimura et al., 2003; Ringli et al., 2002; Samaj et al., 2002, 2004; Vantard and Blanchoin, 2002). Intriguingly, recent advancements suggest that tip-growth of root hairs is driven by actin polymerization (Baluska et al., 2000b; Baluska and Volkmann, 2002; Jiang et al., 1997; Miller et al., 1999; Nishimura et al., 2003; Vantard and Blanchoin, 2002).

To address the role of endosomes in actin-driven plant cell tip growth, F-actin- and endosome-specific stably-transformed transgenic GFP-reporter lines of *A. thaliana* and *Medicago truncatula* have been established in our lab and are used for the *in vivo* visualization of both actin and endosomes. The endosomal marker (GFP-FYVE) contains two tandemly repeated FYVE domains from the mouse endosomal Hrs protein (Gillooly et al., 2000). In this thesis it is shown that plant endosomes are labelled by the GFP-FYVE fusion construct, in a

similar way to two other endosome specific reporters, constructed from the plant Rab GTPases Ara6 (Ueda et al., 2001) and RabF2a (Haas et al., 2007). Their localization and motile behaviour is analyzed in detail and suggest a surprising new link between actin-driven polar tip growth of root hairs and the actin polymerization-propelled motility of endosomes in plants.

1.3. THE SYNTAXIN SYP121

Syntaxins are members of the SNARE (soluble N-ethyl-maleimide sensitive factor attachment protein receptor) family, which mediate secretory vesicle targeting and membrane fusion. In the *A. thaliana* genome a total of 54 SNARE genes have been identified so far, which all possess a highly conserved coiled-coil domain (SNARE motif) and a transmembrane domain at their C-terminus (Uemura et al., 2004). They are classified in five groups representing the degree of their similarities to the synaptic SNAREs, as Qa-SNAREs (Syntaxins), Qb-SNAREs (SNAP Ns), Qc-SNAREs (SNAP Cs), R-SNAREs (VAMPs) and SNAP (SNAP Ns and Cs) (Bock et al., 2001). Membrane fusions of vesicles are aided by the so called SNARE complex, which contains at least one copy of the Qa-, Qb-, Qc-, and R-SNARE motifs. Distinct SNARE complexes are believed to be specific for determining the intracellular destination of vesicles (Jahn et al., 2003; Jahn and Scheller, 2006).

Eighteen out of the 54 SNAREs belong to the Qa group, which is thought to regulate the transport between the plasma membrane and endosomes (Uemura et al., 2004). To this group belongs the protein syntaxin, SYP121 (PEN1), which was found in a screening of Arabidopsis mutants for non-host penetration resistance against a powdery mildew fungus. The conidiospores of the barley powdery mildew *Blumeria graminis* f. sp. *hordei* germinate on Arabidopsis, but just 10% of the sporelings are successful in penetrating the epidermal cells. Normally, the cell forms a cell wall deposition (papilla) directly beneath the penetration site to stop further ingrowth of the fungal hypha, however, in the case of successful penetration a hypersensitive-response is elicited, leading to cell death. In a screen for decreased penetration resistance, the syntaxin SYP121 (PEN1) was identified as an important factor that is needed to stop hyphal penetration (Collins et al., 2003). The SYP121 (PEN1) has a homologue in *Nicotiana tabacum*, SYR1, which is thought to determine the abscisic acid sensitivity of K^+ and Cl^- channels in guard cells. It is localized to the plasma membrane and expressed throughout the plant, including the roots, suggesting that it contributes to cellular

homeostasis as well as to signalling (Geelen et al., 2002). Collins and coworkers (Collins et al. 2003) showed that it localizes to the plasma membrane and accumulates at papillae upon pathogen infection. Furthermore, it is present on endomembrane compartments with a diameter of about 1µm (Collins et al., 2003; Assad et al., 2004). However, nothing is known on the expression and localization of the protein in cells of Arabidopsis roots. In the current work, the localization of GFP-SYP121 in different cells of the root, especially the root hairs, is examined and its possible role in polarized exo/endocytosis is discussed.

1.4. *A. THALIANA* SYNAPTOTAGMINS

Synaptotagmins are encoded by a large gene family in mammals. In the human genome sixteen isoforms exist with different expression patterns and functions. All of them are believed to be Ca^{2+} dependent regulators of exocytosis and/or endocytosis (Chapman, 2002; Poskanzer et al., 2003; Tang et al., 2006). Some examples for the function of human synaptotagmins are the Ca^{2+} dependent regulation of neurotransmitter release at the synapse (syt1, Koh and Bellen, 2003), peptide hormone secretion (i.e. dense-core vesicle exocytosis, Iezzi et al., 2004), plasma membrane repair (Andrews, 2005) and the compensatory synaptic vesicle endocytosis (Poskanzer et al., 2003). The synaptotagmin proteins have a conserved common structure. They possess an N-terminal transmembrane sequence, which is followed by a linker of variable length and two distinct C2 domains, C2A and C2B (Südhof, 2002). Numerous experiments have shown that these two C2 domains are Ca^{2+}- and phosphatidylinositol-4,5-bisphosphate [PtdIns(4,5)P_2]- binding domains (Arac et al., 2006). Whereas the C2A domain is able to bind three Ca^{2+} ions, the C2B domain is capable of binding two Ca^{2+} ions (Südhof, 2002). The human syt1 is the best studied synaptotagmin so far. It is located at the nerve synapses and is required as a Ca^{2+} sensor for the fast fusion of synaptic vesicles. Neurotransmitter-carrying synaptic vesicles are exocytosed in a SNARE-dependent manner after presynaptic depolarization. Synaptotagmin interacts with the SNARE complex by binding to syntaxin and SNAP-25. The depolarization of the presynaptic membrane causes Ca^{2+} influx, which is sensed by syt1. Upon Ca^{2+} binding, syt1 draws the SNARE complex closer to the target membrane and causes fusion (Arac et al., 2006; Meldolesi and Chieregatti, 2004). In the absence of Ca^{2+} the C2A and C2B domains are binding only weakly to negatively charged phospholipids like phosphatidylinositol-4,5-

bisphosphate [PtdIns(4,5)P_2] in the target membrane. Upon the interaction with Ca^{2+}, the C2 domains bind with higher affinity to PtdIns(4,5)P_2 and insert into the target membrane (Hui et al., 2006; Martens et al., 2007), which should induce a positive membrane curvature. As a consequence, vesicle and target membrane get drawn closer to one another and are able to fuse (Arac et al., 2006; Martens et al., 2007).

Sequence analysis of various animal and plant genomes revealed the presence of synaptotagmin-like genes in all animals and land plants. On the other hand, there is no evidence of synaptotagmin genes in unicellular organisms or those with simple forms of multicellularity (Craxton, 2004). The Arabidopsis genome contains six members, SytA to SytF, which belong to this protein family. They are characterized by the same domain pattern as their animal counterparts. However, it is completely unknown, whether the function of these proteins is similar or overlapping with that of the better characterized synaptotagmin isoforms in mammals.

To address the question of what these proteins are doing in plants, we first wanted to get an overview of the expression and intracellular localization of the members of this protein family. Therefore, the promoter regions of all six genes were cloned and promoter:β-glucoronidase (GUS) fusion vectors were prepared to visualize the expression of these genes in *A. thaliana*. Furthermore, the cDNA´s of all six genes have been cloned and GFP fusions were generated to get information about the cellular localization of the proteins. In collaboration with the laboratory of Prof. Botella, University of Malaga, Spain, we have obtained biochemistry data indicating similar Ca^{2+} and phospholipid binding capacities for the plant synaptotagmin-like proteins. As a first experimental strategie to address the function of the protein, a SytA T-DNA mutant line was studied, which is hypersensitve to salt stress in certain conditions.

2. MATERIALS AND METHODS

2.1. MOLECULAR BIOLOGY

All molecular work and preparation of media was done according to the protocols of Sambrook et al. (2001) and enzymes were used accordingly to the manufacturers advices. All chemicals and reagents used for the experiments were purchased from Boehringer-Mannheim (Mannheim, Germany), MBI Fermentas (New York, USA), Merck (Darmstadt, Germany), Pharmacia (Uppsala, S), Roth (Karlsruhe, Germany), Serva (Heidelberg, Germany) or Sigma (Munich, Germany) unless otherwise stated.
The bacterial strains used in this study are *Escherichia coli* DH10 for standard clonings, *Agrobacterium tumefaciens* GV3101 for stable transformation of *Arabidopsis thaliana* and transient transformation of *Nicotiana tabacum* and *Agrobacterium rhizogenes* ARqua1 for transformation of *Medicago truncatula* roots.

2.1.1. ACTIN CYTOSKELETON VECTORS

The coding region of AtFim1 (At4g26700) was amplified from pGEX-Fim1 (Kovar et al., 2000; McCurdy and Kim, 1998) by PCR with the proof reading polymerase PFU (Promega, USA). Restriction enzyme sites had been added to the primers to ligate the open reading frame to the SpeI site of pCAT-GFP (Reichel et al., 1996), resulting in pGFP-Fim1. In order to generate a construct containing just the second actin-binding domain, pGFP-Fim1 was digested with BamHI and SpeI, the fragment recovered from an agarose gel and ligated in frame into a modified pCAT-GFP, resulting in pGFP-FABD2 (see also Ketelaar et al., 2004a). The stop codon of the GFP reading frame was removed by site-directed mutagenesis (Chameleon Mutagenesis Kit, Stratagene). The expression plasmid contained the 35S promoter of Cauliflower Mosaic Virus (CaMV) with a duplicated transcriptional enhancer, the Tobacco Etch Virus leader sequence functioning as a translational enhancer and the polyadenylation signal of the CaMV 35S RNA. For the generation of stably transformed *A. thaliana* plants the expression cassettes were excized by SdaI and cloned into the PstI site of the binary vector pCB302 (Xiang et al., 1999). The binary vector constructs, pCB-GFP-Fim1 and pCB-GFP-FABD2, were introduced into *A. tumefaciens* strain GV3101 (pMP90) by electroporation (Cangelosi et al., 1991).

2.1.2. FYVE LABELLED ENDOSOME VECTORS

The sequences of two FYVE domains from the mouse Hrs protein were connected with the linker sequence QGQGS and fused to the N-terminus of enhanced green fluorescent protein (plasmid pEGFP-C3 from Clontech, USA) as described before (Gillooly et al., 2000). This gene construct was cut out using NheI and SalI and cloned into the XbaI and SalI restriction sites of the binary vector pBLT221, thereby putting its expression under the control of the CaMV 35S promotor. The resulting binary vector was introduced into *A. tumefaciens* GV3101 and *A. rhizogenes* ARqua1.

For DsRedT4 (Bevis and Glick, 2002) tagging, the tandem FYVE domain was PCR-amplified and cloned in frame with DsRedT4 within the vector pRTL2 under the control of the CaMV 35S promotor.

The coding sequence for ARA6-GFP under control of the CaMV 35S promoter and nopaline synthase terminator (Ueda et al., 2001) was excised with HindIII and EcoRI and was inserted into the corresponding sites of pBI121 (Clontech). The resulting vector was introduced into *A. tumefaciens* strain C58C1 (lab of T. Ueda).

AtRabF2a cDNA was PCR amplified introducing BamHI and XbaI restriction sites, to insert the open reading frame into a modified pCAMBIA expression vector with eYFP at the N-terminus under the control of the CaMV 35S promoter (lab of E. Nielsen).

2.1.3. SYNAPTOTAGMIN VECTORS

For constructing the promoter:β-glucuronidase (GUS) fusion constructs, genomic DNA from *A. thaliana* ecotype Columbia-0 was extracted with a genomic DNA preparation Kit (Qiagen), according to the manufacturers instructions. For each promoter region of the six synaptotagmin members was a fragment of about 2 kb upstream of the translation start codon PCR amplified and cloned into the binary pΔGusBin19 (Topping et al., 1991) vector (see Table I). The final vectors carried kanamycin resistance for bacteria and plants and were transformed into *A. tumefaciens* strain GV3101 by electroporation. Selection was carried out on kanamycin containing half strength MS plates. The T2 generation was used for the histochemical localization of GUS activity. Plant samples were vacuum infiltrated for 30 min with substrate solution (100 mM sodium phosphate buffer, pH 7.0, 10 mM EDTA, 0.1%

Triton X-100, 0.5 mM potassium ferricyanide, 0.5 mM potassium ferrocyanide, and 1 mM 5-bromo-4-chloro-3-indolyl glucuronide) and incubated at 37°C for up to 12 h. For observation the samples were mounted in mounting medium (Chloral hydrate 240 g, H_2O 90 g, glycerol 30 g) and examined with a Leica MZ FL III.

Table I. promoter:β-glucuronidase (GUS) fusion constructs

gene of interest	bp upstream of ATG	Resulting vector
SytA	1506	pΔGus-proSytA
SytB	2009	pΔGus-proSytB
SytC	2100	pΔGus-proSytC
SytD	2007	pΔGus-proSytD
SytE	2019	pΔGus-proSytE
SytF	2016	pΔGus-proSytF

For cellular localization of the synaptotagmins GFP fusion constructs were designed as open reading frame (ORF)-GFP fusions as shown in Table II. Each ORF was PCR amplified out of cDNA from *A. thaliana* ecotype Columbia-0 adding suiting restriction sites and firstly cloned into the t-tailed pGem-Easy vector. Out of there it was subcloned into the 35S-GFP-Nos carrying expression vector pCAT-GFP (Reichel et al., 1996). For agrobacterium mediated transformation the complete expression cassettes, 35S-Syt-GFP-Nos, have been excised and cloned into the binary vector pCB302 (Xiang et al., 1998), which were transformed into *A. tumefaciens* strain GV3101 by electroporation. In addition to this several constructs of truncated SytA-GFP were designed (see Table II).

Table II. synaptotagmin-GFP fusion constructs

gene	locus (AGI)	bp	aa	construct name
SytA	At2g20990	1623	541	pSytA-GFP
SytB	At1g20080	1605	535	pSytB-GFP
SytC	At5g04220	1620	540	pSytC-GFP
SytD	At5g11100	1722	574	pSytD-GFP
SytE	At1g05500	1680	560	pSytE-GFP
SytF	At3g18370	2445	815	pSytF-GFP
C2AB of SytA		112-1623	38-541	pGFP-C2AB

2.2. PLANT MATERIAL, CULTIVATION AND TRANSFORMATION

In this study the ecotype Columbia (Col-0) of *A. thaliana* was used for all stable transformations. The plants were grown at 22°C at a 16-h day/8-h night cycle on one-half strength Murashige and Skoog medium including vitamins, 1% (w/v) sucrose and 0.4% (w/v) Phytagel. Liquid culture medium had the same composition without Phytagel. Where medium with low levels of calcium was needed, the concentration of MS was reduced to one-tenth. Strong and healthy grown Arabidopsis plants on soil were used for *A. tumefaciens* mediated transformation with the different binary vectors, using the floral-dip method by Clough and Bent, 1998. Transformed plants (T1) were selected by screening on plate for green fluorescent seedlings with a Leica MZ FL III fluorescence binocular equipped with a gfp3 emission filter (Leica) or on soil by spraying with the according selection medium. In case of selection for kanamycin on plates, the Phytagel was replaced by 1.5% of bactoagar and supplemented by 50µg/ml kanamycin. The fluorescent/surviving seedlings were transferred to soil and propagated by selfing. For microscopic studies T3, T4 and T5 plants were used, the seedlings were grown on vertical oriented Petri dishes. Four-day-old seedlings were mounted in liquid medium using a spacer of one layer of parafilm between slide and coverslip and were vertically adapted overnight, prior to microscopy.

M. truncatula cv. Jemalong were grown on a modified Fahraeus medium containing 1% agar (Boisson-Dernier et al., 2001) on square 12-cm plastic dishes (Greiner, Austria). Transformation of the roots were carried out accordingly to the protocol of Boisson-Dernier et al. (2001) using *A. rhizogenes* strain ARqua1 harboring the different binary vectors. About 3-6 weeks later the screening by fluorescence (see above) was carried out and plants with transformed roots were put individually into square 12-cm plastic dishes for microscopic studies.

N. tabacum was grown on soil for 4 weeks at 25°C and leaves were transiently transformed via *A. tumefaciens* leave infiltration method according to Batoko et al. 2000. The bacterial optical denisty (OD_{600}) used for infiltration was 0,05.

2.3. MICROSCOPY

The confocal microscopy was carried out on either a Leica TCS 4D or a Leica SP5, both equipped with argon and/or krypton laser. For excitation of GFP and FDA the 488 nm line of the argon laser was used and as emission filters were either a 515 nm long pass, a 530 nm band pass or the setting of the Acousto Optical Beam Splitter (AOBS) to 500 to 560 nm used. *A. thaliana* samples mounted in slide chambers were examined using a 40x oil immersion lens. Where it was needed the seedlings mounted in slide chambers where stored vertically in glass cuvettes for 24 hours prior to observation. *M. truncatula* roots growing on agar were covered with bioFolie 25 (Sartorius AG, Vivascience Support Center, Göttingen, Germany) and examined with a 63x water-immersion objective. From transiently transformed leaves of *N. tabacum* pieces of about 1 cm^2 were cut out and mounted between slide and coverslip in tap water. DsRed fluorescence was imaged using excitation at 543 nm and a long pass 620 nm emission filter. The red fluorescent dye FM4-64 was excited by the 488 nm laser line and emission was filtered between 620 and 710 nm. Serial confocal optical sections were taken at different step sizes. Projections of serial confocal sections and contrast enhancement were done using image processing software (Scion Image; Scion Corporation; Photoshop, Adobe Systems Inc., Mountain View, CA, USA; Leica Application Suite Advanced Fluorescence, Leica Microsystems, Mannheim, Germany). For growth and curvature measurements seedlings were observed directly on the Petri dishes with a 10x lens mounted on an inverted Leica DMIRB microscope equipped with CCD-camera, or the Petri dishes were placed on a standard PC scanner. Analysis and measurements were made with Image-Pro Plus 4.1 (Media Cybernetics, L.P.).

2.4. DRUG TREATMENTS AND FLUORESCENT DYE STAINING

Following drugs where used with the different plant systems: 2,3-butanedione monoxime (10 mM), latrunculin B (1 μM for *A. thaliana* and 10 μM for *M. truncatula*), jasplakinolide (1 μM/5μM), brefeldin A (35 μM for *A. thaliana* and 100 μM for *M. truncatula*), wortmannin (10 μM), and oryzalin (1 μM). The drugs were diluted in culture medium and directly added to the roots of transgenic *M. truncatula* or *A. thalinana*. Regarding FM4-64, stock solution (1 mg/ml) was prepared in DMSO and used at 17.5 μM for *M. truncatula* and at indicated

concentrations for *A. thaliana*. Before FM4-64 treatment, plants were incubated for 25 minutes at 6°C to slow down endocytosis. Drug treatment, FM4-64 staining or plasmolysis in transformed *T. nicotiana* leaves was either performed with excised leave pieces or the liquids were injected into the leave prior to excision. FM4-64 was used at 5 µM, NaCl for fast plasmolysis at 500 mM, A23187 at 10 µM in addition to either 10 mM $CaCl_2$ or 10 mM EGTA. All substances where diluted in tap water. The staining of Arabidopsis seedlings for living and dead cells was done with FM4-64 (5 µM) and Fluorescein diacetate (FDA, 5 µg/ml).

2.5. HISTOCHEMICAL ß-GLUCORONIDASE (GUS) STAINING

Seedlings of the T2 generation of stable transformed promoter-GUS *A. thaliana* plants or single organs of these were stained for ß-Glucoronidase activity according to the protocol described by Sieburth et al. (1997). Plant samples were vacuum infiltrated for 10 min with substrate solution (100 mM sodium phosphate buffer, pH 7.0, 10 mM EDTA, 0.1% Triton X-100, 0.5 mM potassium ferricyanide, 0.5 mM potassium ferrocyanide, and 1 mM 5-bromo-4-chloro-3-indolyl glucuronide) and incubated at 37°C for up to 12 h. Plant tissues were mounted in mounting medium, containing chloral hydrate, glycerol and water. The stained seedlings or organs were examined using a Leica MZ FL III binocular equipped with a CCD camera.

3. RESULTS

3.1. LIVE CELL IMAGING OF THE ACTIN CYTOSKELETON IN ARABIDOPSIS

3.1.1. GFP-FABD2 ALLOWS *IN VIVO* VISUALIZATION OF F-ACTIN IN ALL CELL TYPES.

Two different variants of GFP-fusion proteins based on *A. thaliana* fimbrin were tested. The whole molecule fused to GFP and just the C-terminal actin-binding domain fused to the C-terminus of GFP. The resulting GFP-FABD2 (Ketelaar et al., 2004a) fusion protein allowed generation of transformed seedlings which had all cells labelled with the fluorescent F-actin reporter. Extensive arrays of longitudinal actin bundles and dynamic network of actin filaments could be documented in elongated epidermal cells of the hypocotyl (Fig 1 A). In trichomes of primary leaves, a prominent F-actin cage was present around the nucleus and longitudinal filament bundles reached into the trichome tips (Fig 1 B, inset). Stomata cells showed thick filament bundles arranged in dense partially radial arrays throughout the cortex and a more prominent meshwork around the nucleus (Fig 1 C), similar to what has been shown previously (Kost et al., 2000).

In lateral root cap cells expressing GFP-FABD2 a system of long and thick F-actin bundles filled the cell cortex (Fig 1 D). Dense F-actin networks, reported in an earlier study (Collings et al., 2001), were absent from statocytes. Maybe due to the characteristics of the 35S promotor, the level of expression in the lateral cap was always higher than in statocyte cells. In single optical sections through the root cap, at the middle plane of the columella, just a diffuse, patchy pattern of GFP-FABD2 was visible (Fig 1 E, stars). In this section the lateral root cap cells (Fig 1 E, diamonds) showed a lower overall signal due to the fact that the thick filaments at the cell cortex were cut perpendicularly. Again, in contrast to the findings of Collings et al. (2001) who examined other plant species, no distinct F-actin bundles could be observed in the statocytes of transgenic *A. thaliana* plants. In the meristematic zone of the root, interphase cells exhibit very fine and highly dynamic meshworks without any thicker bundles of F-actin (Fig 1 F). Mitotic cells had a F-actin-depleted zone (Fig 1 G, star) at around the equator, whereas F-actin accumulated at the plasma membrane which is facing the spindle poles (Fig 1 G). During cytokinesis this overall actin polarity is still maintained. Fig 1 H shows a cytokinetic cell with strongly labelled cross-walls and F-actin depleted at the lateral plasma membrane areas. The phragmoplast F-actin could be observed at different stages (Fig 1 H, I, arrows) of cytokinesis.

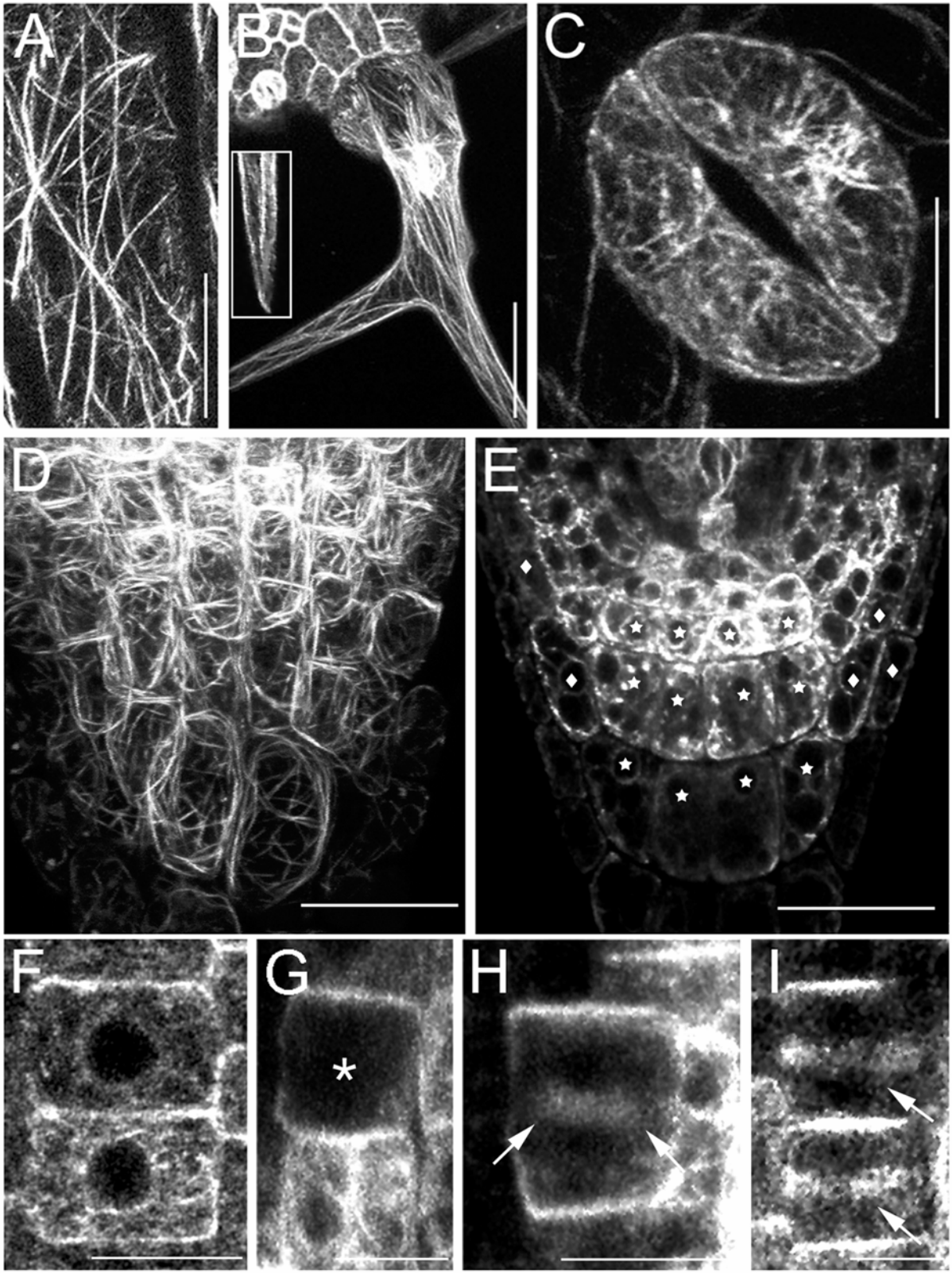

Fig 1. *In vivo* visualization of F-actin using GFP-FABD2 in different cell types of Arabidopsis.

A: epidermal cell of the hypocotyl. B: trichome. C: guard cells. D: lateral root cap cells. E: single optical section through the root cap including statocytes (asterisks), peripheral root cap cells (diamonds). F: interphase cells of the meristem . G: mitotic cell (asterisk). H and I: phragmoplast F-actin at different stages of cytokinesis (arrows). Scale Bars A, D, E = 20 µm; B = 50 µm; C, F-I = 10 µm.

Moving towards the root base, the transition zone exhibited a very special actin pattern. Fig 2 A gives an overview of developmental stages in the cortex cell layer from apical meristem to elongation zone, with the transition zone interpolated in-between them. While dividing cortex cells of the meristem showed fine meshworks throughout their cytoplasm, F-actin of the cortex cells at the transition zone became bundled, enclosing the nucleus and attaching to the F-actin rich cross walls. These F-actin bundles appeared first when the cortex cells cease divisions and enter the transition zone (Fig 2 B). Later on, when elongation of the cortex cells starts, the F-actin bundles around the nucleus as well as the labelling at the cross walls got more prominent (Fig 2 C, E). Finally, in fully elongated cortex root cells, mostly longitudinal filament bundles as well as a fine and highly dynamic network of F-actin occured at the cortex cells (Fig 2 G).

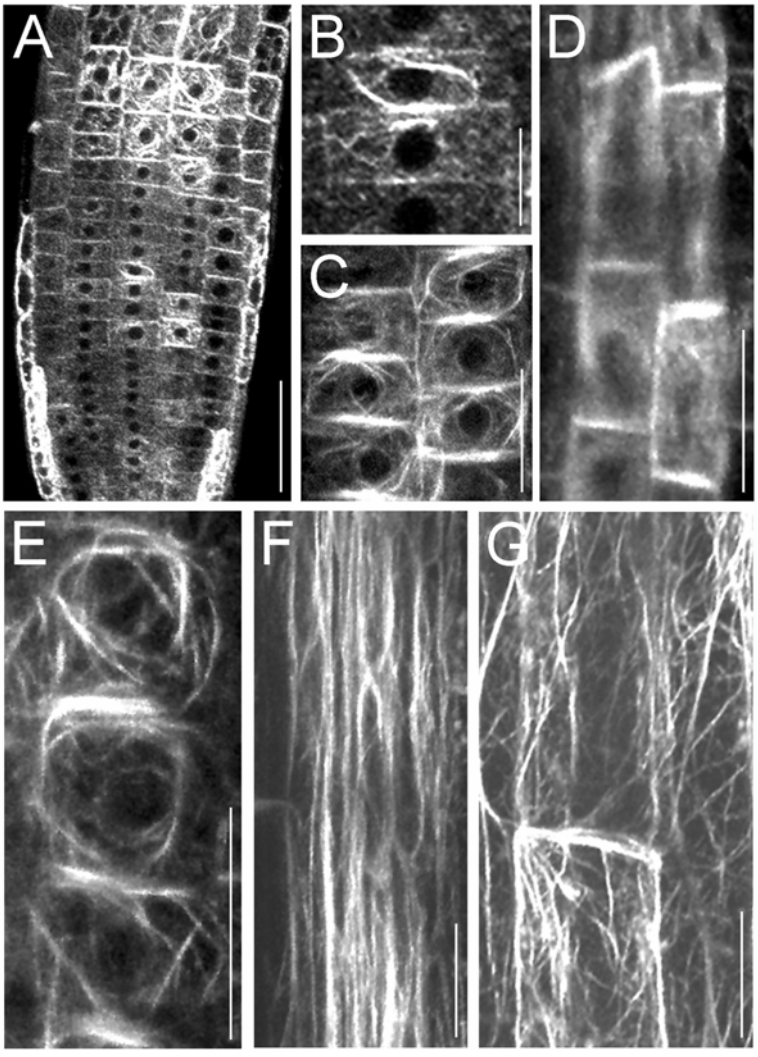

Fig 2. In vivo visualization of F-actin using GFP-FABD2 in the transition and elongation zone of Arabidopsis roots.
A: overview from meristem to early elongation zone within root cortex layer.
B: higher magnification of cells entering the transition zone.
C and E: cortex cells leaving the transition zone and starting with elongation.
D: endodermis cells within the transition zone.
F: elongated endodermis cells. G: elongated cortex cells.
Scale Bars A = 50 µm; B-G = 20 µm.

Nearly the same pattern was observed in cells of the endodermis (Fig 2 D, F). Non-elongated endodermis cells had a strong signal at the cross walls with some actin stretches around the nucleus (Fig 2 D, poorly resolved due to depth of focal plane). Whereas fully

elongated endodermis cells showed no strong signal at cross walls. Instead, longitudinally filament bundles run throughout the entire length of the cell (Fig 2 F).

The actin cytoskeleton is very important for polar growth, which occurs in tip-growing root hairs. At every stage of the root hair development the actin cytoskeleton could be observed properly (Fig 3). In early root hair bulges, an extensive meshwork of F-actin patches and bundles was present at the cell cortex (Fig 3 A). At a somewhat later stage, when the root hair began to grow by tip growth, filament bundles still extend in the direction of the tip and then disperse into a very fine and dynamic meshwork at the very apex (Fig 3 B). The same pattern of organization was seen at the tip of fast growing root hairs (Fig 3 C). Due to their motile activity, small bundles or possibly single actin filaments right at the tip, were just about visible in movies. Fig 3 D is an image taken from a low resolution, but fast scanned time lapse series. Small filaments moving around the tip of the root hair are slightly visible. Actin patches (Fig 3 D, arrows) were always associated with the tip region of growing hairs. Full grown root hairs showed big filament bundles throughout the whole cell merging right into the tip and back (Fig 3 E). To test, whether the fusion construct somehow had a stabilizing effect on F-actin, the F-actin depolymerizing drug latrunculin B (LatB) has been applied. Fig 3 F-H show root tricho- and atrichoblast cells before (F) and after 4 minutes of 400 nM LatB treatment (G). Fig 3 H shows the same cells after 25 min 400 nM LatB treatment and following 50 min of washing out. It is obvious, that the prominent as well as the fine F-actin depolymerized to shorter F-actin filaments or even to G-actin. It seems that the depolymerized actin becomes a bit accumulated in the very tip of the outgrowing root hair bulge (Fig 3 G, arrow). After LatB was washed out, thicker and more densely packed F-actin filaments were rebuilt and appeared at the outgrowing root hair tip (Fig 3 H).

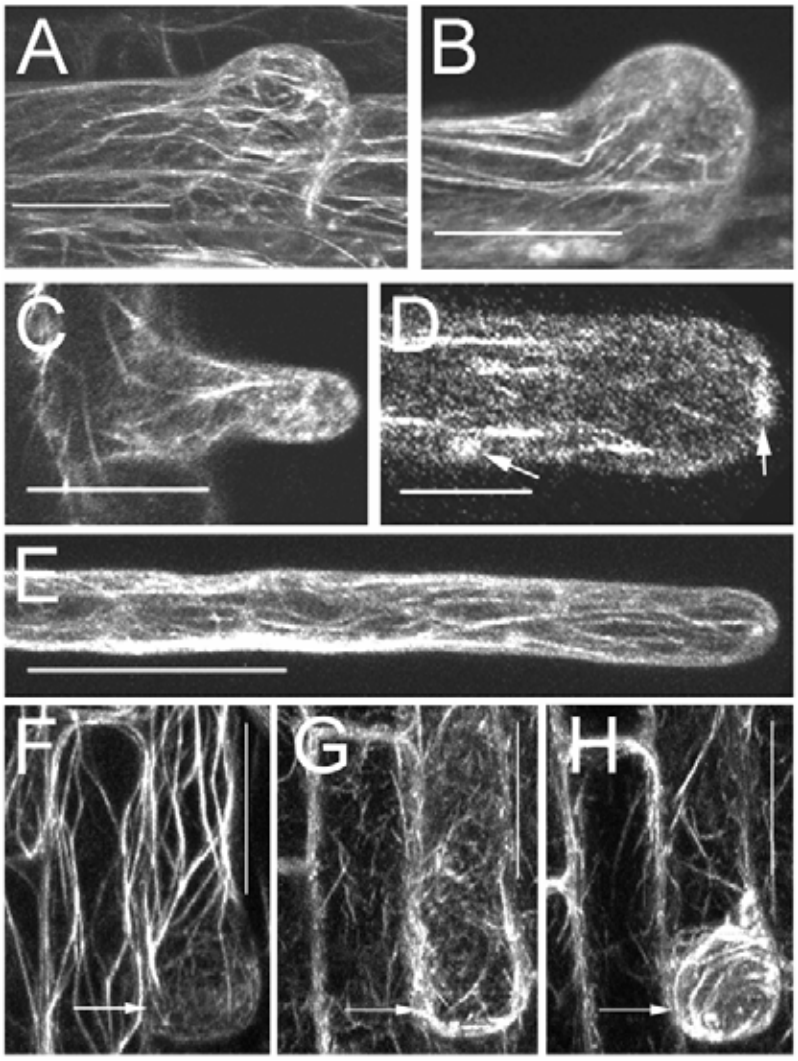

Fig 3. *In vivo* visualization of F-actin using GFP-FABD2 in all stages of root hair development.
A, early bulge.
B, late bulge, beginning tip-growth.
C, young growing root hair.
D, tip of fast growing root hair, with thin filament bundles and actin patches (arrows).
E: growth-terminated root hair.
F: root epidermis cells with outgrowing bulge (arrow).
G: same cells as in F, after LatB treatment.
H: same cells as in G, after washing out of LatB.
Scale Bars A-D, F-H = 20 µm; E = 25 µm.

3.1.2. COMPARISON WITH OTHER IN VIVO F-ACTIN MARKERS

Examination of transgenic *A. thaliana* seedlings transformed with GFP-Fim1 (GFP-fused to the N-terminus of the entire fimbrin 1 molecule) showed unusual patterns of F-actin distributions in epidermal cells of the hypocotyl (Fig 4 A). The cortical actin cytoskeleton appeared as a dense, interwoven meshwork without any preferential orientation. In epidermal cells (Fig 4 B) of the root, however, there were almost no filamentous structures visible exept for a diffuse signal in cytoplasmatic strands. The same was true for epidermis and cortex cells in the transition zone (Fig 4 C).

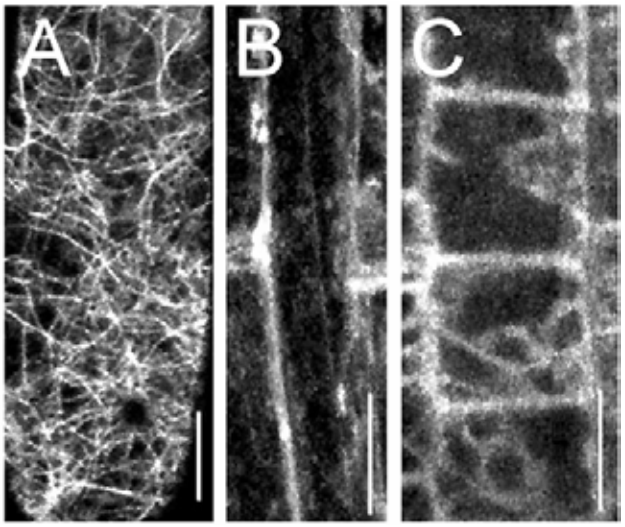

Fig 4. *In vivo* visualization of GFP-Fim1 labelled structures in different cells of Arabidopsis showed no distinct filamentous actin.
A, hypocotyl cell.
B, root epidermal cell.
C, cortex cells within the transition zone of the root apex.
Scale Bars A = 10 µm; B, C = 20 µm.

Transgenic *M. truncatula* roots transformed with plastin-GFP (GFP-fused to the C-terminus of a truncated human T-plastin, Timmers et al., 2002) showed yet another pattern of the actin cytoskeleton. In root epidermis cells, thick, filamentous interwoven structures formed a coarse actin network and the nuclei were always prominently labelled (Fig 5 A). A closer look at root hairs revealed that only occasionally F-actin bundles were visible, whereas most of the cytoplasm was filled with a diffuse signal (Fig 5 B) which could correspond to the endoplasmic reticulum rather than to the actin cytoskeleton.

Seedlings which express GFP-mTn (GFP-fused to the N-terminus of mouse talin, Kost et al., 1998, 2000) showed a similar kind of F-actin arrangements as that seen with GFP-FABD2 in most cell types. However, in lateral root cap cells the very prominent filamentous actin network seen with GFP-FABD2 (Fig 1 D) was not visible, instead, just a diffuse cytoplasmic signal occurred (Fig 5 C). Nearly the same situation was found in the root cap statocytes (Fig 5 C compare to Fig 1 E). On the other hand, in root epidermis cells the F-actin was very much like that seen after labelling with GFP-FABD2, i.e., exhibiting big longitudinal filaments and a randomly arranged fine F-actin network (Fig 5 D). In addition, a strong background of GFP signal in the cytoplasm was always present as well as a labelling of the nuclei (Fig 5 E). The same pattern could be observed in growing root hairs, where nearly the complete root hair showed a diffuse signal with some prominent F-actin bundles included (Fig 5 F). The actin states in the other parts of GFP-mTn seedlings such as cortex, endodermis, and stele cells of the transition zone could not be compared due to the fact that there was no signal detectable. The same is true for the entire meristem.

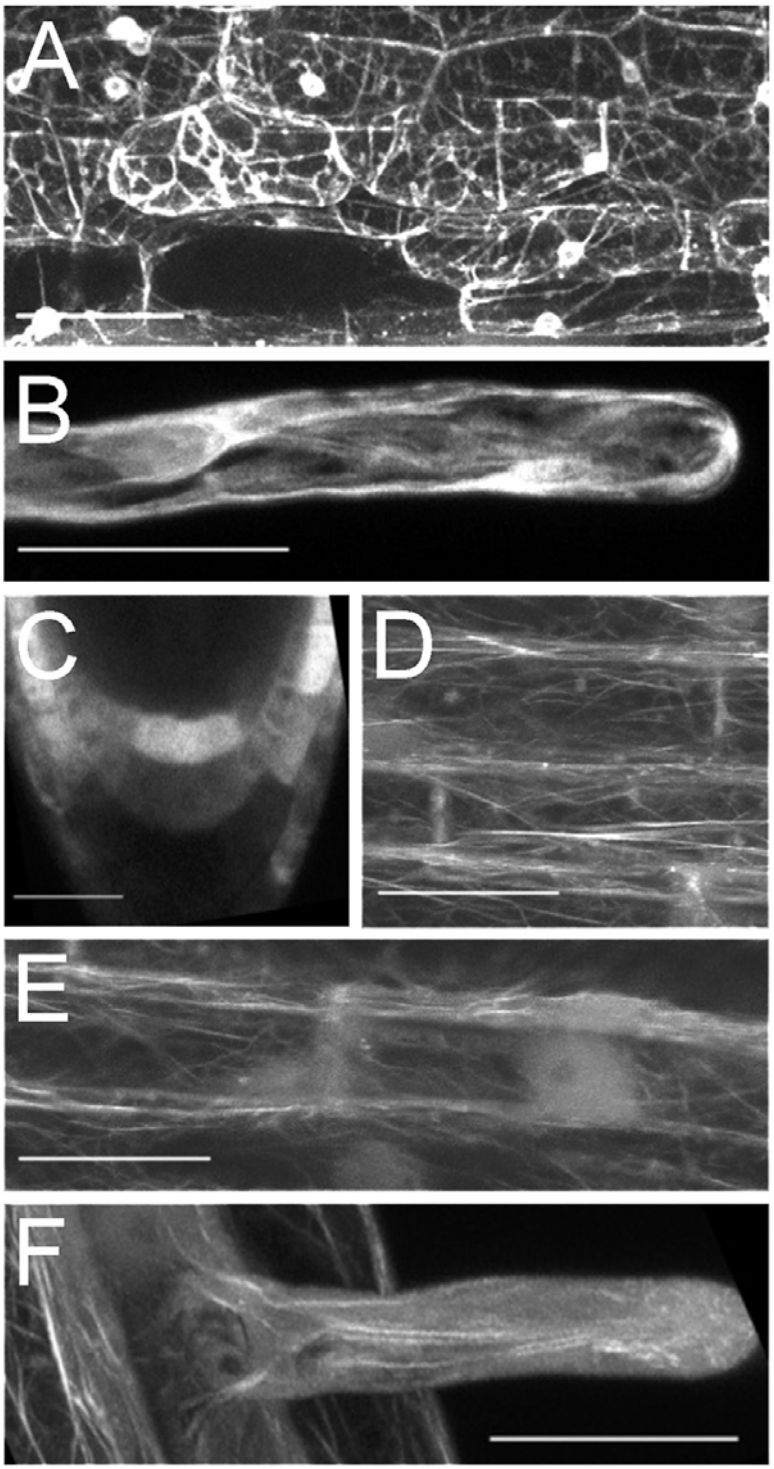

Fig 5. GFP-plastin and GFP-mTn expressed in *M. truncatula* and *A. thaliana* (in comparison to GFP-FABD2 in Fig 2 and 3).
A: GFP-plastin labelled thick filament bundles and the nuclei of Medicago root epidermal cells.
B: a diffuse signal of GFP-plastin is detectable in Medicago root hair.
C: GFP-mTn transgenic Arabidopsis with weak and diffuse signal in lateral root cap cells and statocytes.
D and E: GFP-mTn labelled in root epidermal cells filament bundles, fine F-actin networks and nuclei.
F: GFP-mTn root hairs showed few actin bundles and a huge diffuse background.
Scale bars A–F = 25 µm.

3.1.3. ARABIDOPSIS STABLY TRANSFORMED WITH GFP-FABD2 SHOW NORMAL GROWTH IN RESPONSE TO LIGHT, DARKNESS AND GRAVITY

In order to rule out that the GFP-FABD2 construct interfers with endogenous fimbrin-based processes, the growth rates of root hairs were determined, as well as the responses of roots to gravistimulation and hypocotyls to darkness (Table III A-C; Fig 6). All these parameters

showed values corresponding well to those found in wild-type *A. thaliana* seedlings. These data clearly indicate that the GFP-FABD2 lines are well suited for physiological experiments, including photo- and gravitropic responses which both depend on the polar transport of auxin. In all other situations tested, no significant deviation of growth values from those found in wild-type plants could be scored. Moreover, we did not detect any phenotypic changes in the GFP-FABD2 seedlings. In comparison to WT and GFP-FABD2 seedlings, the GFP-mTn seedlings showed a slightly decreased hypocotyl growth and significantly slower gravitropic response (Table III A-C, Fig 6).

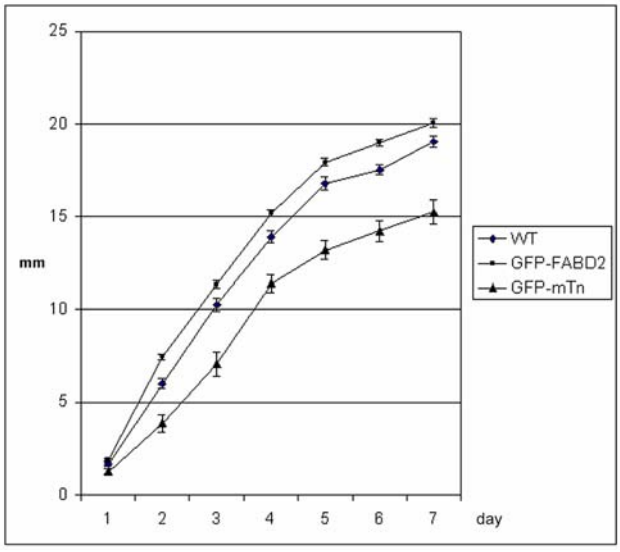

Fig 6. Plot showing hypocotyl length of etiolated wild-type, GFP-FABD2 and GFP-mTn seedlings measured each day until day seven after germination on vertical Petri dishes. Whereas wild-type and GFP-FABD2 seedlings grew with almost the same speed, the GFP-mTn seedlings showed a gradual reduction of growth speed resulting in a shortend hypocotyl length after 7 days (see also Table III B).

Table III. A: the growth speed of root hairs was measured for 30 min only on fast growing hairs longer than 20 μm of seedlings grown on top of vertical Petri dishes. The growth rates were calculated to μm/min and then averaged. Both transgenic lines show a slightly increased growth speed compared to wild-type root hairs.

B: the hypocotyl length of etiolated seedlings was measured each day until 7 days after germination. The difference of the growth speed of GFP-mTn (3.1 mm/24h) compared to wild-type (3.6 mm/24h) results in a diminished hypocotyl length of GFP-mTn seedlings after 7 days of growth.

C, seedlings were germinated in the dark and grown vertically for 2 days before the plates were re-oriented by 90 degrees. The angle of the root curvature was measured 18 hours after re-orientation. GFP-mTn seedlings show a significant (ANOVA, p=0.000) delay in the graviresponse in comparison to wild-type seedlings.

A	growth speed (μm/min)	average growth speed (μm/min)	STDEV	SE
WT (n=34)	0.7 - 1.76	1.39	0.29	0.05
GFP-FABD2 (n=29)	1.11 - 2.04	1.62	0.23	0.04
GFP-mTn (n=33)	0.96 - 2.08	1.59	0.28	0.05

B	Hypocotyl length one day after germination in mm (SE)	Hypocotyl length seven days after germination in mm (SE)	Average growth rates between 2 and 5 days after germination in mm/24h
WT (n=33)	1.65 (0.10)	19.03 (0.28)	3.6
GFP-FABD2 (n=45)	1.88 (0.07)	20.05 (0.24)	3.5
GFP-mTn (n=7)	1.26 (0.14)	15.25 (0.66)	3.1

C	Average root curvature 18h after re-orientation, degrees (SE)	p-value of ANOVA against WT
WT (n=22)	76.35 (2.64)	
GFP-FABD2 (n=28)	79.50 (1.62)	0.316
GFP-mTn (n=23)	59.87 (2.72)	0.000

3.2. PI(3)P MARKED ENDOSOMES

3.2.1. A TANDEM FYVE-CONSTRUCT RECOGNIZES PLANT ENDOSOMES

In both yeast and mammals, the phosphoinositide PI(3)P accumulates preferentially in endosomal membranes (Gillooly et al., 2000) and binding of FYVE-domain proteins to PI(3)P is sufficient to target endosomal proteins to these subcellular compartments. For plants it is known, that a classical *A. thaliana* FYVE domain binds specifically to PI(3)P in vitro (Jensen et al., 2001). Therefore, we were interested to know if the tandem FYVE domain would be sufficient for targeting to endocytic compartments in plants. To this end, the FYVE domain from the mouse Hrs protein was tandemly fused (Gillooly et al., 2000) to the C-terminus of GFP or DsRedT4, respectively. Particle bombardment was employed to transiently express the fusion proteins (GFP-FYVE; DsRed-FYVE) in onion epidermal bulb scale cells. Confocal imaging revealed fluorescently-labelled motile organelles, which were positive also for the endosome-specific plant Rab GTPases Ara6 and RabF2a, when pDsRed-FYVE and Ara6-GFP or YFP-RabF2a were transiently co-expressed. In the case of Ara6 and FYVE, the merged images showed a co-localization between the two fusion proteins in small and punctate, motile organelles (Fig 7 C, yellow arrowheads), but not in larger static organelles, which were binding the GFP-FYVE reporter exclusively (Fig 7 C, red arrowheads). Coexpression of pDsRed-FYVE and pYFP-RabF2a also showed complete co-localization within small motile organelles (Fig 7 D-F).

Previously, Ara6 and RabF2a labelled compartments have been shown to accumulate newly endocytosed FM4-64 (Ueda et al., 2001). To determine, whether FYVE-labelled compartments have endosomal identity, a double labelling of stably transformed *M. truncatula* roots expressing GFP-FYVE with the red fluorescent styryl dye FM4-64 have been performed. This endocytic tracer binds to the plasma membrane and becomes rapidly incorporated into the cell through bulk-flow endocytosis (Ueda et al., 2001). Upon the exposure of root hairs to FM4-64 for five minutes, a fluorescent signal was observed on all FYVE-labelled endosomes (Fig 7 G-I). The GFP-FYVE labelled endosomes were located in the vesicle-rich tip region of root hairs and co-localized with FM4-64 labelled endosomes (Fig 7 I). Taken together, the fluorescently-labelled FYVE reporter co-localizes with the plant endocytic Rab GTPases Ara6 and RabF2a on endosomes which accumulate internalized FM4-64.

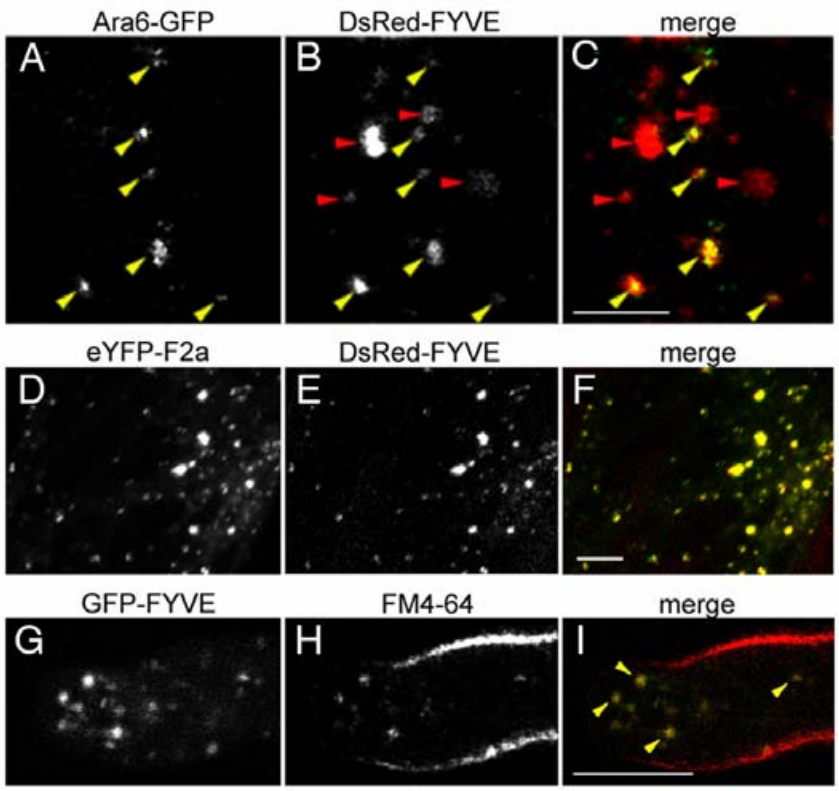

Fig 7. A-C: transient co-expression of endosomal markers Ara6-GFP with DsRed-FYVE in onion epidermal bulb scale cells. Simultaneous two-channel confocal imaging revealed that these two fusion proteins co-localize in several smaller compartments, while few larger FYVE-labelled compartments are not positive for Ara6.

D-F: transient co-expression of eYFP-RabF2a and DsRed-FYVE in epidermal bulb scale cells showed a complete co-localization of both markers.

G-I: FM4-64 applied to transgenic *M. truncatula* roots expressing GFP-FYVE construct. After 5 min of exposure to FM4-64, FYVE-labelled endosomes in root hairs were enriched also with FM4-64.

Yellow arrowheads indicate co-localization between Ara6 and FYVE (A-C), as well as between FM4-64 and FYVE (G-I).

Scale bars A-I = 10 µm.

3.2.2. MOTILE ENDOSOMES ARE PRESENT IN ALL ROOT CELLS

After identification of the GFP-FYVE labelled plant endosomes in *M. truncatula* root hair cells, the pattern of their distribution in other root cells was analyzed. In stably transformed *M. truncatula* roots, GFP-FYVE was detected on highly motile endosomes in all root cells. GFP-FYVE labelled endosomes were especially abundant in root cap and meristem cells (Fig 8 A, B). In the small meristem cells, the GFP-FYVE labelled endosomes appeared evenly distributed

throughout the cytoplasm and excluded from the nuclei (Fig 8 B, stars). GFP-FYVE was localized to endosomes that moved without any preference for a specific subcellular location. In *A. thaliana* roots, a similar distribution of FYVE-tagged endosomes was found. In peripheral root cap cells (Fig 8 C, D), GFP-FYVE endosomes were somewhat bigger than in the central statocytes (Fig 8 C, star).

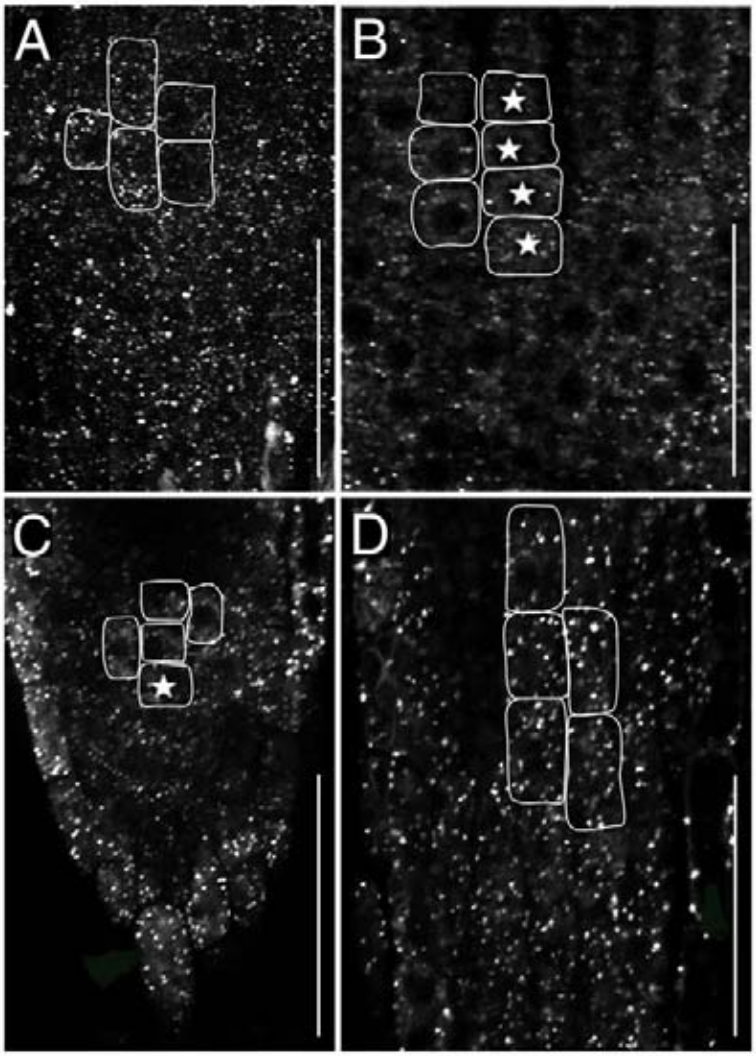

Fig 8. Localization of GFP-FYVE labelled endosomes in *M. truncatula* and *A. thaliana* roots.
A: abundant FYVE-labelled endosomes in all cortical cells of stable transformed roots of *M. truncatula*.
B: in deeper meristem cells GFP-FYVE localized endosomes around centrally positioned nuclei.
C: in stable transformed roots of *A. thaliana*, FYVE-labelled endosomes were abundant in all cells, but with a smaller diameter in the central statocytes.
D: FYVE-labelled endosomes evenly distributed in peripheral root cap cells.
Some cells are outlined using white lines, position of some nuclei is indicated with stars.
Scale bars A-C = 50 µm; D = 25 µm.

3.2.3. PLANT ENDOSOMES ARE PRESENT AT SITES OF ACTIN-DRIVEN POLAR GROWTH

Both atrichoblasts (non-hair cells) and trichoblasts (hair cells) of *M. truncatula* exhibited a uniform distribution of GFP-FYVE labelled endosomes throughout the length of the cell (Fig 9 A), but in the trichoblasts FYVE-endosomes became enriched at the outgrowing bulges (Fig 9 A, B). At a later stage, when hairs had already emerged and were actively growing, GFP-FYVE endosomes were extraordinarily motile and present at the vesicle-rich and organelle-depleted tip

zone of the root hairs (Fig 9 C). When root hair growth ceased, this distribution was rapidly lost and GFP-FYVE accumulated on larger structures, which were distributed throughout the length of the root hair (Fig 9 D). Occasionally, fully grown root hairs showed only a few large endosomal aggregates without any preferential localization (Fig 9 E).

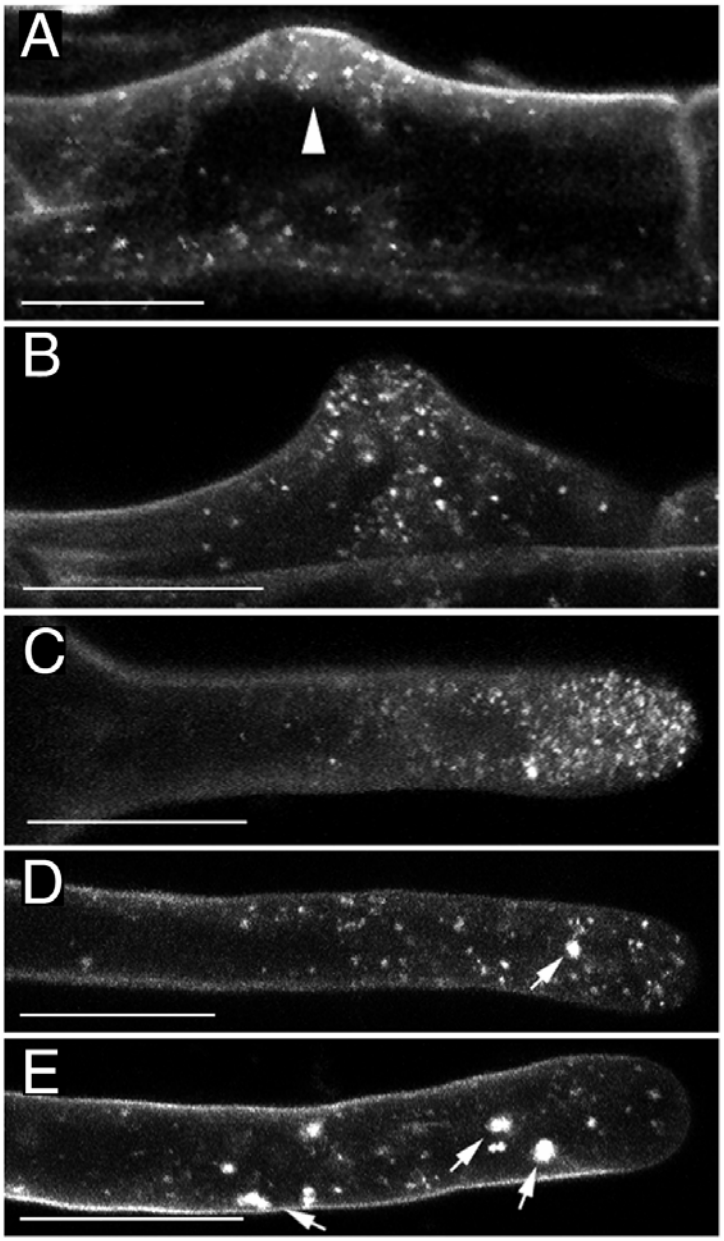

Fig 9. GFP-FYVE in root hairs of *M. truncatula.*

A: FYVE-labelled endosomes present at the bulging site of the trichoblast.

B: further polarization of GFP-FYVE towards the out-growing bulge.

C: FYVE-labelled endosomes, highly motile at the tip of tip-growing root hairs.

D: root hair in cessation of tip growth, showed enlarged endosomes with random distribution.

E: Non-growing mature root hair with only few enlarged endosomes outside of the root hair tip.

The arrowhead indicates the root hair bulge and the arrows indicate enlarged ndosomes.

Scale bars A-E = 20 µm.

To confirm that this pattern is not restricted to legume roots, the distribution of GFP-FYVE compartments in stably transformed *A. thaliana* was examined as well. Exactly as in Medicago, Arabidopsis root hairs showed FYVE-labelled endosomes preferentially present within outgrowing bulges (not shown) and at the tips of polarly growing root hairs (Fig 10 A). Growing hairs exhibited abundant endosomes from the tip up to 30 µm downward the root hair shank, but retracted from the tips in mature hairs, once growth had ceased (Fig 10 B). However,

unlike this situation in Medicago, FYVE-based endosomes did not form enlarged structures in mature root hairs of Arabidopsis. Rather, endosomes became just a little bit larger and spread throughout the entire root hair (Fig 10 A).

To determine, if the endosomal Rab GTPases, Ara6 and RabF2a, were also present at the tips of growing root hair cells, stably transformed *A. thaliana* seedlings expressing Ara6-GFP or YFP-RabF2a, respectively, were investigated. Both these Rab GTPase reporters labelled membrane compartments that distributed within growing tips. Very similar patterns of distribution of Ara6-labelled endosomes, to those described above for the GFP-FYVE construct, in both rapidly growing hairs (Fig 10 C) and hairs with ceased tip growth (Fig 10 D) have been scored. Furthermore, the growing and growth-terminated root hairs of eYFP-RabF2a transformed *A. thaliana* seedlings showed the same distribution pattern of endosomes as that shown for the transgenic FYVE and Ara6 seedlings (Fig 10 E, F).

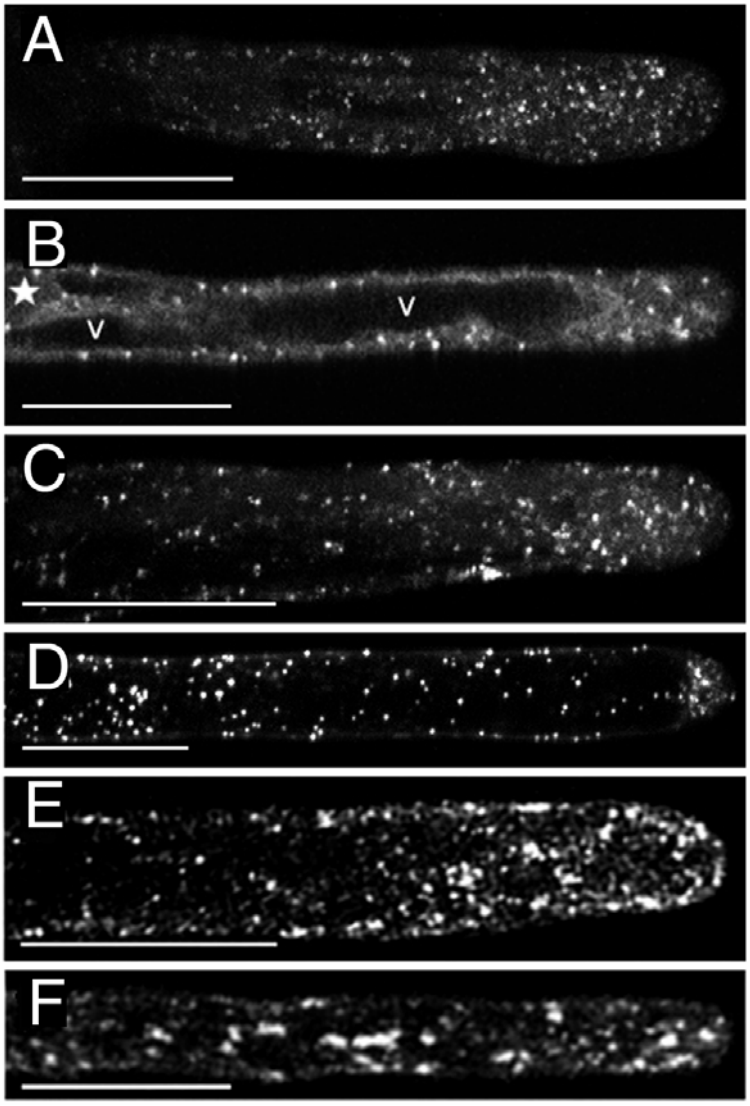

Fig 10. Different GFP-based endosome marker in root hairs of *A. thaliana.*

A, B: GFP-FYVE labelled endosomes in the tip of growing (A) and evenly distributed in growth-terminated (B) root hairs.

C, D: similar distributions were scored also for Ara6-labelled endosomes in growing (C) and growth-ceasing root hairs (D).

E, F: also eYFP-RabF2a-labelled endosomes showed a similar distribution in growing (E) and growth-terminated (F) root hairs.

Star in b indicates the position of nucleus and v the vacuole.

Scale bars A-F = 25 µm.

3.2.4. MOTILE F-ACTIN PATCHES IN ROOT HAIR TIPS

Both the preferential tip accumulation as well as the highly dynamic motility of the GFP-FYVE and YFP-RabF2a labelled membranes suggested a role of the actin cytoskeleton in the subcellular distribution of these endosomal compartments within growing root hair cells. Because an intact actin cytoskeleton is also required for expansion of root hair cells (Baluska et al., 2000b; Baluska and Volkmann, 2002; Gilliland et al., 2002; Jiang et al., 1997; Miller et al., 1999; Ringli et al., 2002; Samaj et al., 2002; Vantard and Blanchoin, 2002), the potential link between actin based motility and subcellular distribution of the GFP-FYVE/Ara6/YFP-RabF2a endosomes and cell expansion in root hair cells was investigated. Interestingly, this motility did not appear to be completely random based on the observed presence of these compartments at the tips of root hairs. *In vivo* analysis of root hair tips, transformed with the GFP-FABD2 construct visualizing F-actin (see chapter 3.1; Ketelaar et al., 2004), revealed mobile F-actin patches (Fig 11 A, C). The rate of tip growth and cell morphology did not show obvious differences to wild type root hairs (data not shown).

The F-actin patches resembled closely the above described endosomes with respect to speed, locations and directions of movements. Generally, in the tips of growing root hairs of *M. truncatula* as well as of *A. thaliana*, abundant actin-patches and very dynamic short actin filaments (Fig 11 A, C) could be detected. However, non-growing root hairs showed prominent actin bundles, which protruted up to the extreme tip (Fig 11 B, D), while enlarged actin patches were still present but less motile.

Treatment of root hairs with 1µM jasplakinolide resulted in the formation of thick actin structures composed of presumably aberrantly bundled F-actin, which were formed at or near the root hair tip (Fig 11 E-H). In time series, it is obvious that these structures are polarly organized and move towards the hair tip. Finally, they stopped their movements completely and associated tightly with the very tips of jasplakinolide-treated root hairs (Fig 11 H).

Fig 11. Root hairs of *M. truncatula* (A, B) and *A. thaliana* (C-H) transformed with GFP-FABD2.
A: growing root hair without thick actin bundles at the tip and some actin patches.
B: non-growing root hair with thick actin bundles throughout the complete cell.
C: typical actin distribution in a growing Arabidopsis root hair, with prominent actin patches near the tip.
D: thick actin bundles throuhgout the complete non-growing root hair.
E: growing Arabidopsis root hair tip without treatment (E).
F: after 12 min treatment with 1 µM jasplakinolide, the first larger paracrystalline-like F-actin bundle appeared at the tip.
G-H: after 40 and 80 min treatment with jasplakinolide, even larger paracrystalline-like structures of bundled F-actin were tightly associated with the very tips.
Scale bars A-D = 20 µm; E-H = 10 µm.

3.2.5. ACTIN POLYMERIZATION PROPELS ENDOSOMES

The observation that F-actin patches were present at the tips of root hairs and displayed similar motility characteristics as endosomes labelled with GFP-FYVE and Ara6/RabF2a reporter constructs suggested that perhaps the dynamics of these compartments was intimately linked to the actin cytoskeleton. To identify the driving forces behind the motility of these plant endosomes, time-lapse confocal imaging of root hair tips was performed. A single focal plane in the middle of the tip was monitored for 70 seconds. The experiment revealed that the motile behavior of

endosomes was highly variable (Fig 12). In some rare cases endosomes were nearly stationary, displaying restricted motility of only a few micrometers forwards and backwards (Fig 12 F, red marked letters). Alternatively, stationary compartments suddenly initiated movements and dashed away at high speed. Other GFP-FYVE endosomes displayed slow and directional movements (Fig 12 F, number 2), while yet others displayed sustained, rapid motility (Fig 12 F, number l).

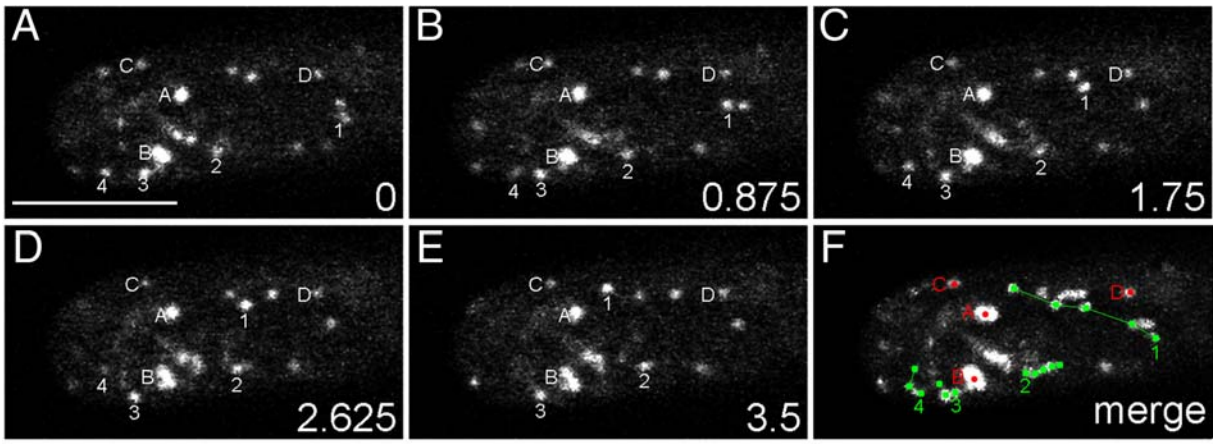

Fig 12. Time-lapse imaging of GFP-FYVE in Medicago root hair tips.

A-E: subsequent pictures of the same tip revealed, that individual endosomes follow different patterns of motility, where some were rather stationary (see endosomes marked with capital letters A, B, C, D in each picture) what is denoted as resting phase. Other endosomes were moving slowly (endosomes marked with numbers 2, 3, 4) or rapidly (number 1).

F: merged picture of the series before, with inserted trajectorys.

Scale bar in A = 10 µm.

Table IV. Speed and rest times of the GFP-FYVE labelled endosomes in *M. truncatula* root hair tips

	speed range [µm/sec]	average rest time [sec]	time spent stationary [%]
control (n=100)	0.09 - 17.77	1 - 4	26 - 39
BDM (n=54)	0.11 - 18.92	0 – 1*	0 – 10*
LatB (n=48)	0 - 1.04*	2.5 - 4.35	55 – 67*

Significant differences between treated and control root hairs are indicated by star.

For the control 100 endosomes out of 11 root hairs, for the BDM treatment 54 endosomes out of three root hairs and for LatB treatment 48 endosomes out of three root hairs were measured.

In order to ascertain on which cytoskeletal elements and processes these endosomal movements depended, the effect of several drugs was tested. In the untreated root hair tips, the majority of endosomes changed their position within 14-28 seconds (Fig 13 A-C). Measurements and subsequent statistical analysis of the movements revealed an average speed of 0.54 µm/sec (0.21 µm/sec SE) for the GFP-FYVE labelled endosomes (Table IV). During the period of observation time, they spent up to 40% of this period as stationary organelles, the duration of resting time was in the range of 1-4 seconds.

Upon application of 10 mM of 2,3-butanedione monoxime (BDM), a general myosin ATPase inhibitor (Samaj et al., 2000), GFP-FYVE labelled endosomes continued to display subcellular movements, even if we extended the treatment for up to one hour (Fig 13 D-F). While overall motility of organelle and cytoplasmic streaming was not negatively affected (data not shown), the characteristics of endosome motility was altered in the presence of BDM. Detailed quantitative analysis revealed a dramatically changed resting time of the endosomes in BDM treated root hairs. The BDM treated FYVE-labelled endosomes spent less than 10% of the observed time in a stationary phase as compared to 40% in control conditions. Application of 10 µM latrunculin B (LatB), an efficient F-actin depolymerizing agent (Gibbon et al., 1999; Baluska et al., 2001b), resulted in almost instant inhibition of endosomal movements (Fig 13 G-I). Treatment with the microtubule depolymerizing drug, oryzalin (10 µM), had no discernible effect on endosomal motility (data not shown).

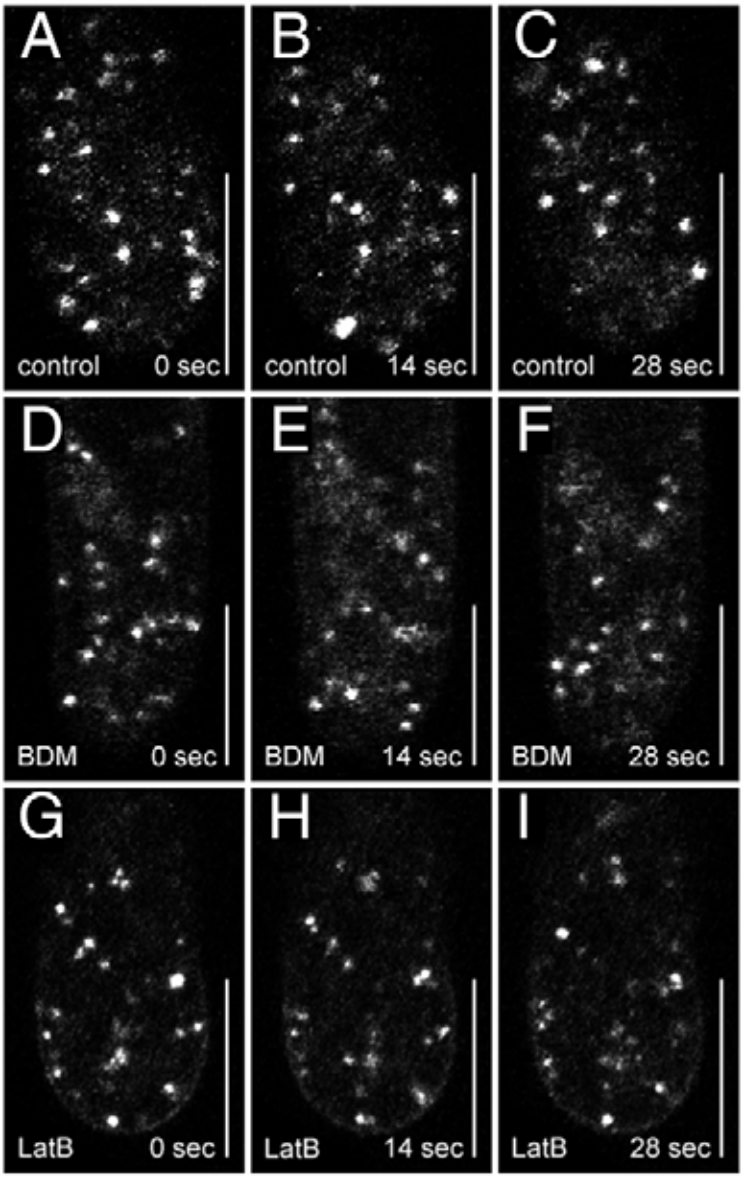

Fig 13. FYVE-labelled endosomes in Medicago root hairs during 28 sec time lapse imaging.
A-C: without treatment, rapid motilities of tip-localized endosomes were scored.
D-F: the movement was not inhibited by the myosin motor inhibitor BDM.
G-I: LatB stopped instantly all movements of the endosomes. See also Table III.
Scale bars A-I = 10 µm.

3.2.6. BREFELDIN A, WORTMANNIN, AND JASPLAKINOLIDE AFFECT GFP-FYVE ENDOSOMES

To test if endosomal movements were influenced by inhibitors of membrane trafficking through endomembrane compartments, brefeldin A (BFA) and wortmannin were applied to root hairs of *M. truncatula*. The effect of BFA was traceable after ten minutes (Fig 14 A) in the form of an enlargement of FYVE-labelled endosomes which concomitantly slowed down their motility. After 60 min of exposure to 100 µM BFA, a significant inhibition of endosomal motility and further enlargement of endosomes (Fig 14 B) became apparent. Two hours of BFA treatment resulted in large agglomerates of aggregated endosomes (Fig 14 C, arrows), known as the ‘BFA compartments’ in plant cells, with a greatly reduced motility. Exposure of

hairs to 10 µM wortmannin produced similar, although less prominent, effects on FYVE-labelled endosomes (Fig 14 D-F).

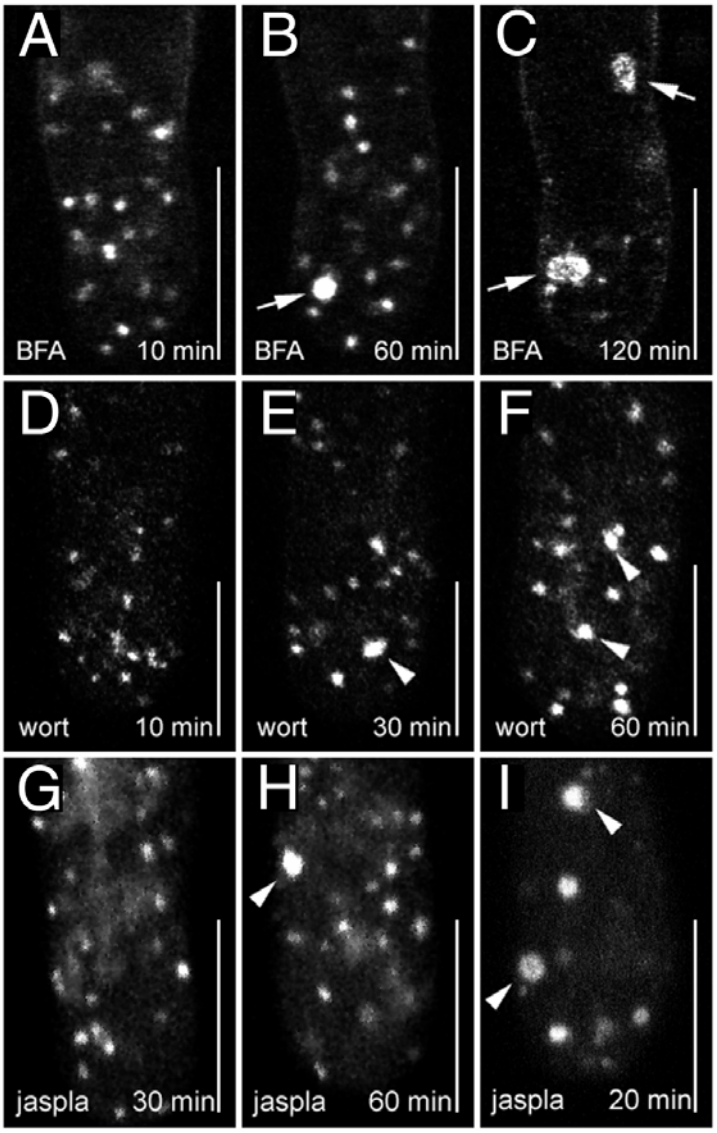

Fig 14. The effect of BFA, wortmannin and jasplakinolide on GFP-FYVE endosomes in Medicago root hairs.
A-C: BFA inhibited the motility, caused enlargement (arrows) and aggregation of FYVE-labelled endosomes.
D-F: similar, but less dramatic effects (arrowheads) were induced also with wortmannin.
G: 1 µM jasplakinolide treatment resulted after 30 min in inhibition of the motility of the FYVE-labelled endosomes.
H: after 60 min of exposure first larger aggregates (arrowhead) appeared.
I: Treatment with 5 µM jasplakinolide for 20 min resulted in the same effects, the motility was greatly decreased and the endosomes were enlarged (arrowheads).
Scale bars A-I = 10 µm.

After scoring the dramatic changes of the actin cytoskeleton upon jasplakinolide treatment, GFP-FYVE expressing root hairs were as well tested with 1 µM and 5µM jasplakinolide (Fig 14 G-I). The data revealed, that FYVE-based endosomes considerably enlarged in hairs treated with jasplakinolide, suggesting that dynamic F-actin is essential also for their morphology. With the increasing time of exposure and concentration of jasplakinolide, endosomes slowed down their movements.

3.3. SYNTAXIN SYP121

3.3.1. INTRACELLULAR LOCALIZATION OF GFP-SYP121 IN ROOT CELLS

In order to investigate which kind of vesicles contain SYP121, the intracellular localization of GFP-SYP121 in the root of stable transgenic *Arabidopsis* seedlings (Collins et al., 2003; Assad et al., 2004) were examined. Due to the ubiquitously expressing 35S promoter, the fluorescence signal and therefore fusion protein expression was high in all cells of the root cap as well as in the epidermal and cortex cell layers (Fig 15 A, B). The GFP-SYP121 signal predominantly labelled the plasma membrane of the root cap cells (Fig 15 A), but at a higher magnification, it can be seen to be abundant within vesicles, which are evenly distributed in the entire cytoplasm of the cortex cells (Fig 15 B). In contrast to this, the tip-growing root hair cells had abundant GFP-SYP121-labelled vesicles, which were highly polarised towards the growing tip. This tip-localization of GFP-SYP121-labelled vesicles is generally maintained from very young root hairs (Fig 15 E) to full grown root hairs (Fig 15 C, D). Furthermore, GFP-SYP121 accumulated in endosomal derived cell plates of dividing cells at all stages (Fig 15 F). These latter findings further suggest the endosomal nature of the GFP-SYP121-labelled vesicles, since it is already known that the tip growth of root hairs and the formation of the cytokinetic cell plate is driven by endosomal secretion (Dhonukshe et al., 2006; Ovecka et al. 2005).

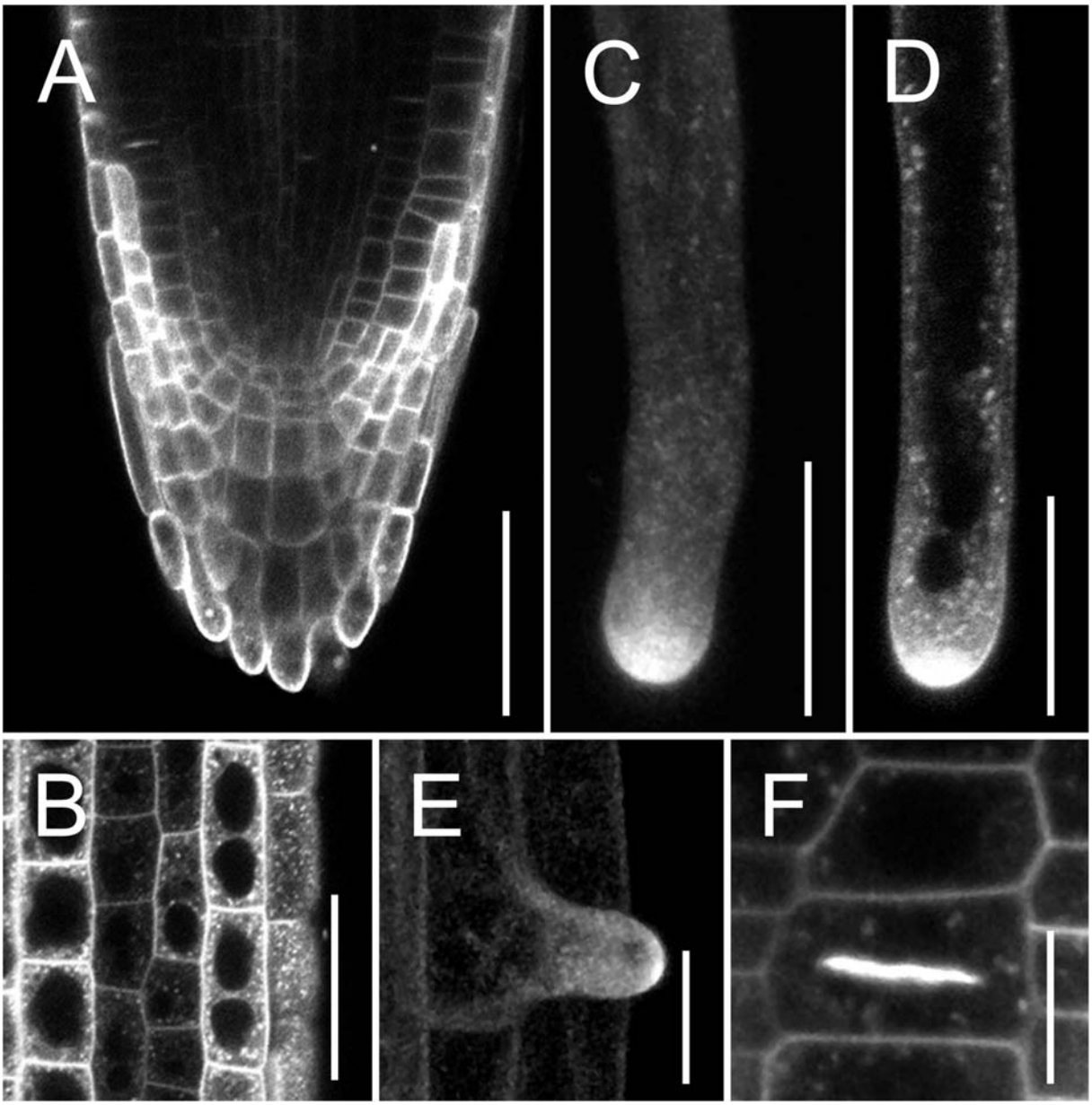

Fig 15. *In vivo* visualization of GFP-SYP121 in transgenic *A. thaliana* root cells.

A: overview of the complete root tip in a median longitudinal optical section, showing high expression in root cap cells at the plama membrane.

B: higher magnification of epidermal cells of the elongation zone revealed evenly distributed vesicles.

C: projection of a growing root hair with polarized distribution of GFP-SYP121 vesicles at the tip.

D: a growth-terminating root hair, displaying a vanishing polarized distribution.

E: projection of a young, rapidly growing root hair.

F: meristem cell with prominent labelled cell plate.

Scale Bars A = 50 µm; B = 40 µm; C, D, E = 20 µm; F = 10 µm.

3.3.2. SYP121 ACCUMULATES IN ENDOSOMAL BFA-INDUCED COMPARTMENTS AND ITS TIP-LOCALIZATION IS F-ACTIN DEPENDENT

Brefeldin A (BFA) exposure results in an aggregation or enlargement of endosomal compartments (see chapter 3.2; Baluska et al. 2002; Samaj et al. 2005). In roots, GFP-SYP121-labelled vesicle aggregates appeared within 30 min of BFA treatment, as shown in epidermal cells of the root transition and elongation zones (Fig 16 A, B). The GFP-SYP121-labelled vesicles in growing root hairs showed a strong response to BFA. After 30 min, the tip-polarisation of GFP-SYP121 disappeared and large BFA compartments emerged (Fig 16 C). To address the driving force behind the polarised SYP121 distribution in root hairs, the effect of the F-actin-disintegrating drug cytochalasin D (CD) was tested. Fig 16 D shows a normally growing root hair with its characteristic tip focused GFP-SYP121 localization. The density profile of the GFP signal in false colors shows clearly the high signal (white) at the root hair tip. The CD treated root hair in Fig 16 E has lost this clear tip focalisation. Although the vesicles are still concentrated at the tip region, this phenomenon is less pronounced.

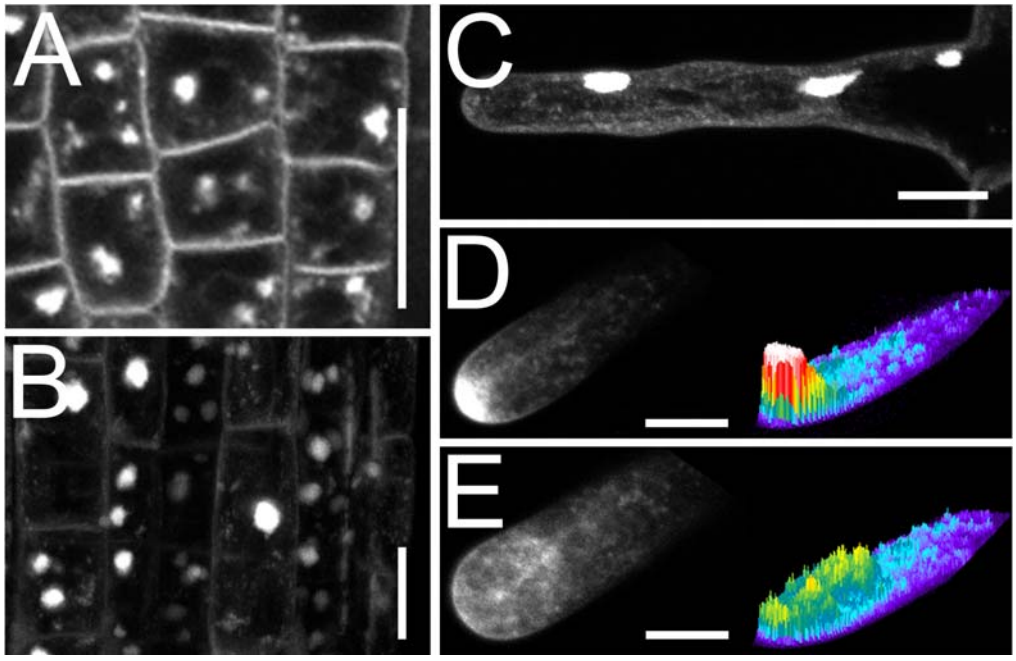

Fig 16. Live imaging of inhibitor treated GFP-SYP121 root cells.

A: epidermal cells of the transition zone after 35µM BFA treatment for 30 min showing SYP121 aggregations.

B: the same aggregates were found in epidermal cells of the elongation zone after the treatment with BFA.

C: in root hairs, exposed to BFA, GFP-SYP121 aggregates almost completely into few large BFA compartments.

D: microscopic image of a growing root hair with its normal tip focused GFP-SYP121 localization and the corresponding density profile (white = high fluorescence density, blue = low density).

E: microscopic image of a growing root hair after exposure to 1µM Cytochalasin D and the corresponding density profile.

Scale Bars A-C = 20 µm, D, E = 10 µm.

3.3.3. SYP121 CO-LOCALIZES PARTIALLY WITH THE ENDOCYTIC TRACER FM4-64

The red fluorescent dye FM4-64 serves as endocytic marker (for plant cells, see Ueda et al., 2001; Samaj et al. 2005). After a short application to the roots of transgenic GFP-SYP121 plants, a partial co-localization of GFP-SYP121 and FM4-64 is visible. In Fig 17 A, a growing root hair tip is shown after incubation with FM4-64 for 2 min. The typical tip focused localization of GFP-SYP121 (left) and a similar localization of FM4-64 (middle) is visible. The merged image (right) shows a high degree of co-localization (yellow color) of the green (GFP-SYP121) and red (FM4-64) channel. At the very tip, there is a high rate of co-localization, both at the plasma membrane and within the vesicles. However, some 10 μm behind the very tip, the signals divide into two different populations of vesicles which show only occasional overlap. The root hair tip in Fig 17 B is imaged after incubation with FM4-64 for 5 min. Only the merged image of the green and red channels is shown. The tip focused co-localization is clearly visible. After 10 min of labelling with FM4-64, the seedling was treated with BFA to block secretion and to induce formation of endocytic BFA-induced compartments. After 60 min of incubation, large BFA-induced compartments aggregate with a strong signal from both GFP-SYP121 and FM4-64 (Fig 17 C). The same kind of co-localization appears in cortex cells of the transition zone after the incubation of the roots for 50 min with BFA and then for 10 min with FM4-64 (Fig 17 D). The GFP-SYP121 vesicles accumulate within BFA-induced compartments (left), in which the signal from the endocytic tracer FM4-64 can also be detected (middle). In the merged image (right) co-localization of the signals of the two channels is visible, but proportional differences appear. Whereas, the GFP-SYP121 to a large degree is transferred from the plasma membrane into the BFA-induced compartments (green), the FM4-64 (red) still has a much higher signal at the plasma membrane. This indicates that the SYP121 vesicles are part of the endocytic network (Samaj et al. 2005) or that these vesicles are recycled during their function at the plasma membrane.

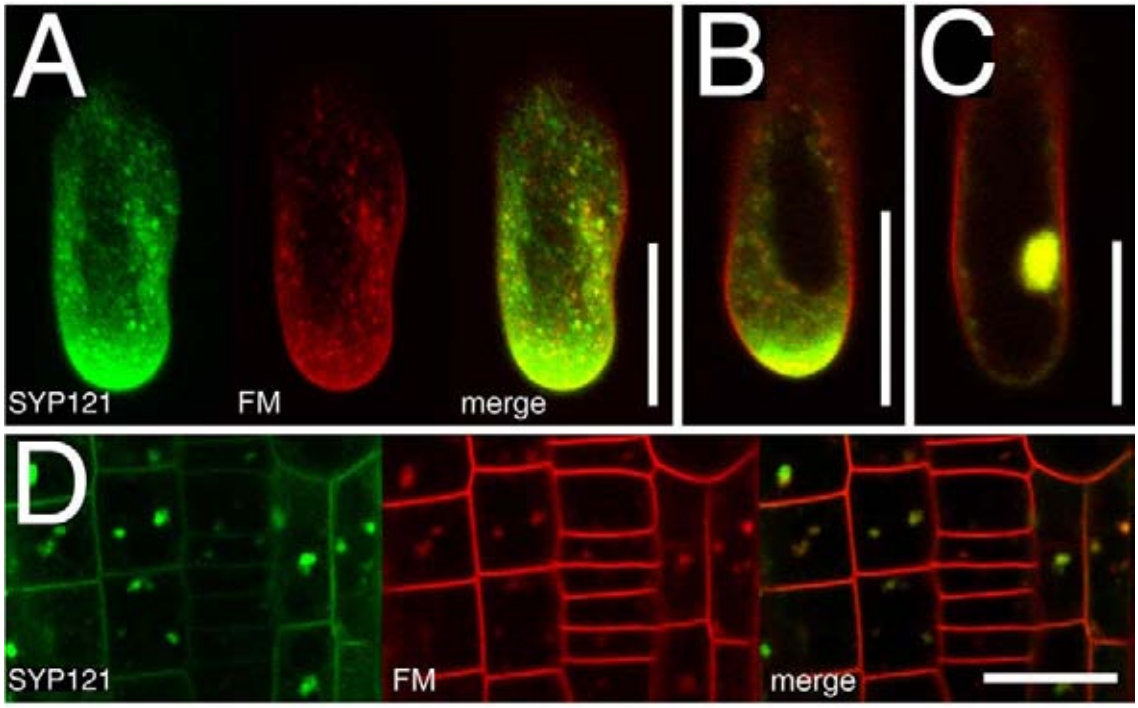

Fig 17. GFP-SYP121 and FM4-64 co-localization.
A: root hair from GFP-SYP121 transgenic seedling incubated for 2 min with FM4-64, resulting in partial co-localization (yellow color in the merge picture).
B: merged image of a growing root hair after 5 min of FM4-64 treatment.
C: merged image after staining for 10 min with FM4-64 and subsequent incubation for 60 min with BFA.
D: cortex cells of the transition zone were treated for 50 min with BFA and then incubated with FM4-64 for 10 min, resulting in a co-localization of GFP-SYP121 and the FM dye in BFA induced compartments.
Scale Bars A-D = 20 µm.

3.4. SYNAPTOTAGMIN EXPRESSION AND LOCALIZATION

3.4.1. EXPRESSION PATTERN OF SYNAPTOTAGMINS

The six members of the synaptotagmin-like gene family have all a similar gene structure according to databases and prediction programs. At the N-terminus there is a transmembrane domain or in case of SytF a predicted signal peptide. Followed by a linker the two or three, respectively, C2 domains are tandemly arranged. As a kind of exception the SytF sequence shows similarities at the C-terminus to coiled-coil domains (Fig 18). All genes have a predicted structure of 11 to 13 exons building ORF´s from 1605 bp to 2445 bp (see Table II in Material and Methods).

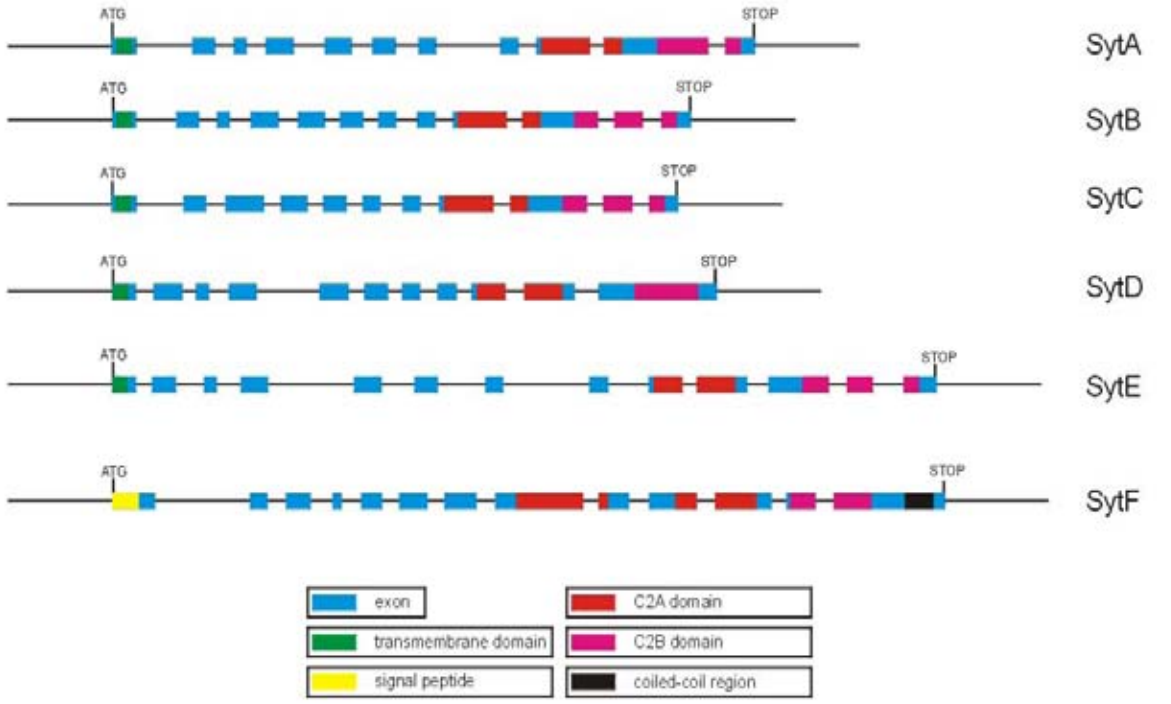

Fig 18. Exon/intron structure of the six synaptotagmin members.

The expression pattern of this gene family was first analysed using publicly available Affymetrix microarray data (Zimmermann et al., 2004; www.genevestigator.ethz.ch) and is shown in Fig 19. The remarkable points are the strong expression of SytA and SytE in almost all types of tissue and the exclusive expression of SytB in stamen. Furthermore, SytC is expressed in cotelydons and leaves and to a weaker degree in roots.

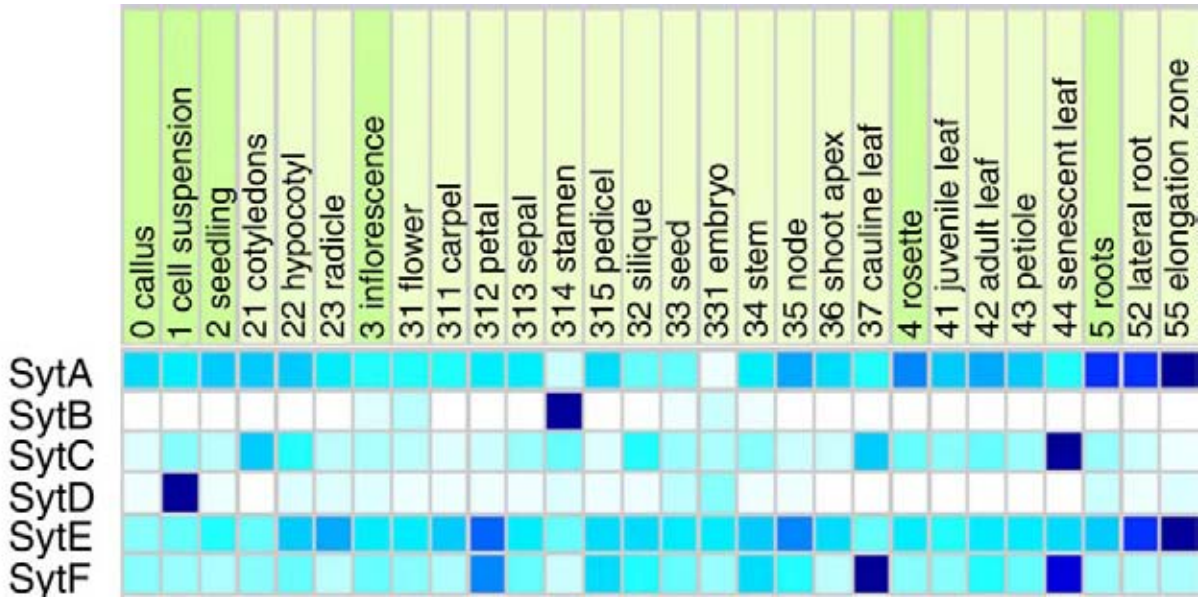

Fig 19. Expression pattern of the six Arabidopsis synaptotagmin-like genes, calculated from Affymetrix microarrays using Genevestigator (www.genevestigator.ethz.ch). Dark blue color represents high expression and white color represents no expression of the particular gene in the paticular tissue.

SytD appears to be strongly expressed in suspension cells and just weakly in embryo and roots. An average expression shows SytF, with peaks in cauline and senescent leaves. These data come from a lot of different experiments and laboratories and are only used to get a first idea of the expression program of the synaptotagmins.

To gain further insight where and when the six different synaptotagmins are expressed, promoter:β-glucuronidase (GUS) reporter gene transcriptional fusion constructs were designed. The promoter regions where defined as 2 kb long DNA fragments directly upstream of the translation start codon, where possible. In case of SytA, a 1,5 kb long genomic DNA fragment (for exact sizes, see Material and Methods 2.1.3) upstream of ATG was amplified and used as promoter region. After stable introduction of these fusion constructs into *A. thaliana*, at least five transformed lines of each family member were analyzed.

For SytA in almost all cells of different developmental stages a strong GUS activity was detected (Fig 20). The vascular tissue as well as epidermal cells of cotelydons and leaves were stained (Fig 20 A). GUS activity was also monitored in trichomes and root hairs (Fig 20 B, C) as well as in all cells of the main root and lateral roots. Interesting to note are higher intensities of GUS activity in the vascular tissue of the elongation zone and of cells of the root cap (Fig 20 D).

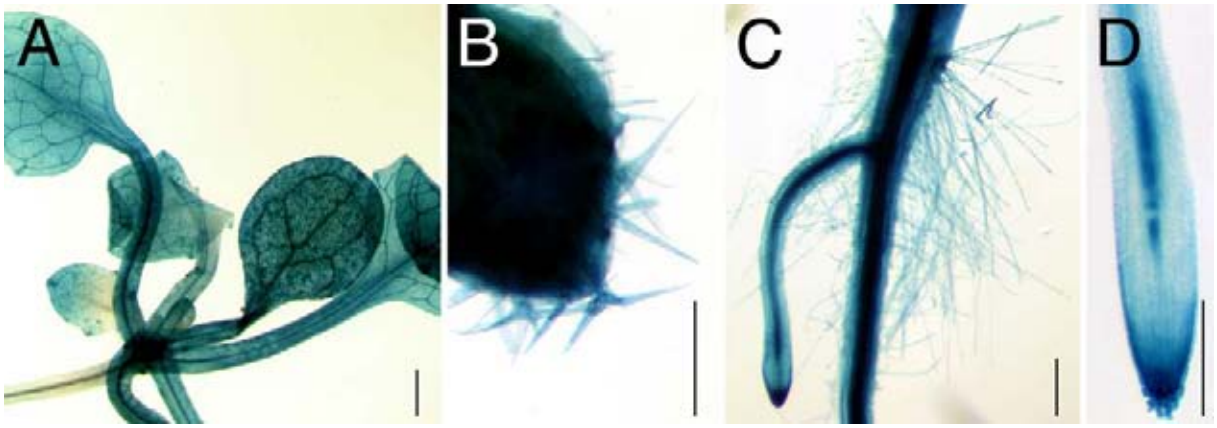

Fig 20. promoterSytA:GUS localization in Arabidopsis tissues and organs.

A: GUS activity in the whole seedling in all cells.

B: GUS activity in trichomes.

C: GUS activity in main and lateral roots and root hairs.

D: GUS activity in the root tip is stronger in vascular tissue of the elongation zone and in root cap cells.

Scale Bars A = 1 mm; B, D = 200 µm; C = 500 µm.

The picture was for the closest relative of SytA, SytB completely different. The only prominent expression was localized to developing pollen (Fig 21 A, B). A very faint activity could be monitored in the secretory cells of the peripheral root cap (Fig 21 C).

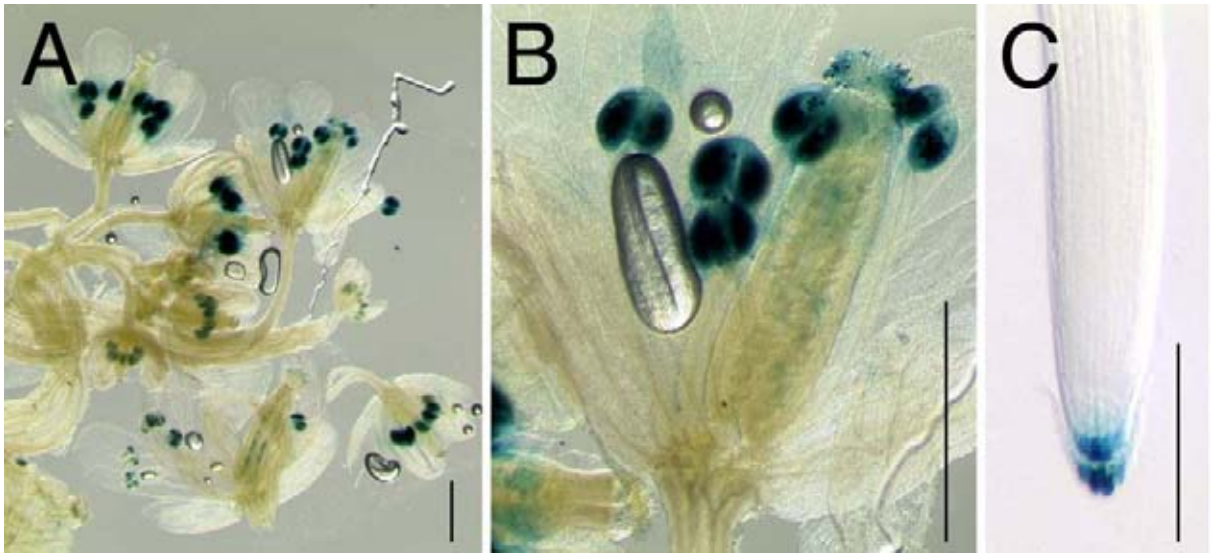

Fig 21. promoterSytB:GUS localization in Arabidopsis tissues and organs.
A: flowers with strongly stained stamen.
B: close up from A.
C: the secretory cells of the root cap exhibited a faint GUS activity.
Scale Bars A, B = 1 mm, C = 200 µm.

The expression program of SytC was different from SytA and SytB. In the green parts of the plants, GUS activity was exclusively found in stomata (Fig 22 A). Also the stomata of the hypocotyl had a clear signal (Fig 22 B). The expression in the roots differed strongly from the

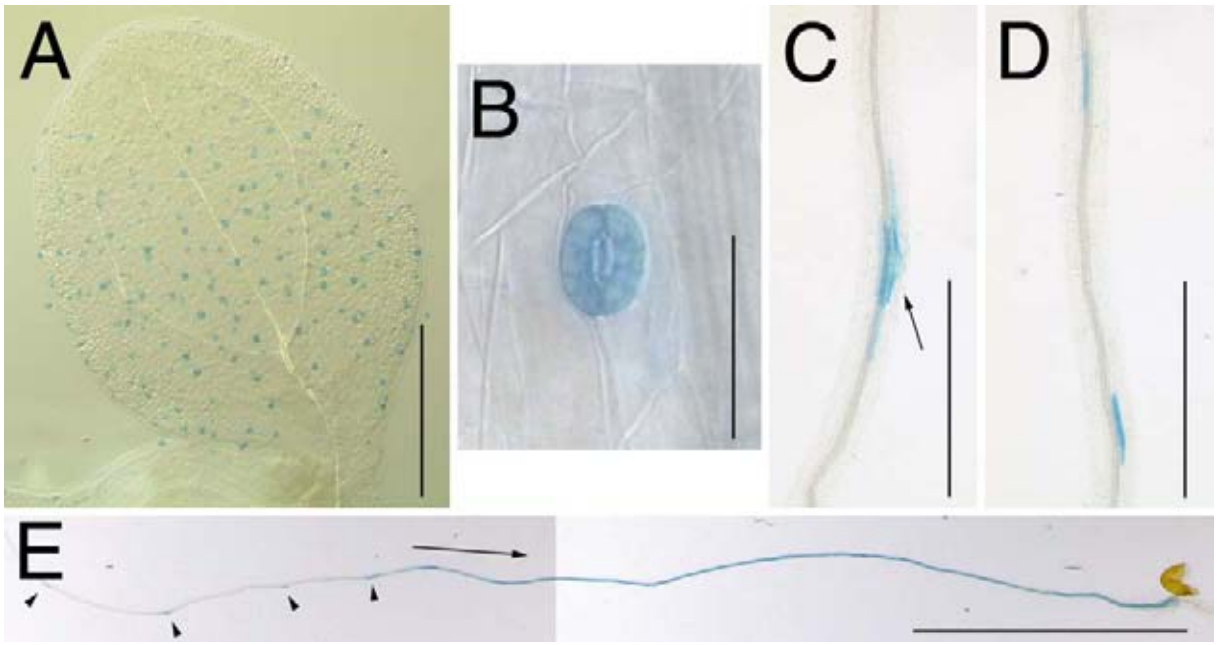

Fig 22. promoterSytC:GUS localization in Arabidopsis tissues and organs.

A: in leaves, GUS activity localized only to stomata.

B: stomata of the hypocotyl displayed GUS activity as well.

C: outgrowth of a lateral root (arrow) with only a few GUS positive cells.

D: two single cells showing GUS activity, presumably at places of later lateral root outgrowth.

E: root with GUS activity in single cells (arrowheads) and in all vascular tissue of older parts of the root (arrow).

Scale Bars A, C-E = 500 µm, B = 50 µm.

others. The signal emerged in single cells which are the points of later lateral root outgrowth (Fig 22 C arrow, D). In a complete root it is obvious that at the beginning, in younger root parts, only single cells show expression (Fig 22 E, arrowheads) and, when the root becomes older the GUS activity is spread to all the vascular tissue (Fig 22 E, arrow).

In case of the promoter analysis of SytE there was found no GUS signal at all in at least 10 transformed lines. GUS activity of SytD promoter lines was restricted to vascular tissue in the hypocotyl, leaves as well as in roots (Fig 23 A, B). In roots there was a slightly stronger signal detected in the elongation zone and at the outgrowth points of lateral roots (Fig 23 B, C). The SytF promoter lines showed only a low activity of GUS in the root meristem and in cells of the root cap (Fig 23 D, E).

Fig 23. promoterSytD:GUS and promoterSytF:GUS localization in Arabidopsis tissues and organs.
A: SytD-GUS activity in the vascular tissue of hypocotyl and leaves.
B: SytD-GUS signal in vascular tissue of the roots and at points of lateral root outgrowth.
C: SytD-GUS in stelar cells of the elongation zone.
D, E: SytF-GUS activity restricted to the meristem and certain cells of the root cap.
Scale Bars A = 1 mm, B-D = 200 µm, E = 100 µm.

3.4.2. INTRACELLULAR LOCALIZATION IN *A. THALIANA* AND *N. TABACUM*

For examination of the intracellular localization of the synaptotagmin proteins, complete ORF-GFP fusion constructs were constructed and stably introduced in Arabidopsis plants with agrobacterium-mediated gene transfer. More than 20 transformed lines could be isolated which showed resistance upon the selection marker, but all of them exhibited a very low level of GFP signal. Confocal microscopy of the roots (Fig 24 A-C) revealed the green fluorescence signal emerging primarily from the plasma membrane (PM) and structures inside the cells remembering the endoplasmatic reticulum (ER). The best expression could be observed in cells of the epidermis and in the root cap. The epidermal and root cap cells had a labelling at the PM and in diffuse pattern inside the cell (Fig 24 A, left and right). In the close-up of the transition and elongation zone, it is more obvious that the PM was not everywhere labelled with the same intensity. The cross walls between adjacent cells were stronger labelled than the longitudinal ones (Fig 24 B). Also the intracellular diffuse pattern, excluding nucleus and

vacuoles were more eminent. Interestingly, at older parts of the root, the stronger labelling of the cross walls vanished and the ER-like structure became more recognizable and aggregates inside appeared (Fig 24 C).

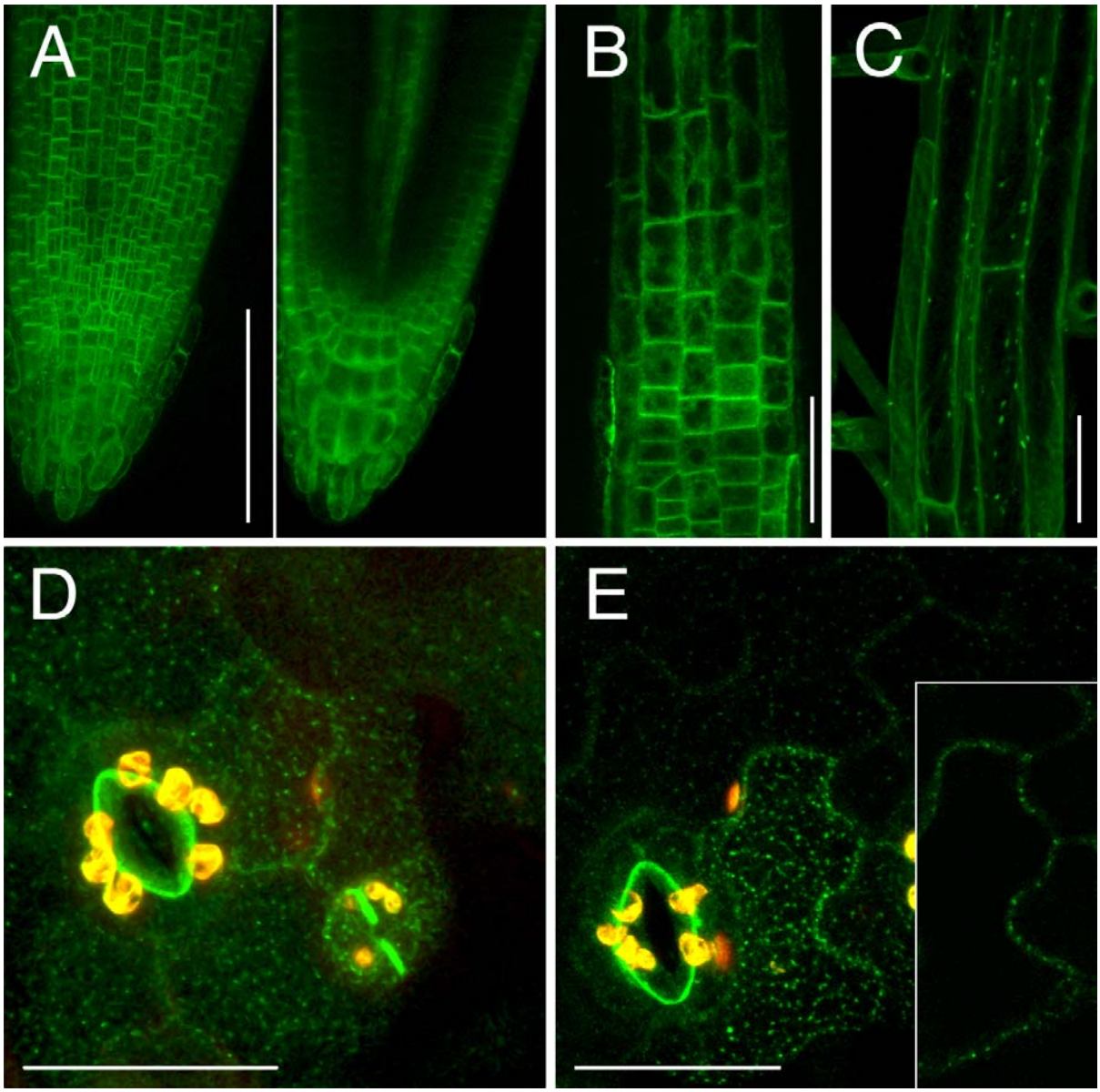

Fig 24. SytA-GFP expression in stable transformed Arabidopsis.

A: projection and single optical section of a root tip, SytA-GFP localized predominantly to the PM.

B: a projection of the epidermal cell layer at the transition and elongation zone shows a dominant signal from the cross walls and from diffuse pattern inside the cells.

C: epidermis cells at an older root part displayed a ER-like structure.

D: projection of the top half of leaf epidermis cells, including stomata. SytA-GFP localized to non-moving spots at the PM and to the “cross walls” of young stomata cells.

E: projection and single optical section (as inset) of an epidermal cell, similar to D.

The yellow color from the plastids in D and E results from the auto-fluorescence recorded in red and green channel due to high laser settings.

Scale Bars A = 100 µm, B, C = 50 µm, D, E = 25 µm.

The epidermal cells of the leaves show a spot-like structures all around the cell at the PM. Fig 24 D and E are projections of the upper halves of epidermal cells and stomata and show these not moving spots on the top of the cells. Noticeable is also the very strong signal emerging from the “cross-walls” of the young stomata. The inset in Fig 24 E makes the positioning of the spots at the surface of the cells clear. It is a single optical section from the shown projection and exhibits only spots at the PM/wall of the adjacent cells.

Due to the fact that the expression level was very low in the transgenic Arabidopsis seedlings, *N. tabacum* leaves were infiltrated with agrobacteria harbouring the SytA-GFP construct. This method gives usually a high expression in the epidermis cells and is well suited for localization experiments. In Fig 25 A and B transformed cells expressing SytA-GFP at moderate and low levels are shown. With a moderate expression (Fig 25 A), stable bright spots (arrows) at the plasma membrane connected by highly mobile ER tubules (arrowheads) were visible, which were just faintly visible at a lower expression level (Fig 25 B). The inset in Fig 25 B is a single optical section at the middle plane of the cell demonstrating the plasmodesmata-like appearance of these spots between two cells. To define the significance of the transmembrane domain, a GFP construct missing this domain was expressed in tobacco leaves as well (Fig 25 C). GFP-C2AB was evenly distributed throughout the cytosol and also inside the nucleus (open star). In addition to this, a ER marker, GFP-ER (Haseloff et al., 1997), introduced into tobacco leave cells only shows the highly mobile ER tubules like SytA-GFP, but is lacking the bright stable spots at the PM/ER junctions (Fig 25 D). After plasmolysing the SytA-GFP transformed leave cells with 500 mM NaCl for two hours and additional staining of the PM with FM4-64, it became obvious, that SytA-GFP is closely associated with the PM. SytA-GFP was localized to distinct parts of the PM, partly on the retracted PM of the protoplast, in Hechtian strands and in spots, which were still attached to the cell wall (Fig 25 E). This was more obvious visible in a projection of the upper half of a plasmolysed epidermal cell (Fig 25 F). The membrane of the protoplast (Fig 25 F, arrowheads) was attached to the cell wall with many Hechtian strands (Fig 25 F, arrow) which were labelled with SytA-GFP.

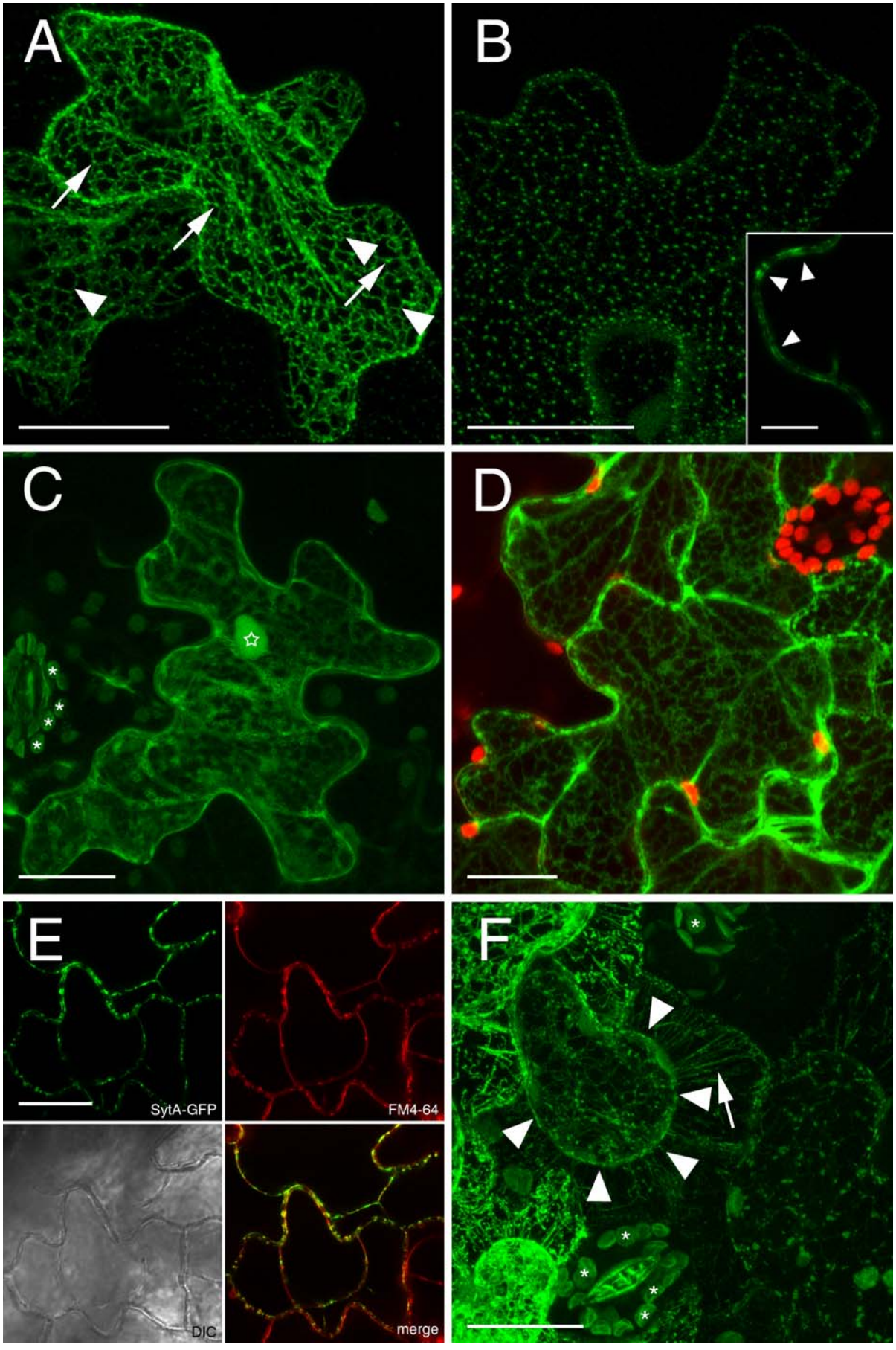
A
B
C
D
E
SytA-GFP
FM4-64
DIC
merge
F

Fig 25. GFP constructs expressed in *Nicotiana tabacum* epidermal leave cells.
A: SytA-GFP localized within mobile ER-tubules (arrowheads) connecting stable spots (arrows) at the PM in a projection of the top half of the cell.
B: SytA-GFP expressed in lower amounts, only the brighter spots are visible. The inset shows a single optical section at the middle plane of the cell with plasmodesmata like structures (arrowheads).
C: GFP-C2AB expressed in tobacco shows a cytosolic distribution and nucleus localization (open star).
D: GFP-ER expressed in tobacco epidermis cells shows the ER as highly mobile tubules.
E: SytA-GFP expressing cell, plasmolysed with 500mM NaCl and staining with FM4-64. SytA-GFP is shown on the upper left, the red fluorescence of the FM4-64 is displayed at the upper right. The lower right shows a merge of the two channels, revealing co-localization by the yellow color at spots at the PM. On the lower left the corresponding DIC image is shown.
F: projection of a salt plasmolysed cell showing SytA-GFP in Hechtian strands (arrow) and at the membrane of the retracted protoplast (arrowheads).
Auto-fluorescence of chloroplasts is indicated by asterisk.
Scale Bars A-F = 25 µm, inset in B = 10 µm.

The synaptotagmins are Ca^{2+} sensing/binding proteins, therefore its was interesting, if there is a change in the localization of the fusion protein upon Calcium addition or depletion. These kind of experiments can be performed with the Ca^{2+} ionophore Calcimycin A23187. The drug A23187 enables Ca^{2+} ions to cross biological membranes, the direction depending on the concentrations in- and outside the cell. The Ca^{2+} concentration inside the cell could be increased via application of extra Calcium or decreased by application of the Ca^{2+} chelating agent EGTA. Upon increase of the intracellular Ca^{2+} concentration, the immobile spots at the proclaimed ER/PM junctions vanished, the underlying ER formed bigger tubes and large aggregates of the fusion protein could be observed (Fig 26 A, B). On the contrary, upon removing Ca^{2+} from the cells, the SytA-GFP spots keep in place and may even be more focused (Fig 26 C, D). In case of both treatments, a PM labelling with brighter spots is still visible in single optical section through the middle of the cells (Fig 26 B, D).

Fig 26. SytA-GFP transformed tobacco leave cells with different Calcium levels.
A, B: the transformed leave was treated 1h with 10µM A23187 and 10mM $CaCl_2$. In A a projection of the half cell and in B a single optical section from the middle plane is shown. The immobile spots disappeard into huge aggregates and the ER-like structure formed bigger tubes.
C, D: the transformed leave was treated 1h with 10µM A23187 and 10mM EGTA. In C a projection of the half cell and in D a single optical section from the middle plane is shown. The immobile spots and the ER appeared similar to not treated cells.
Scale Bars A-D = 25µm.

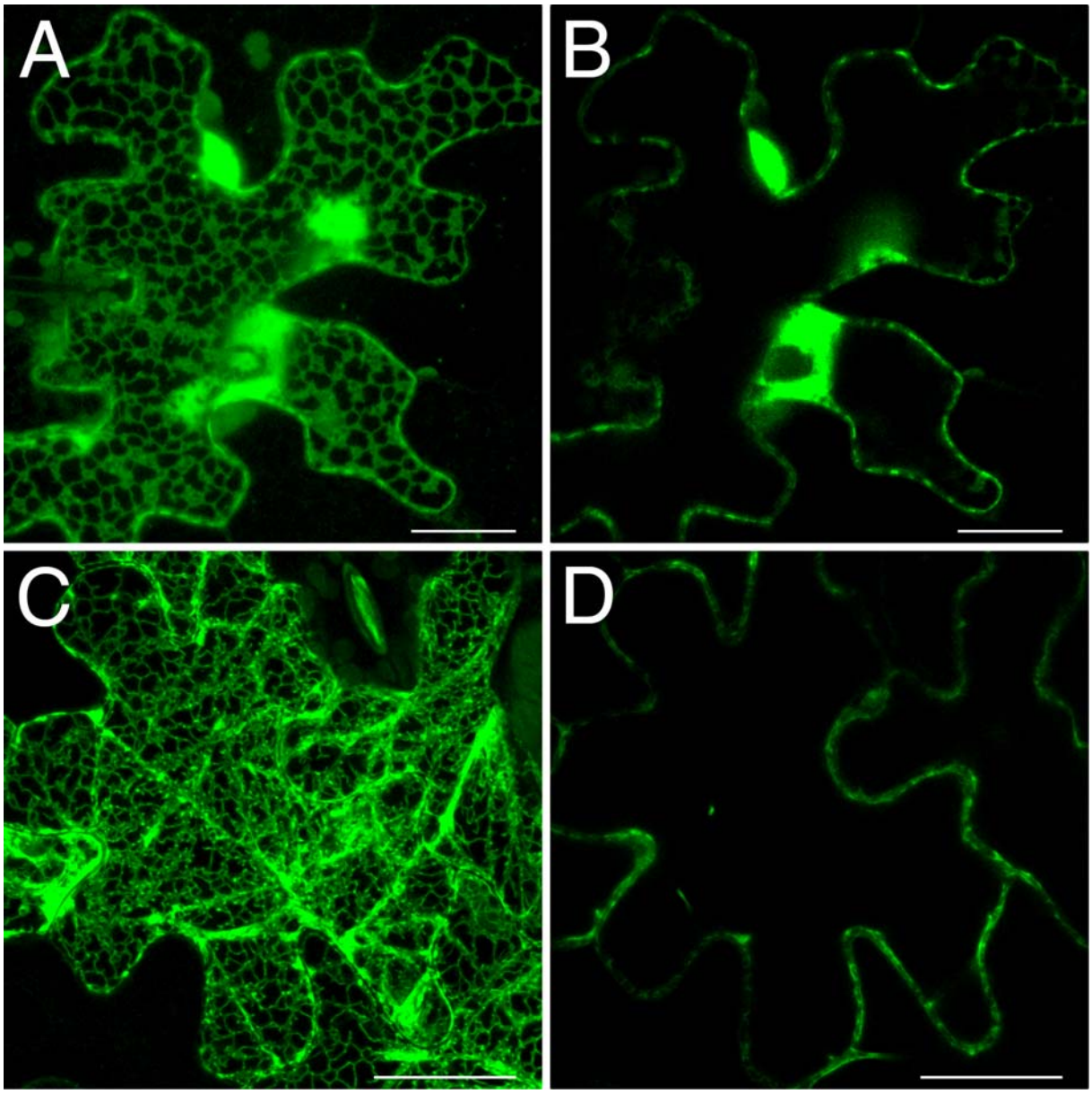

3.4.3. CHARACTERIZATION OF THE SYTA T-DNA LINE

WT and SytA T-DNA mutant (mSytA) seedlings were germinated on normal half-strength MS plates and after three days transferred to slide chambers and kept for at least 24 hours in vertical position. After this adaptation the medium was exchanged to low Calcium containing medium, one-tenth MS, with different salt concentrations. After another 24 hours in the treatment medium the seedlings were examined with the microscope. The lowest concentration of salt with an effect on the seedlings was found at 50 mM NaCl. The WT seedlings showed normal root and root hair growth (Fig 27 A, B). In contrast to this, the

mSytA seedlings showed at this concentration severe defects at the root hairs (Fig 27 C, D). The root hairs were much shorter, had often abnormal bulges or were exploded. The growth of the root was in a non significant manner decreased. At salt concentrations over 100 mM NaCl and low calcium, root hairs of mutant seedlings were not anymore outgrowing at all and the root growth was stopped.

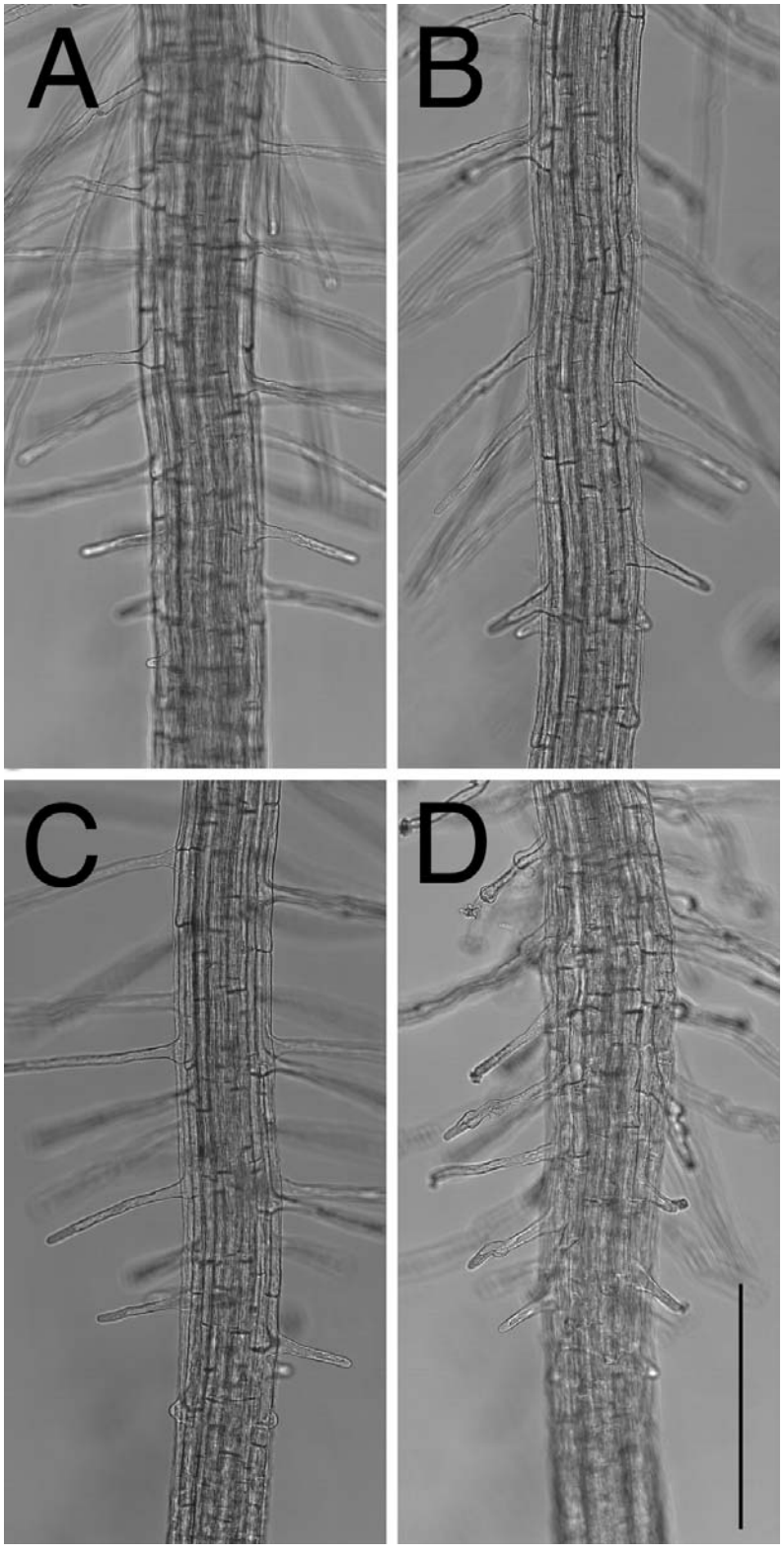

Fig 27. WT and mSytA seedlings before and after treatment with salt.
A: WT root growing in half-strength MS medium.
B: WT root growing for 24 hours in one-tenth-strength MS medium containing 50 mM NaCl showed normal growth.
C: mSytA root growing in half-strength MS medium.
D: mSytA root growing for 24 hours in one-tenth-strength MS medium containing 50 mM NaCl showed severe defects in root hairs and root elongation.
Scale Bar 25 µm.

To document the influence of salt to the cells of WT and mSytA seedlings, a double staining with FM4-64 and fluorescein diacetate (FDA) was prepared (Gunse et al., 2003). The endocytic tracer dye FM4-64 was in this case used as a marker for intact plasma membranes. Using short labelling times, like 30 seconds, the chance that the dye is incorporated into the cells via endocytosis is ruled out. If there is a strong labelling inside the cells, the dye must have been penetrated the cell through a wounded plasma membrane and absorbed into the endomembranes directly. To further harden this point, the staining was simultaneously done with FDA, to show living cells with an intact plasma membrane. The first set of experiments was performed with a high concentration of salt, regarded to salt shock treatment. Therefore, the roots of four days old seedlings of WT and mSytA were transferred to MS medium containing 200 mM NaCl for one hour. The WT roots showed after the treatment mostly living cells indicated by the bright green fluorescence and only occasionally bright red fluorescent dead cells within the meristem and the transition zone (Fig 28 A). In case of the

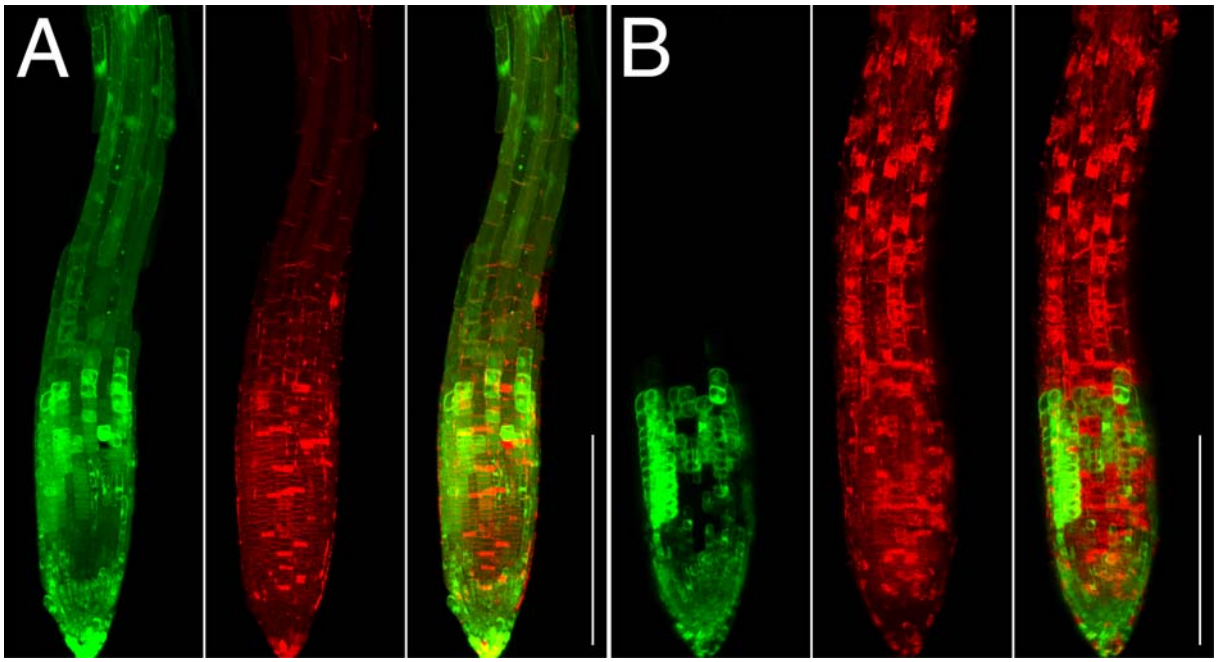

Fig 28. WT and mSytA seedlings after 1h 200 mM NaCl stained for live and dead cells after salt shock treatment.

A: FDA (green), FM4-64 (red) and merged image of salt treated WT seedling. Most cells of the root tip are intact, shown with the green color and the red color at the PM and just occasionally inside the cells.

B: FDA (green), FM4-64 (red) and merged image of salt treated mSytA seedling. Most cells are dead, only a few exhibit green fluorescence and all others are penetrated by FM4-64.

Scale Bars A, B = 250 µM.

mutant seedlings the picture is completely different. Almost all cells from the elongation zone on, show a strong red fluorescence inside the cells and only the cells from the root cap, meristem and transition zone show clusters of green fluorescence, indicating living cells (Fig 28 B).

In a second set of experiments, the cell viability of seedlings exposed to different concentrations of NaCl in low Calcium-concentration medium were tested. The seedlings were placed on petri dishes containing 1/10 MS medium enriched with 50, 75, 100, 125 mM NaCl, as well as 100 and 125 mM NaCl supplemented with 3 mM $CaCl_2$ and stained after different time periods. After three hours treatment (Fig 29) a clear difference between WT and mutant seedlings, with respect to the NaCl concentration, was obvious. The WT seedlings showed first dead cells (Fig 29 arrows) at 75 mM NaCl between elongation and root hair zone. At 100 mM NaCl the first few cells in meristem and transition zone appeared dead, which number increased at 125 mM NaCl. The supplement of 3 mM $CaCl_2$ rescued this salt phenotype completely, no dead cells were anymore found inside meristem and transition zone. The dead cells in the root hair zone of the WT seedling at 125 mM NaCl and 3 mM $CaCl_2$ are due to damages by tweezers during the staining process.

The situation in the SytA mutant background appeared similar, even so more severe. Cells of the root hair zone died already at 50 mM NaCl and at the meristem and transition zone at 75 mM NaCl. Above this concentration of salt, almost all epidermal and cortical cells from the root hair zone on were dead and bigger clusters of dead cells appeared in meristem and transition zone. Interestingly, the $CaCl_2$ supplementation at 100 mM NaCl was able to rescue the phenotype partially. Almost no dead cells were found at the meristem and much less at the root hair zone. The 3 mM $CaCl_2$ supplement at 125 mM NaCl could not rescue the seedling but diminish the damages in comparison to the situation without extra Ca^{2+}. These experiments of the cell viability after salt stress show clearly that synaptotagmin A plays a role in the answer of the cell to low cocentrations of salt as well as to salt shock treatment.

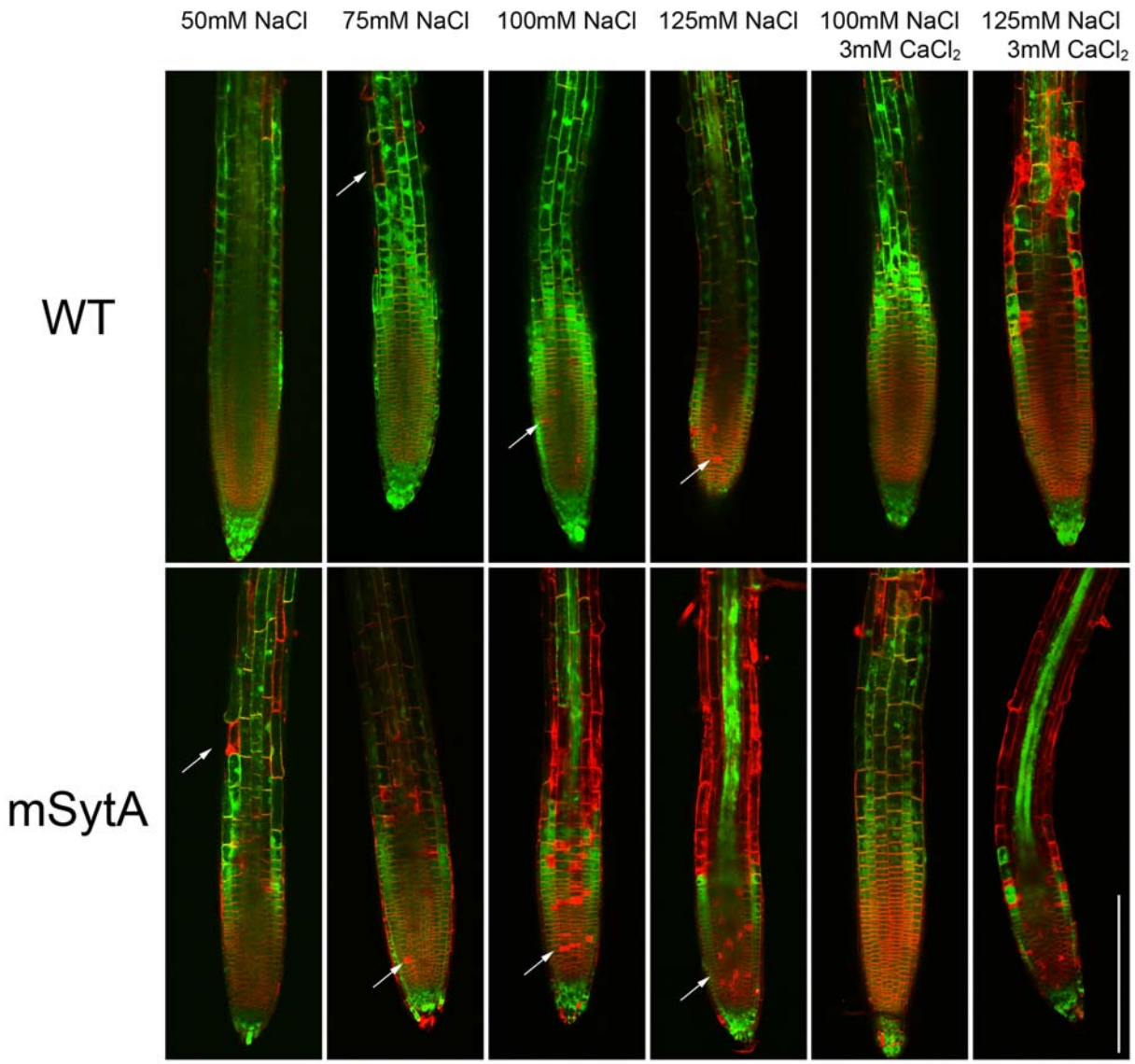

Fig 29. WT and mSytA seedlings after 3h growing on different concentrations of NaCl stained for live and dead cells.

Merged images of FDA (green) and FM4-64 (red) channels for WT and mSytA seedlings growing on 50, 75, 100, 125 mM NaCl and 100, 125 mM NaCl including 3 mM $CaCl_2$.

WT: first dead cells at root hair zone at 75 mM NaCl and in meristem and transition zone at 100 mM. Supplementation with calcium protects the cells at 100 and 125 mM NaCl.

mSytA: first dead cells appear at 50 mM NaCl in the root hair zone and at 75 mM in meristem. At 100 and 125 mM NaCl many cells in meristem, transition zone and root hair zone are dead. Supplementation with calcium protects the cells of the root tip at 100 mM NaCl and to a smaller dergree at 125 mM NaCl.

Arrows indicate dead cells or clusters of dead cells.

Scale Bar 250 uM.

4. DISCUSSION

4.1. THE ACTIN CYTOSKELETON

A. thaliana seedlings stably transformed with the GFP-FABD2 fusion construct provide us with the unique opportunity to study the actin cytoskeleton in vivo in all cell types throughout the plant body in the course of organ development. In addition to the already well characterized trichomes, we are now in the position to answer critical questions related to *in vivo* roles of the actin cytoskeleton within cells of the root cap, meristem, transition zone, root hairs, as well as diverse stelar cell types. In particular, we can study the involvement of the actin cytoskeleton in the redistribution of auxin throughout the root apices which is closely related to vesicle recycling (Baluska et al., 2003a; Geldner et al., 2003; Muday et al., 2000). Furthermore, the GFP-FABD2 construct is also suitable for visualization of the actin cytoskeleton in other monocot and dicot plant species including *Allium cepa*, *Medicago truncatula*, *Vicia faba* and tobacco BY-2 suspension cells (our unpublished data).

As recently reported by Wang et al. (2004) the BD1/2-GFP construct also based on *A. thaliana* fimbrin 1 is well suited to represent the actin cytoskeleton in great detail in a similar fashion as GFP-FABD2 in cells of the elongation zone, of the root upward to the hypocotyl and to the leaves. However, as far as the lower portions of the root including the transition zone, the apical meristem and the root cap are concerned, BD1/2-GFP and all other variants tested by Wang et al. (2004) have reported mainly a diffuse cytoplasm-based distribution of actin, which is not consistent with our present view of the actin cytoskeleton in these areas of the root, even though some controversy remains (see below). This gap in our capability to observe in vivo the architecture and dynamic of the actin cytoskeleton in the proximal regions of the root organ has now been closed with the availability of the GFP-FABD2 transgenic *A. thaliana* line.

GFP-mTn transgenic lines also have some shortcomings as we report here. This is in agreement with reports from other labs (Ketelaar et al., 2004b; Wang et al., 2004). For instance, GFP-mTn is not useful for studies on the redistributions of F-actin in dividing cells, because meristematic cells at the root apex are either devoid of reporter gene expression or the expressed fusion protein is diffusely distributed in cells of that developmental stage. In contrast, the dividing cells of GFP-FABD2 transformed root apices had a high enough level of expression allowing the in vivo tracking of F-actin redistribution throughout mitosis and cytokinesis in the spatial context of the entire tissue. In accordance with previously published

data on dividing root apex cells obtained using Steedman's wax embedding technique (Baluska et al., 1997b), interphase cells show a meshwork of F-actin arrays encasing the central nucleus and connecting it to the plasma membrane, without any distinct polarity of actin-enriched domains. However, as soon as cells enter mitosis, they disassemble and deplete F-actin in the central part of the cell and accumulate dense F-actin layers under the plasma membrane domains facing the spindle poles, whereas the lateral plasma membrane domains, which in preprophase are occupied by the preprophase band of microtubules are depleted in F-actin (Baluska et al., 1997b, 2000a; see also Fig 1 F-H). This rapid and dramatic redistribution of the actin cytoskeleton suggests that meristematic cells express their inherent polarity along the root axis even though it becomes structurally manifested only in mitotic and cytokinetic cells. During cytokinesis, parent cells maintain the distribution of F-actin-enriched domains (polar cross walls) and depleted domains (lateral walls) as was described for mitosis. In addition, they assemble F-actin also in microtubule-dependent phragmoplasts navigating cell plate vesicles into the mid-line destined to be the future new cell wall between the daughter cells. F-actin localization by GFP-reporters in structures resembling a phragmoplast has previously been reported by Wang et al. (2004).

With the GFP-FABD2 transgenic line we have the ideal opportunity to re-investigate *in vivo* the major developmental switch occurring in the F-actin distribution of cells advancing from the meristem to the elongation zone with the transition zone interpolated in between (Baluska et al., 1997b, 2000a, 2001a,b). A previous immunofluorescence study, using Steedman's wax sectioning, revealed that cells in the transition zone assemble prominent actin bundles which are initiated at the nuclear surface and remain in lateral contact with the centrally positioned nuclei. Subsequently, these actin bundles extend towards the non-growing cross-walls harbouring numerous plasmodesmata and align laterally along their plasma membrane (Baluska et al., 1997b). It has been hypothesized that both the nuclear envelope as well as the plasma membrane domains underneath the cross-walls act as some kind of actin filament organizing centres (AFOCs) which would define the structural polarity of these cells as they are preparing for rapid elongation (Baluska et al., 2000a; Volkmann and Baluska, 1999). Conceivably, there has always been some concern on the reliability of these observations, because the specimens had to be chemically fixed and fixation, being a rather slow process, might allow some aberrant redistributions of actin filaments. Here, it is shown convincingly that living root cells of *A. thaliana* exhibit the same pattern of F-actin distribution and perform the same sequence of restructuring, which had been deduced from the fixed material. I.e., actin filaments start bundling at lateral domains of the nuclear surface

and then progressively protrude out towards the polar cross-walls. This phenomenon is here for the first time documented in living root cells of Arabidopsis. The pharmacological approaches revealed that the arrangement of the actin cytoskeleton plays a crucial role in the onset of rapid cell elongation (Baluska et al., 1997b, 2001b; Volkmann and Baluska, 1999). Genetic approaches confirmed the significant role of the actin cytoskeleton during rapid cell elongation as well (Barrero et al., 2002, 2003; Dong et al., 2001; Gilliland et al., 2002; Nishimura et al., 2003; Ramachandran et al., 2000; Ringli et al., 2002).

The possibility of visualizing F-actin in cells of the transition zone is fundamental also for understanding the potential role of the actin cytoskeleton in gravitropism of the root, because the graviresponse is initiated in this particular zone of the root via differential speed with which cells traverse this developmental stage and begin to elongate (Baluska et al., 1996, 2001a). Here, it is shown that root growth and its graviresponse (see Table III) in GFP-FABD2 transgenic seedlings is very similar to wild type plants. In contrast to GFP-mTn seedlings, which have a slightly decreased hypocotyl growth and a significantly slower gravitropic response. Moreover, etiolated hypocotyls undergo rapid growth in both wild-type and GFP-FABD2 plants. Last but not least, root hairs are well-known to be extremely sensitive to environmental perturbations resulting in the cessation of tip-growth. This sensing of the environment involves the actin cytoskeleton and signalling components such as mitogen-activated protein kinases (Samaj et al., 2002, 2004). Importantly, root hairs of GFP-FABD2 transgenic seedlings show growth rates slightly exceeding those scored for root hairs of wild-type roots (see Table III). Moreover, in contrast to GFP-mTn root hairs showing predominantly diffuse signal at their apices, GFP-FABD2 root hairs reveal dynamic populations of thin, presumably unbundled F-actin dynamically protruding up to the very tips of growing root hairs. Besides dynamic F-actin elements, we scored also motile patches of F-actin moving vigorously within apices of growing tips. Elucidating the role of these structures will require further studies but the current data suggest that they are associated with early endosomes (see Results 3.2 and Discussion 4.2). Jasplakinolide is a potent drug inducing overpolymerization of F-actin (Bubb et al., 2000; Samaj et al., 2002; Sawitzky et al., 1999) and its application to root hairs expressing GFP-FABD2 construct induces rapid transformation of dynamic F-actin elements and patches into large and thick spindle-shaped aggregates. In contrast, Latrunculin B at concentrations of 400 nM results in a complete, but reversible breakdown of the GFP-FABD2-labelled actin cytoskeleton in root hairs as well as in cells of the root body.

By employing the GFP-FABD2 plants, the controversial issue of the state of the actin cytoskeleton in root cap cells can be now re-adressed, especially in the gravisensing statocytes positioned in the middle part of root caps, which have previously been studied by using fluorochrome-conjugated phalloidin (Collings et al., 2001). Filamentous actin structures seen in this study can certainly be taken as an indication for the presence of actin, however, due to the filament-stabilizing properties of phalloidin, the status of the actin cytoskeleton in these cells still remains controversial. Our present data provide in vivo confirmation of the absence of robust F-actin bundles within root cap statocytes which are otherwise assembling in all other postmitotic root cells and reported by GFP-FABD2. Root cap statocytes are equipped with large amyloplasts which sediment towards their physical bottom in a process which is counteracted by residual actomyosin-based forces (Volkmann and Baluska, 1999). Weak actomyosin forces combined with the absence of robust cytoskeletal elements, which would trap and restrain them in the deeper cytoplasm, should allow large and heavy amyloplasts to sediment along the gravity vector (Baluska et al., 1997a; Baluska and Hasenstein; 1997).

4.2. ENDOSOMES AND TIP GROWTH

In this *in vivo* approach, the specific localization of the PI(3)P reporter, GFP-FYVE, to dynamic and motile endosomal compartments is shown. Their identity was confirmed *in vivo* using the endocytic tracer FM4-64 as well as GFP/YFP constructs of the endosome-specific plant Rab GTPases, Ara6 and RabF2a. Furthermore, the motility of these plant endosomes in root hairs of both *M. truncatula* and *A. thaliana* were characterized to be actin dependent. The observations highlight both conserved as well as unique aspects of plant endosomes with regard to mechanisms controlling membrane trafficking and subcellular dynamics. Based on the well documented and highly conserved PI(3)P-binding capacity of the FYVE-domain (Gillooly et al., 2000; Jensen et al., 2001), it can be assumed that plant endosomes identified here are likely enriched with PI(3)P. This is fully in agreement with the situation in yeast and mammalian cells. However, in contrast to animal and fungal endosomes, the motility of which is accomplished along microtubules driven by dyneins and kinesins (Nielsen et al., 1999; Wedlich-Söldner et al., 2000, 2002), the subcellular motility of plant endosomes relies fully upon polymerization and dynamics of actin.

In yeast and animals, endosomal membranes accumulate PI(3)P (Gillooly et al., 2000) due to the specific recruitment of PI(3)K by the endosome-localized Rab GTPases Vps21 and

Rab5 (for review see Zerial and McBride, 2001). It has previously been shown, that in transiently transformed *A. thaliana* protoplasts, overexpression of a FYVE-domain containing fragment of the mammalian EEA1 protein, which is different from the FYVE construct used in the present study, resulted in its targeting to subcellular membranes thought to partially overlap with a prevacuolar-like compartment. This construct consisted of a Rab5 binding motif and a FYVE-domain containing zinc finger motif (Kim et al., 2001; Sohn et al., 2003). Therefore, it was not clear, if the FYVE-domain was sufficient for the subcellular targeting to plant membranes. Unlike the EEA1 carboxy-terminal domain construct (Kim et al., 2001), the here characterized Hrs GFP-FYVE construct consists only of two FYVE domains and does not contain a Rab GTPase binding domain. Therefore, the sole targeting determinant is based on the PI(3)P binding specificity of the double FYVE domains, which localize the reporter construct to plant endosomal compartments. The endosomal identity of these compartments is demonstrated by labelling with GFP-reporters of two plant endosomal Rab GTPases, both being highly similar to mammalian Rab5 and yeast Vps21p. This raises the possibility that the recruitment of PI(3)K and subsequent accumulation of PI(3)P on endosomal membranes is a conserved feature not only in animals and yeast but also in plants.

Spatially controlled, and signal-mediated actin polymerization is crucial for maintaining motilities and shapes of animal cells (Goode et al., 2000). Walled plant cells are non-motile and believed to expand just by the force of turgor pressure. But recent advances in the studies of the two tip growing plant cell types, pollen tubes and root hairs, surprisingly indicated that actin polymerization-driven expansion of the cell periphery might be at the heart of this highly polarized growth of walled plant cells (Baluska et al., 2000b, 2002; Baluska and Volkmann, 2002; Gibbon et al., 1999; Gilliland et al., 2002; Jiang et al., 1997; Ketelaar et al., 2004; Miller et al., 1999; Nishimura et al., 2003; Ringli et al., 2002; Samaj et al., 2002, 2004; Vantard and Blanchoin, 2002; Vidali et al., 2001). In full agreement with this notion, the current results indicate, that actin-dependent tip growth is tightly linked to the actin polymerization-driven movements of plant endosomes.

The present work shows that motile endosomes are present at outgrowing bulges of root hairs. The significance of this finding could be that endosomes participate in the reorganization of the cell´s architecture when trichoblasts accomplish the developmentally unique signal-mediated switch in cell polarity from uniaxial cell expansion to the lateral initiation of tip growth (Baluska et al., 2000b, 2001b; Baluska and Volkmann, 2002; Gibbon et al., 1999; Gilliland et al., 2002; Jiang et al., 1997; Miller et al., 1999; Ringli et al., 2002; Samaj et al., 2002, 2004; Vidali et al., 2001). It is known that the bulging area of a hair-

forming trichoblast organizes a dense actin meshwork via recruitment of actin, profilin, ADF, ROPs (Rho-GTPases of plants), and mitogen-activated protein kinases (Baluska et al., 2000b; Baluska and Volkmann, 2002; Gilliland et al., 2002; Jiang et al., 1997; Jones et al., 2002; Miller et al., 1999; Ringli et al., 2002; Samaj et al., 2002). Motile endosomes might participate in the recruitment of molecular components essential for the local assembly of the actin cytoskeleton, which drives polarized tip growth (Baluska et al., 2000b; Baluska and Volkmann, 2002; Gilliland et al., 2002; Jiang et al., 1997; Miller et al., 1999; Nishimura et al., 2003; Ringli et al., 2002; Samaj et al., 2002, 2004; Vantard and Blanchoin, 2002). This is the case in budding yeast, where the endosomal protein Cdc50p recruits the profilin-binding formin, Bni1p, to sites of polarized growth in budding yeast (Misu et al., 2003).

The close relationship between the endosomal compartment and the dynamics of the actin cytoskeleton in the tip region of the growing root hair is demonstrated by the effects obtained by Brefeldin A treatment. In the BFA-treated root hairs endosomes enlarged and subsequently became rather stationary, while tip growth came to a stop. This is in agreement with previous work, which has shown that fine tip-focussed F-actin meshworks disappear from tips of root hairs, when they stop growing due to their exposure to BFA, whereas some F-actin cables remain preserved in other regions of the root hairs (Samaj et al., 2002). Apparently, any changes to the actin cytoskeleton affect tip growth in root hairs. Recently it was shown that different ACT2 Arabidopsis mutants have defects in root hair tip growth (Gilliland et al., 2002; Nishimura et al., 2003; Ringli et al., 2002), whereas the thick actin cables underlying cytoplasmic streaming are not affected. Another set of recent data revealed that RNAi-mediated depletion of actin interacting protein 1 (AIP1) inhibited growth of root hairs and induced formation of unusually thick actin bundles which protruded up to the very tips of short root hairs showing ‘ballooning’ of their apices (Ketelaar et al., 2004).

The question then remains, whether myosins play a role in actin-based endosome dynamics. The current data indicate that this does not seem to be the case. Myosins most likely are not directly involved in driving motility of endosomes at growing tips, because BDM has no inhibitory effect on endosomal movements in this subcellular domain. Similarly microtubules, which are the favoured long-range motility tracks in mammalian systems (Goode et al., 2000), are not essential for the motility of plant endosomes, because depolymerization of microtubules did not inhibit rapid motility of FYVE/Ara6/RabF2a-based endosomes, as it also does not inhibit tip growth per se (Baluska et al., 2000b; Miller et al., 1999). The only cytoskeletal drug, which almost instantly blocks the motility of endosomes, both at the tip and in the shank, is latrunculin B. Taking these facts together it may be

proposed, that plant endosomes, which are even particularly dynamic within the very tips of root hairs lacking prominent cytoskeletal tracks (Baluska et al., 2000b; Ketelaar et al., 2004; Miller et al., 1999) could be moved by actin-comet-tails. Comet tail movement has originally been discovered in animal cells infected with pathogenic bacteria of the genus Listeria, but later it has been recognized as a more widespread motility phenomenon in animal cells (May et al., 1999). Comet tail movement requires the actin-binding protein complex Arp2/3. It is therefore important to note that the Arabidopsis genome contains genes of the Arp2/3 complex (Deeks and Hussey, 2003; McKinney et al., 2002) and that mutants of the Arp2/3 complex show aberrant root hair phenotypes (Mathur et al., 2003a,b). Furthermore, Arp3-like protein is reported to be enriched at tips of early root hairs as well as in association with multivesicular endosomes (Van Gestel et al., 2003). Fine meshworks of F-actin are affected in cells of Arabidopsis mutants defective in proteins of the Arp2/3 complex (Mathur et al., 2003a,b; Nishimura et al., 2003). It is therefore justified to conclude that actin comet-tail movements of endosomes is a plant cell-specific version of this peculiar motility phenomenon and it may be noted that this corresponds well with the observation that endosomes, phagosomes, and pinosomes in animal cells often use actin polymerization for their motilities (Taunton, 2001).

Besides tip growth and endosome motility, invagination of the plasma membrane during the early endocytosis is well known to be dependent on actin polymerization (Engqvist-Goldstein et al., 2004; Kaksonen et al., 2003). In budding yeast, endocytic vesicles which have pinched off the plasma membrane use dynamic actin comet tails for rapid transport deeper into the cytoplasm, when endocytic complexes serve as nucleation sites for burst-like actin polymerization (Engqvist-Goldstein et al., 2004). These events are known to be abundant especially at sites of polar growth in yeast cells, which in some respects, resembles tip growth of plant cells (Pelham and Chang, 2001; Pruyne and Bretscher, 2000; Smith et al., 2001). Intriguingly, yeast actin patches are propelled by actin polymerization (Carlsson et al., 2002; Pelham and Chang, 2001; Smith et al., 2001). In both plants and yeast, polar expansion occurs in cells that are constrained by robust cell walls. Mechanistically, it would make sense when secretory cargo as well as endocytic traffic are recruited from and delivered into zones of high actin polymerization. Because the delivery of newly synthesized cell wall components via exocytosis would result in localized surplus of membrane material, concomitant active endocytosis would also be predicted within these zones of high actin dynamics. Actin-driven endosomes might even push against the plasma membrane similarly like actin-driven microbial pathogens (Goldberg, 2001) and lysosome-based melanosomes

(Scott et al., 2002) which produces long filopodia facilitating their cell-to-cell spreading. But how can local actin polymerization drive expansion of walled plant cells? This problem could be perhaps solved, if one considers that actin-driven endosomes participate in cell wall turnover (Baluska et al., 2002), and hence contribute to the plasticity of the wall. A similar scenario is attractive also for the fungal endosomes accumulating at sites of polar growth (Walther and Wendland, 2004; Wedlich-Söldner et al., 2000) and cell wall remodelling during cell separation (Wedlich-Söldner et al., 2000, 2002), as well as for yeast actin patches (Pruyne and Bretscher, 2000). Besides explaining actin-driven polarized growth in walled cells, the present data could potentially also shed fresh light on the elusive actin polymerization-driven spots/foci at the actin-based protrusive surfaces of animal and human cells (Kaksonen et al., 2000; Rochlin et al., 1999; Weiner et al., 1999) because these too, were linked with endosomes (Kaksonen et al., 2000). In conclusion, actin-propelled endosomes are inherently linked with polarized growth of root hairs and future studies should reveal if this new link is relevant also to other eukaryotic cells that show polarized growth.

4.3. THE SYNTAXIN SYP121

The syntaxin SYP121, which is already known to have a role in the defence of fungal non-host penetration into plant cells, belongs to the huge family of SNARE proteins. These proteins are believed to specify the intracellular destination of the multitude of endomembrane vesicles and compartments. Complementary SNAREs are localized to different membrane compartments (Uemura et al., 2004) and as they approach each other, interaction can take place by the formation of tri- or tetrameric bundles of coiled helices. This interaction draws donor and acceptor membranes closely together so that they make contact and fuse (Pratelli et al., 2004). Previous studies in plants have shown that SYP121 is involved in the polarised vesicle secretion of protective wall materials at the site pathogen penetration. SYP121 accumulates at the site of papilla formation and has also been observed associated with vesicles and compartments, which accumulate in the vicinity of the forming papillae (Assaad et al., 2004). In Arabidopsis, SYP121 is required for penetration resistance to the non-host fungus Blumeria graminis. Similarly in barley, which is the host of B. graminis, the SYP121 orthologue ROR2 is required for penetration resistance (Collins et al., 2003). An and coworkers (An et al., 2006a) suggested that if ROR2 mediates vesicle secretion at the plasma membrane (PM), then less membrane material will be delivered to the PM in ror2 mutants.

The PM requires both secretion and endocytosis to maintain membrane homeostasis and, as a result, endocytosis would be reduced in cells of the ror2 mutant. Alternatively, if SYP121/ROR2 regulates membrane trafficking between the PM and endosomal compartments, then these syntaxin mutants would also have reduced formation of endosomes. Available evidence suggests that the group of SYP1 syntaxins (SYP111/112, SYP121-125 and SYP131/132) may regulate the transport between the plasma membrane and endosomes. This is based on the observation that GFP-SYP111 co-localizes with the dye FM4-64, which is internalized following an endocytic pathway (Uemura et al., 2004).

The localization of a SYP121 is described to be at the PM in Arabidopsis protoplasts (Uemura et al., 2004), at the PM in intact cells and in vesicles (Collins et al., 2003) and in cellular compartments (possibly endosomes) induced upon fungal infection (Assad et al., 2004). Uemura and coworkers (Uemura et al., 2004) reported expression profiles for all the 54 plant syntaxins, including SYP121. These RT-PCR based experiments showed a weak expression of SYP121 in flowers, leaves and stems and a strong expression in roots. This is where the current study sets in. Because of the strong expression that has been observed in the root tissue, the already existing stable expressing 35S-GFP-SYP121 Arabidopsis line (a generous gift of Hans Thordal-Christensen, The Royal Veterinary and Agricultural University, Denmark) was used for the experiments. Special focus was given to the root epidermal cells and the tip-growing root hairs. The GFP tagged protein was found at the PM, in intracellular vesicular structures and in forming cell plates of dividing cells in the meristem, similar to the Knolle protein, which is a syntaxin member known as SYP111 (Lauber et al., 1997). Upon BFA treatment, endosomes and TGN elements aggregate and form BFA-compartments that show typically a perinuclear localization (Samaj et al., 2004; Geldner, 2004; Grebe et al., 2003; Geldner at al., 2003). This suggests that BFA blocks the secretory pathways, but not the first steps in endocytosis (Samaj et al., 2005). The finding here, that GFP-SYP121 shifts from the population of small vesicles seen in untreated cells into the large BFA-compartments after application of the drug is a clear evidence that this syntaxin is continually recycled from the plasma membrane into the endosomal compartment. The same situation is seen in tip growing root hairs. In untreated cells, SYP121 is present in a highly motile, apical vesicle population, from where it disappears and shifts into large non-motile membrane aggregates after BFA treatment. This is exactly the same behaviour seen with the double FYVE-reporter construct (see chapter 3.2) and it is therefore not surprising that FM4-64 partially co-localizes with the SYP121 vesicles and that experimental actin depolymerisation by Cytochalasin D destroys the tip high gradient of SYP121 vesicles/endosomes. The conclusion from these data can only be

that SYP121 is a plasma membrane component becoming recycled through the endosomal recycling machinery. This explains the role of SYP121 in the host resistance against fungal penetration. Papilla formation requires a sharp increase in localized secretion and this in turn increases compensatory endocytosis so that a short circuit builds up between the area of the plasma membrane around the papilla and the surrounding cortical population of endosomes. By this way a high density of molecular components required for targeted secretion could be maintained at the infection site. It is even possible, that endosomes are removed from other, nonaffected areas of the cell where they had been engaged in recycling of wall precursor material and become redirected towards the infection site, delivering not only the components of the secretory machinery but also their wall precursor material. Such a more direct contribution of endosomes to secretion has benn demonstrated for the process of cytokinetic cell plate formation, guard cell dynamics and tip-growing cells (Dhonukshe et al. 2006, Ovecka et al., 2005, Sutter et al., 2007). The classic view is, that secretion solely relies on a Golgi-based synthesis and delivery of secretory vesicles from the TGN. However, the data of this thesis and the examples discussed here rather suggest that endosomal recycling is a component part of secretion in cases, where a rapid, localized response requires a supply of wall precursor material faster than new synthesis can provide (Samaj et al., 2005, Baluska et al., 2005; Dhonukshe et al. 2007).

4.4. *A. THALIANA* SYNAPTOTAGMINS

From recent molecular neurobiology data it is evident, that there are many different possibilities for synaptotagmin functions in animals. The protein domain substructure of synaptotagmins suggests, that all of them are closely related to one another and that their major function settles in the area of endomembrane transport, fusion and the maintenance of structural integrity of membranes (Chapman, 2002; Poskanzer et al., 2003; Tang et al., 2006). I.e., it has been shown that syt1 closely interacts with the SNARE complex to trigger the synchronous neurotransmitter release upon arrival of a Ca^{2+} signal (Koh and Bellen, 2003). On the other hand, the animal synaptotagmin 7 (syt7) apparently participates in the resealing of disrupted plasma membranes by a mechanism, which closely resembles the neuronal Ca^{2+}-regulated exocytosis (Andrews, 2005). Requirements for molecular machineries to fulfil such basic function should be present in all eukaryotic organisms including plants, i.e., plant cells must have mechanisms for the maintenance and repair of the plasma membrane. However,

until recently, candidate genes or proteins have not been identified, which could take part in these processes. In a recent genomic survey (Craxton, 2004) synaptotagmin-like genes have been identified in Arabidopsis and this marks the beginning of synaptotagmin research in plants. In collaboration with the laboratory of Miguel Botella (Department of Molecular Biology and Biochemistry, University of Málaga, Spain), some biochemical key features of synaptotagmin A have been studied. From this work we know, that the binding capacities of plant synaptotagmins for Ca^{2+} and phospholipids is quite similar to the animal counterparts (Schapire and Voigt et al. 2007, submitted).

In the current thesis work, which is the first comprehensive description of the synaptotagmin gene family in plants, the focus lies on the characterization of the expression pattern of the synaptotagmin gene family, their cellular localization and the possible function of sytA. In the genome of Arabidopsis there are six members of synaptotagmin-like genes. They possess all a very similar domain structure consisting of an N-terminal transmembrane domain, followed by a linker of different length. Behind this linker two C2 domains are tandemly arranged, C2A and C2B, with the exception of SytF, which has the lowest degree of sequence similarity, where three C2 domains are placed one after the other. These C2 domains enable the protein to link to phospholipids and bind Ca^{2+} ions in a defined manner. SytF is also different in some other aspects from the rest of the family. Domain prediction software labels the N-terminus as a signal peptide rather than a transmembrane region and at the C-terminal end a possible coiled-coil region is located. Whereas the members SytA to SytE are all built of 535-574 amino acids, SytF is more than 250 amino acids longer. These differences of SytF result probably in a different function, whereas the structure of the other Syts suggests a higher degree of redundancy. SytA and SytB are closest to each other, but are expressed in different tissues. Whereas SytA is expressed in almost every vegetative cell, SytB is highly expressed in pollen and to a minimal degree in root cap cells. The phenomenon, that pollen specific genes are slightly expressed in root cap cells is not uncommon (personal communication). The expression pattern of SytC is unique, as it is located only in stomata of the green parts of the plant body, whereas in roots the expression of SytC is seen in the lateral root initials and in the older parts of the root it is also present in all cells of the vascular tissue. This makes the SytC an interesting candidate for stomata regulation and the regulation of lateral root formation. Guard cells change their volume during opening and closing of the stoma, and with it, the size of the PM surface area undergoes cyclical changes. Consequently, enlargement of surface area by exocytosis and decrease of surface area by endocytosis as well as very active vesicle trafficking in the guard cell cytoplasm must accompany the cycles of

stomata opening and closure (Meckel et al., 2005; Sutter et al., 2007). The expression pattern of SytC in the root highly resembles the auxin distribution before and during lateral root outgrowth, which could implicate a role for SytC in auxin vesicle traffic (Dubrovsky et al., 2006).

SytD is expressed in the vascular tissue throughout the seedling and the most different isoform SytF appears to be expressed only in the apical meristem of the root. The method of investigating the expression pattern of genes with promoter:GUS fusion constructs is widely used, but also not completely unfailing (Sieburth and Meyerowitz, 1997). If possible, the promoter region included a 2 kb nucleotide piece upstream of the start codon, however, it is impossible to know, whether there are other regulatory elements located further upstream or even elsewhere. In comparison with the data obtained from the publicly available RNA microarray database (Zimmermann et al., 2004), the promoter:GUS expression pattern for SytA, SytB and SytC is fitting well with the data presented here. Whereas the rest of the expression data is at variance with our data. According to the microarray data, SytD is almost exclusively expressed in suspension culture cells, SytE is expressed everywhere and SytF is highly expressed in leaves. But, microarray data should be interpreted with care, because they represent a combination of experiments from different laboratories. It can only be speculated why in our hands the SytE promoter:GUS fusion showed no expression at all. Either the promoter is not located in the 2 kb genomic DNA segment upstream of the translational start codon as denoted above or there are other negative regulatory elements which prevent translation.

Because the SytA protein is expressed in virtually all cells and tissues, it was picked as the best suited candidate for the study of its intracellular localization. The coding region was cloned behind the CaMV 35S promoter and stably introduced into the Arabidopsis genome. Even if the expression levels of the fusion protein was very low in all examined independent lines, with confocal microscopy it was possible to visualize its localization. The low expression levels may be a reaction of the organism to counterbalance artificial expression of the fusion protein with the expression of the endogenous SytA gene. However, expression was sufficiently high for analysis and showed that the localization varied from the root to the leaves. In roots the fusion protein was mostly found at the PM of cross walls and to a slighter degree in a diffuse pattern in the cell lumen. Stronger expression was observed in the root cap and in root epidermis cells. Only in older root epidermal cells, the diffuse pattern inside the cell was reminiscent of an ER-specific staining. In contrast to this, in the leaves the protein was observable in a punctate structure at the PM, both in the top view as well as in optical

sections through the middle of the cell. The pattern seen in single optical sections through the middle of the cell resembles closely plasmodesmata structures as seen with specific plasmodesmata-reporter constructs (Oparka et al., 1997). A strong labelling signal was observed at the walls between two guard cells which build the stomata. The punctate structures could be connections to non-motile points of the ER, which could resemble physical connections of the ER reaching out through the PM into the cell wall space. Such domains of the ER in plant cells have been known for a long time (Knebel et al. 1990). The ER labelling pattern is not so different between the root and the leaves. In the root, especially in the root tip, the cells are quite tightly connected to each other, especially at their polar cross walls, indicating a more efficient communication within the longitudinal cell files rather than between them in radial direction (Baluska et al., 2003b). This, together with the smaller size of the cells, could have the consequence that punctuate structures become very dense and may optically appear as solid line. It is therefore very likely that this labelling pattern represents a dense packing of plasmodesmata. The ER-like labelling in older epidermis cells is explainable due to the fact that the protein may locally accumulate at “busy”-spots where synthesis occurs, but this needs further clarification in the future.

However, because of the overall low expression level in the Arabidopsis seedlings, inhibitor and co-localization experiments were not easy to perform. For these kinds of experiments, another method of fusion protein expression appeared to be more favourable, such as Agrobacterium driven transient leave transformation in tobacco plants, which is an often used method to express fusion proteins and locate them in living tissue. Expression of the SytA-GFP construct in epidermis cells of *N. tabacum* resulted in a similar pattern as in the stable transgenic lines of Arabidopsis. In cells with low, middle and high expression levels, the same punctate structures at the ER/PM/cell wall junctions were labelled. The difference between the different expression levels was that the more fusion protein was inside the cells the more was located in the ER and thereby the the punctate pattern became obscured. This and the fact that the punctate structures were essentially non-motile, prompted the idea that they constitute junctions between the ER, PM and the cell wall. These structures appeared as well in single optical sections through the middle plane of neighbouring cells, resembling plasmodesmata.

The results obtained with the other fusion construct containing only the C2AB domain of SytA, lacking the N-terminal transmembrane domain were much different from those of the complete SytA sequence. This construct localized diffusely to the cytoplasm including the nucleus. This clearly indicates the importance of the N-terminus, including the

transmembrane domain, for targeting of the protein to its proper intracellular compartment. It is obvious that SytA has to be inserted to the membrane of the correct compartment in order to be able to function properly. Staining with plasma membrane dye FM4-64 and plasmolysis also indicated that the SytA-GFP fusion protein is located in or at the PM, in the retracting protoplast as well as in Hechtian strands and in spots attached to the wall. Furthermore, the fusion protein was able to react to changes of the intracellular Ca^{2+} concentration. With the Calcium ionophore A23187, which enables Ca^{2+} to cross membranes, it is possible to in- or decrease the intracellular Ca^{2+} level depending on the Ca^{2+} concentration in the medium. After strong increase of the Calcium concentration inside the cell (in cytoplasm normally 100-200 nM Ca^{2+}), the fusion protein lost its specific association with the punctate structure at the ER/PM/cell wall junctions and aggregated in huge amounts throughout the entire ER compartment. In contrast to this, a decrease of the internal Ca^{2+} level resulted in an almost unchanged distribution of the fusion protein as compared with the control. This could indicate, that the protein gets “activated” by calcium and relocates from its punctate structures.

The SytA T-DNA line deposited in the SAIL collection (SAIL_775_A08) was isolated by our collaboration partner, the group of Miguel Botella and analyzed here in further detail. The T-DNA is located in the tenth exon and no transcripts could be detected by RT-PCR, and likewise, SytA protein was not detected in western blots of protein samples from the mutant plants. The line was in so far characterized, that it showed a hypersensitivity to high NaCl concentrations at low concentration of external Ca^{2+} in the growth medium. Whereas the WT seedlings can tolerate the salt stress, the mutant seedlings cannot, they react by a complete stop of growth. The lowest concentration of NaCl at which a difference was observed between control and salt treatment was 50 mM NaCl for 24 hours. At that concentration the overall root growth was not affected, but root hairs showed already defects, i.e., tip growth stopped, balloning of the tips occurred or the hair cells even ruptured and died.

This behaviour may be taken as an indication that mutant seedlings cannot compensate salt stress because surface changes at the plasma membrane that go along with osmotic volume changes cannot be executed in the absence of SytA. With increasing salt concentration the effects spread also to the elongating cells of the root, as there is a complete growth stop detectable after applying salt concentrations higher than 100 mM NaCl in the mutant. To further investigate this, four day old seedlings were exposed to a high concentration of salt (200 mM) for a short time, a salt shock. Subsequent staining for live and dead cells showed where the loss of SytA caused cell rupture. Dead cells did not show FDA fluorescence, whereas FM4-64 could enter the ruptured cell, bound to internal membranes and

caused a strong fluorescence signal. The situation after salt stress was as expected. The WT seedlings tolerated the salt in so far, as most of the cells were living after salt stress treatment. On the contrary, the mSytA seedlings had just living cells in the root cap, meristem and transition zone. Probably these zones were guarded by the root cap cells and their formed mucilage. The normally elongating cells could not bear the salt stress and got plasma membrane defects right away, which result in an immediate stop of growth. This point was further strengthend by longer incubation times at lower salt concentrations and also low calcium concentrations. Cells of mSytA seedlings colapsed at lower salt concentrations than WT seedlings and showed overall a stronger reaction to increasing salt concentration. SytA seems to be essential for the answer to the abiotic stress of salt treatment and it can be concluded that it serves in plasma membrane maintaining processes.

Taken together, the Arabidopsis synaptotagmins share a common domain arrangement with their animal counterparts and build a small gene family with their characteristic tandem C2 domains. The different members of this gene family show a differential expression pattern with only small overlap, only SytA is expressed throughout the entire organism in all developmental stages. This expression pattern indicates, that with the exception of SytA, there is probably not a high degree of functional redundancy among family members, however, this needs to be addressed in further mutant studies. For SytA the localization and mutant analysis leads to the hypothesis that the protein is part of the membrane repair process after abiotic stress. The fact, that the mutant seedlings are growing quite well under normal laboratory conditions and only show a phenotype unter salt stress conditions suggests, that SytA does not have a major function in regular membrane maintenance in the unstressed state. Since volume changes occur regularly during normal development, maintenance of the plasma membrane may be regulated in an organ-specific way by the other differentially expressed isoforms of the synaptotagmin family.

5. SUMMARY

In plants, membrane recycling processes are involved in every instance of cell volume changes which occur during growth, development and adaptation to the environment. The thesis work described here addresses membrane recycling on three different levels. (i) The level of the actin cytoskeleton as the major cytoskeletal structure, which supports vesicle trafficking in plant cells. (ii) The level of endosomal dynamics as the major membrane compartment that is involved in membrane recycling at the plasma membrane and (iii) at the level of macromolecular components, which are involved in vesicle fusion.

1) The actin cytoskeleton: After introduction of the GFP-fusion technology, the actin cytoskeleton in plants has initially been studied using a construct containing a mouse talin sequence as reporter. This construct was useful to some extend, but more often failed to give a correct representation of the actin cytoskeleton in plant cells. Here, another construct, GFP-FABD2, has been designed on the basis of the plant fimbrin 1 sequence, which proved to be more reliable, and it is particularly useful as a faithful reporter of the actin cytoskeleton in transgenic *A. thaliana* lines. With this new fluorescent reporter, the structure and dynamic of the actin cytoskeleton is studied in greater detail in correlation with the motile behaviour of endosomal compartments.

2) Endosomal dynamics: A second new GFP-reporter was constructed by using two tandemly linked PI(3)P binding domains (double-FYVE) from a mouse endosomal protein. Since endosomal membranes contain PI(3)P in yeast, animals and plants, the strategy was to identify endosomes by the binding affinity of the FYVE domains to PI(3)P. It turned out that this strategy works well and through co-localization with endosomal markers and other fluorescent dyes and by pharmacological perturbation, the endosomal nature of the labelled membrane compartment is confirmed. The generation of stabe transgenic *A. thaliana* lines allows the detailed analysis of the PI(3)P containing endosomes throughout root tissues. It is further shown, that in tip-growing root hair cells, the GFP-FYVE labelled endosomes accumulate at the growing tip and their movement is based on actin polymerization (rocket tail mechanism) rather than actomyosin interaction (motor-based mechanism).

3) SYP121 as a component of the targeting/fusion machinery: SYP121 has previously been identified by others as a member of the syntaxin family in *A. thaliana*. Here, the distribution of this protein and its behaviour at membrane recycling sites is studied. On the basis of the SYP121 gene sequence, a GFP-reporter was constructed. By co-localization with

endosomal markers it is shown, that SYP121 is present on the endosomal compartment and pharmacological treatments reveal, that it behaves in the same way as the double FYVE-reporter. SYP121 is present at the tip of the growing root hairs and associates with the growing cell plate during cytokinesis. This correlation is lost, when the actin cytoskeleton is depolymerized or when membrane recycling is blocked. Since it has been shown by others, that SYP121 is also present at the site of papilla formation in the course of fungal infection, it is suggested that this member of the t-SNARE family is of importance for a variety of vesicle fusion events, i.e., tip growth, cell plate expansion and papilla formation, and it can also be concluded that plant endosomes are involved in t-SNARE recycling in each of these cases.

4) Synaptotagmin A as a component of the targeting/fusion machinery: synaptotagmins comprise a large family of proteins, originally discovered in neuronal synapses, but afterwards found in many other types of animal tissues. Biochemically they are Ca-dependent, PIP-binding membrane proteins involved in the fusion process during exocytosis. Surprisingly, six closely related proteins exist in plants, termed Synaptotagmin-like proteins which, until now, have remained uncharacterized. Here, the expression pattern of the six members of the *A. thaliana* synaptotagmin gene family are investigated by promoter-GUS fusions, and the localization of their most abundant member, SytA, is studied in detail. Whereas SytA is expressed in almost all cells throughout the plant, the other gene family members show a restricted expression to certain organs or cell types. SytB is found in pollen, SytC in stomata and lateral root initials, SytD in vascular tissue and SytF at low levels in the root meristem and root cap cells. A SytA-GFP gene fusion was constructed and transformed stably into *A. thaliana* as well as transiently into tobacco leaves. SytA-GFP was localized at the plasma membrane in Arabidopsis root cells and in distinct spots at ER/PM junctions. Experimentally raising the Ca^{2+} concentration within the cells results in relocation of the protein to large, spread out aggregates, whereas lowering of the Ca^{2+} concentration had no effect. This demonstrates that SytA-binding to the target membrane is Ca-dependent. The SytA T-DNA mutant line shows a phenotype, dependent on high salt concentrations or moderate salt concentrations together with low Ca-concentrations. Under these circumstances root hairs form ballooning ends, many of them rupture, and the roots stop growing. Many cells in the meristem, transition zone and of the rhizodermis throughout the root die in comparison to wild type roots with increasing salt concentrations. These data suggest that SytA is mainly involved in cell volume regulation in response to salt stress by mediating Ca-dependent vesicle fusion with the plasma membrane, whereas the other members are likely to be involved in development-specific regulation of cell volume changes.

REFERENCES

An, Q., Huckelhoven, R., Kogel, K.H., and van Bel, A.J. (2006). Multivesicular bodies participate in a cell wall-associated defence response in barley leaves attacked by the pathogenic powdery mildew fungus. Cell Microbiol **8,** 1009-1019.

Andrews, N.W. (2005). Membrane resealing: synaptotagmin VII keeps running the show. Sci STKE **2005,** pe19.

Arac, D., Chen, X., Khant, H.A., Ubach, J., Ludtke, S.J., Kikkawa, M., Johnson, A.E., Chiu, W., Sudhof, T.C., and Rizo, J. (2006). Close membrane-membrane proximity induced by Ca(2+)-dependent multivalent binding of synaptotagmin-1 to phospholipids. Nat Struct Mol Biol **13,** 209-217.

Assaad, F.F., Qiu, J.L., Youngs, H., Ehrhardt, D., Zimmerli, L., Kalde, M., Wanner, G., Peck, S.C., Edwards, H., Ramonell, K., Somerville, C.R., and Thordal-Christensen, H. (2004). The PEN1 syntaxin defines a novel cellular compartment upon fungal attack and is required for the timely assembly of papillae. Mol Biol Cell **15,** 5118-5129.

Baluska, F., Volkmann, D., and Barlow, P. (1996). Specialized zones of development in roots: view from the cellular level. Plant Physiol **112,** 3-4.

Baluska, F., and Hasenstein, K. (1997). Root cytoskeleton: its role in perception of and response to gravity. Planta **203,** S69-78.

Baluska, F., Kreibaum, A., Vitha, S., Parker, J.S., Barlow, P.W., and Sievers, A. (1997a). Central root cap cells are depleted of endoplasmic microtubules and actin microfilament bundles: implications for their role as gravity-sensing statocytes. Protoplasma **196,** 212-223.

Baluska, F., Vitha, S., Barlow, P., and Volkmann, D. (1997b). Rearrangements of F-actin arrays in growing cells of intact maize root apex tissues: a major developmental switch occurs in the postmitotic transition region. Eur J Cell Biol **72,** 113-121.

Baluska, F., Barlow, P., and Volkmann, D. (2000a). Actin and myosin VIII in developing root cells. In Actin: a Dynamic Framework for Multiple Plant Cell Functions, C.J. Staiger, F. Baluska, D. Volkmann, and P. Barlow, eds (Dordrecht, The Netherlands: Kluwer Academic Publishers), pp. 457-476.

Baluska, F., Salaj, J., Mathur, J., Braun, M., Jasper, F., Samaj, J., Chua, N.-H., Barlow, P.W., and Volkmann, D. (2000b). Root Hair Formation: F-Actin-Dependent Tip

Growth Is Initiated by Local Assembly of Profilin-Supported F-Actin Meshworks Accumulated within Expansin-Enriched Bulges. Developmental Biology **227,** 618-632.

Baluska, F., Busti, E., Dolfini, S., Gavazzi, G., and Volkmann, D. (2001a). *Lilliputian* Mutant of Maize Lacks Cell Elongation and Shows Defects in Organization of Actin Cytoskeleton. Developmental Biology **236,** 478-491.

Baluska, F., Jasik, J., Edelmann, H.G., Salajova, T., and Volkmann, D. (2001b). Latrunculin B-Induced Plant Dwarfism: Plant Cell Elongation Is F-Actin-Dependent. Developmental Biology **231,** 113-124.

Baluska, F., and Volkmann, D. (2002). Pictures in cell biology. Actin-driven polar growth of plant cells. Trends Cell Biol **12,** 14.

Baluska, F., Hlavacka, A., Samaj, J., Palme, K., Robinson, D.G., Matoh, T., McCurdy, D.W., Menzel, D., and Volkmann, D. (2002). F-Actin-Dependent Endocytosis of Cell Wall Pectins in Meristematic Root Cells. Insights from Brefeldin A-Induced Compartments. Plant Physiol. **130,** 422-431.

Baluska, F., Samaj, J., and Menzel, D. (2003a). Polar transport of auxin: carrier-mediated flux across the plasma membrane or neurotransmitter-like secretion? Trends Cell Biol **13,** 282-285.

Baluska, F., Wojtaszek, P., Volkmann, D., and Barlow, P. (2003b). The architecture of polarized cell growth: The unique status of elongating plant cells. Bioessays **25,** 569-576.

Baluska, F., Liners, F., Hlavacka, A., Schlicht, M., Van Cutsem, P., McCurdy, D.W., and Menzel, D. (2005). Cell wall pectins and xyloglucans are internalized into dividing root cells and accumulate within cell plates during cytokinesis. Protoplasma **225,** 141-155.

Barrero, R.A., Umeda, M., Yamamura, S., and Uchimiya, H. (2002). Arabidopsis CAP Regulates the Actin Cytoskeleton Necessary for Plant Cell Elongation and Division. The Plant Cell **14,** 149-163.

Barrero, R.A., Umeda, M., Yamamura, S., and Uchimiya, H. (2003). Over-expression of Arabidopsis CAP causes decreased cell expansion leading to organ size reduction in transgenic tobacco plants. Ann Bot (Lond) **91,** 599-603.

Batoko, H., Zheng, H.Q., Hawes, C., and Moore, I. (2000). A rab1 GTPase is required for transport between the endoplasmic reticulum and golgi apparatus and for normal golgi movement in plants. Plant Cell **12,** 2201-2218.

Bevis, B.J., and Glick, B.S. (2002). Rapidly maturing variants of the Discosoma red fluorescent protein (DsRed). Nat Biotechnol **20,** 83-87.

Bock, J.B., Matern, H.T., Peden, A.A., and Scheller, R.H. (2001). A genomic perspective on membrane compartment organization. Nature **409,** 839-841.

Boisson-Dernier, A., Chabaud, M., Garcia, F., Becard, G., Rosenberg, C., and Barker, D.G. (2001). Agrobacterium rhizogenes-transformed roots of Medicago truncatula for the study of nitrogen-fixing and endomycorrhizal symbiotic associations. Mol Plant Microbe Interact **14,** 695-700.

Bubb, M.R., Spector, I., Beyer, B.B., and Fosen, K.M. (2000). Effects of jasplakinolide on the kinetics of actin polymerization. An explanation for certain in vivo observations. J Biol Chem **275,** 5163-5170.

Cangelosi, G.A., Best, E.A., Martinetti, G., and Nester, E.W. (1991). Genetic Analysis of *Agrobacterium*. Methods in Enzymology **204,** 384-397.

Carlsson, A.E., Shah, A.D., Elking, D., Karpova, T.S., and Cooper, J.A. (2002). Quantitative analysis of actin patch movement in yeast. Biophys. J. **82,** 2333-2343.

Chapman, E.R. (2002). Synaptotagmin: a Ca(2+) sensor that triggers exocytosis? Nat Rev Mol Cell Biol **3,** 498-508.

Clough, S.J., and Bent, A.F. (1998). Floral dip: a simplified method for *Agrobacterium*-mediated transformation of *Arabidopsis thaliana*. The Plant Journal **16,** 735-743.

Collings, D.A., Zsuppan, G., Allen, N.S., and Blancaflor, E.B. (2001). Demonstration of prominent actin filaments in the root columella. Planta **212,** 392-403.

Collins, N.C., Thordal-Christensen, H., Lipka, V., Bau, S., Kombrink, E., Qiu, J.L., Huckelhoven, R., Stein, M., Freialdenhoven, A., Somerville, S.C., and Schulze-Lefert, P. (2003). SNARE-protein-mediated disease resistance at the plant cell wall. Nature **425,** 973-977.

Cosgrove, D.J. (1999). Enzymes and other agents that enhance cell wall extensibility. Annu Rev Plant Physiol Plant Mol Biol **50**, 391-417.

Craxton, M. (2004). Synaptotagmin gene content of the sequenced genomes. BMC Genomics **5,** 43.

Dhonukshe, P., Baluska, F., Schlicht, M., Hlavacka, A., Samaj, J., Friml, J., and Gadella, T.W. (2006). Endocytosis of cell surface material mediates cell plate formation during plant cytokinesis. Dev Cell **10,** 137-150.

Dhonukshe, P., Samaj, J., Baluska, F., and Friml, J. (2007). A unifying new model of cytokinesis for the dividing plant and animal cells. Bioessays **29,** 371-381.

Dhugga, K.S. (2005). Plant Golgi cell wall synthesis: from genes to enzyme activities. Proc Natl Acad Sci U S A **102,** 1815-1816.

Dong, C.-H., Xia, G.-X., Hong, Y., Ramachandran, S., Kost, B., and Chua, N.-H. (2001). ADF Proteins Are Involved in the Control of Flowering and Regulate F-Actin Organization, Cell Expansion, and Organ Growth in Arabidopsis. The Plant Cell **13,** 1333-1346.

Dubrovsky, J.G., Gambetta, G.A., Hernandez-Barrera, A., Shishkova, S., and Gonzalez, I. (2006). Lateral root initiation in Arabidopsis: developmental window, spatial patterning, density and predictability. Ann Bot (Lond) **97,** 903-915.

El-Din El-Assal, S., Le, J., Basu, D., Mallery, E.L., and Szymanski, D.B. (2004). DISTORTED2 encodes an ARPC2 subunit of the putative Arabidopsis ARP2/3 complex. Plant J **38,** 526-538.

Engqvist-Goldstein, A.E., Zhang, C.X., Carreno, S., Barroso, C., Heuser, J.E., and Drubin, D.G. (2004). RNAi-mediated Hip1R silencing results in stable association between the endocytic machinery and the actin assembly machinery. Mol Biol Cell **15,** 1666-1679.

Friml, J., Benkova, E., Blilou, I., Wisniewska, J., Hamann, T., Ljung, K., Woody, S., Sandberg, G., Scheres, B., Jurgens, G., and Palme, K. (2002). AtPIN4 mediates sink-driven auxin gradients and root patterning in Arabidopsis. Cell **108,** 661-673.

Friml, J., Wisniewska, J., Benkova, E., Mendgen, K., and Palme, K. (2002). Lateral relocation of auxin efflux regulator PIN3 mediates tropism in Arabidopsis. Nature **415,** 806-809.

Geelen, D., Leyman, B., Batoko, H., Di Sansebastiano, G.P., Moore, I., and Blatt, M.R. (2002). The abscisic acid-related SNARE homolog NtSyr1 contributes to secretion and growth: evidence from competition with its cytosolic domain. Plant Cell **14,** 387-406.

Geldner, N. (2004). The plant endosomal system--its structure and role in signal transduction and plant development. Planta **219,** 547-560. Epub 2004 Jun 2022.

Geldner, N., Friml, J., Stierhof, Y.D., Jurgens, G., and Palme, K. (2001). Auxin transport inhibitors block PIN1 cycling and vesicle trafficking. Nature **413,** 425-428.

Geldner, N., Anders, N., Wolters, H., Keicher, J., Kornberger, W., Muller, P., Delbarre, A., Ueda, T., Nakano, A., and Jurgens, G. (2003). The Arabidopsis GNOM ARF-GEF Mediates Endosomal Recycling, Auxin Transport, and Auxin-Dependent Plant Growth. Cell **112,** 219-230.

Gibbon, B.C., Kovar, D.R., and Staiger, C.J. (1999). Latrunculin B Has Different Effects on Pollen Germination and Tube Growth. The Plant Cell **11,** 2349-2363.

Gilliland, L.U., Kandasamy, M.K., Pawloski, L.C., and Meagher, R.B. (2002). Both Vegetative and Reproductive Actin Isovariants Complement the Stunted Root Hair Phenotype of the Arabidopsis act2-1 Mutation. Plant Physiol **130,** 2199-2209.

Gillooly, D.J., Morrow, I.C., Lindsay, M., Gould, R., Bryant, N.J., Gaullier, J.M., Parton, R.G., and Stenmark, H. (2000). Localization of phosphatidylinositol 3-phosphate in yeast and mammalian cells. Embo J **19,** 4577-4588.

Goldberg, M.B. (2001). Actin-based motility of intracellular microbial pathogens. Microbiol Mol Biol Rev **65,** 595-626.

Goode, B.L., Drubin, D.G., and Barnes, G. (2000). Functional cooperation between the microtubule and actin cytoskeletons. Current Opinion in Cell Biology **12,** 63-71.

Grebe, M., Xu, J., Mobius, W., Ueda, T., Nakano, A., Geuze, H.J., Rook, M.B., and Scheres, B. (2003). Arabidopsis sterol endocytosis involves actin-mediated trafficking via ARA6-positive early endosomes. Curr Biol **13,** 1378-1387.

Grebe, M., Friml, J., Swarup, R., Ljung, K., Sandberg, G., Terlou, M., Palme, K., Bennett, M.J., and Scheres, B. (2002). Cell polarity signaling in Arabidopsis involves a BFA-sensitive auxin influx pathway. Curr Biol **12,** 329-334.

Gruenberg, J. (2001). The endocytic pathway: a mosaic of domains. Nat Rev Mol Cell Biol **2,** 721-730.

Gunse, B., Garzon, T., and Barcelo, J. (2003). Study of aluminum toxicity by means of vital staining profiles in four cultivars of Phaseolus vulgaris L. J Plant Physiol **160,** 1447-1450.

Haas, T.J., Sliwinski, M.K., Martinez, D.E., Preuss, M., Ebine, K., Ueda, T., Nielsen, E., Odorizzi, G., and Otegui, M.S. (2007). The Arabidopsis AAA ATPase SKD1 is involved in multivesicular endosome function and interacts with its positive regulator LYST-INTERACTING PROTEIN5. Plant Cell **19,** 1295-1312.

Hamilton, D.A., Roy, M., Rueda, J., Sindhu, R.K., Sanford, J., and Mascarenhas, J.P. (1992). Dissection of a pollen-specific promoter from maize by transient transformation assays. Plant Mol Biol **18,** 211-218.

Haseloff, J., Siemering, K.R., Prasher, D.C., and Hodge, S. (1997). Removal of a cryptic intron and subcellular localization of green fluorescent protein are required to mark transgenic *Arabidopsis* plants brightly. Proceedings of the National Academy of Sciences USA **94,** 2122-2127.

Hepler, P.K., Vidali, L., and Cheung, A.Y. (2001). Polarized Cell Growth in Higher Plants. Annual Review of Cell and Developmental Biology **17,** 159-187.

Hui, E., Bai, J., and Chapman, E.R. (2006). Ca2+-triggered simultaneous membrane penetration of the tandem C2-domains of synaptotagmin I. Biophys J **91,** 1767-1777.

Iezzi, M., Kouri, G., Fukuda, M., and Wollheim, C.B. (2004). Synaptotagmin V and IX isoforms control Ca2+ -dependent insulin exocytosis. J Cell Sci **117,** 3119-3127.

Jahn, R., and Scheller, R.H. (2006). SNAREs - engines for membrane fusion. Nat Rev Mol Cell Biol **7,** 631-643.

Jahn, R., Lang, T., and Sudhof, T.C. (2003). Membrane fusion. Cell **112,** 519-533.

Jedd, G., and Chua, N.H. (2002). Visualization of peroxisomes in living plant cells reveals acto-myosin-dependent cytoplasmic streaming and peroxisome budding. Plant and Cell Physiology **43,** 384-392.

Jensen, R.B., La Cour, T., Albrethsen, J., Nielsen, M., and Skriver, K. (2001). FYVE zinc-finger proteins in the plant model Arabidopsis thaliana: identification of PtdIns3P-binding residues by comparison of classic and variant FYVE domains. Biochem J **359,** 165-173.

Jiang, C.J., Weeds, A.G., and Hussey, P.J. (1997). The maize actin-depolymerizing factor, ZmADF3, redistributes to the growing tip of elongating root hairs and can be induced to translocate into the nucleus with actin. Plant J **12,** 1035-1043.

Jones, M.A., Shen, J.-J., Fu, Y., Li, H., Yang, Z., and Grierson, C.S. (2002). The Arabidopsis Rop2 GTPase Is a Positive Regulator of Both Root Hair Initiation and Tip Growth. The Plant Cell **14,** 763-776.

Kaksonen, M., Peng, H.B., and Rauvala, H. (2000). Association of cortactin with dynamic actin in lamellipodia and on endosomal vesicles. J Cell Sci **113,** 4421-4426.

Kaksonen, M., Sun, Y., and Drubin, D.G. (2003). A pathway for association of receptors, adaptors, and actin during endocytic internalization. Cell **115,** 475-487.

Ketelaar, T., Anthony, R.G., and Hussey, P.J. (2004). Green fluorescent protein-mTalin causes defects in actin organization and cell expansion in Arabidopsis and inhibits actin depolymerizing factor's actin depolymerizing activity in vitro. Plant Physiol **136,** 3990-3998.

Ketelaar, T., Allwood, E.G., Anthony, R., Voigt, B., Menzel, D., and Hussey, P.J. (2004). The actin-interacting protein AIP1 is essential for actin organization and plant development. Curr Biol **14,** 145-149.

Kim, D.H., Eu, Y.J., Yoo, C.M., Kim, Y.W., Pih, K.T., Jin, J.B., Kim, S.J., Stenmark, H., and Hwang, I.I. (2001). Trafficking of Phosphatidylinositol 3-Phosphate from the trans-Golgi Network to the Lumen of the Central Vacuole in Plant Cells. Plant Cell **13,** 287-301.

Knebel, W., Quader, H., and Schnepf, E. (1990). Mobile and immobile endoplasmic reticulum in onion bulb epidermis cells: short- and long-term observations with a confocal laser scanning microscope. Eur J Cell Biol **52,** 328-340.

Koh, T.W., and Bellen, H.J. (2003). Synaptotagmin I, a Ca2+ sensor for neurotransmitter release. Trends Neurosci **26,** 413-422.

Kost, B., Spielhofer, P., and Chua, N.-H. (1998). A GFP-mouse talin fusion protein labels plant actin filaments in vivo and visualizes the actin cytoskeleton in growing pollen tubes. The Plant Journal **16,** 393-401.

Kost, B., Spielhofer, P., Mathur, J., Dong, C.-H., and Chua, N.-H. (2000). Non-invasive F-actin visualization in living plant cells using a GFP-mouse talin fusion protein. In Actin: a dynamic framework for multiple plant cell functions, C.J. Staiger, F. Baluska, D. Volkmann, and P. Barlow, eds (Dordrecht: Kluwer), pp. 637-659.

Kovar, D.R., Staiger, C.J., Weaver, E.A., and McCurdy, D.W. (2000). AtFim1 is an actin filament-crosslinking protein from Arabidopsis thaliana. The Plant Journal **24,** 1-14.

Lauber, M.H., Waizenegger, I., Steinmann, T., Schwarz, H., Mayer, U., Hwang, I., Lukowitz, W., and Jurgens, G. (1997). The Arabidopsis KNOLLE protein is a cytokinesis-specific syntaxin. J Cell Biol **139,** 1485-1493.

Lawe, D.C., Patki, V., Heller-Harrison, R., Lambright, D., and Corvera, S. (2000). The FYVE domain of early endosome antigen 1 is required for both phosphatidylinositol 3-phosphate and Rab5 binding. Critical role of this dual interaction for endosomal localization. J Biol Chem **275,** 3699-3705.

Li, S., Blanchoin, L., Yang, Z., and Lord, E.M. (2003). The putative Arabidopsis arp2/3 complex controls leaf cell morphogenesis. Plant Physiol **132,** 2034-2044.

Lipka, V., Kwon, C., and Panstruga, R. (2007). SNARE-ware: the role of SNARE-domain proteins in plant biology. Annu Rev Cell Dev Biol **23,** 147-174.

Martens, S., Kozlov, M.M., and McMahon, H.T. (2007). How synaptotagmin promotes membrane fusion. Science **316,** 1205-1208.

Mathur, J., Mathur, N., and Hulskamp, M. (2002). Simultaneous visualization of peroxisomes and cytoskeletal elements reveals actin and not microtubule-based peroxisome motility in plants. Plant Physiology **128,** 1031-1045.

Mathur, J., Spielhofer, P., Kost, B., and Chua, N. (1999). The actin cytoskeleton is required to elaborate and maintain spatial patterning during trichome cell morphogenesis in Arabidopsis thaliana. Development **126,** 5559-5568.

Mathur, J., Mathur, N., Kernebeck, B., and Hulskamp, M. (2003). Mutations in Actin-Related Proteins 2 and 3 Affect Cell Shape Development in Arabidopsis. THE PLANT CELL **15,** 1632-1645.

Mathur, J., Mathur, N., Kirik, V., Kernebeck, B., Srinivas, B.P., and Hulskamp, M. (2003). Arabidopsis CROOKED encodes for the smallest subunit of the ARP2/3 complex and controls cell shape by region specific fine F-actin formation. Development **130,** 3137-3146.

May, R.C., Hall, M.E., Higgs, H.N., Pollard, T.D., Chakraborty, T., Wehland, J., Machesky, L.M., and Sechi, A.S. (1999). The Arp2/3 complex is essential for the actin-based motility of Listeria monocytogenes. Current Biology **9,** 759-762.

McCurdy, D.W., and Kim, M. (1998). Molecular cloning of a novel fimbrin-like cDNA from Arabidopsis thaliana. Plant Molecular Biology **36,** 23-31.

McKinney, E.C., Kandasamy, M.K., and Meagher, R.B. (2002). Arabidopsis contains ancient classes of differentially expressed actin-related protein genes. Plant Physiology **128,** 997-1007.

Meckel, T., Hurst, A.C., Thiel, G., and Homann, U. (2005). Guard cells undergo constitutive and pressure-driven membrane turnover. Protoplasma **226,** 23-29.

Meldolesi, J., and Chieregatti, E. (2004). Fusion has found its calcium sensor. Nat Cell Biol **6,** 476-478.

Miller, D.D., Ruijter, D., A., N.C., Bisseling, T., and Emons, A.C. (1999). The role of actin in root hair morphogenesis: studies with lipochito-oligosaccharide as a growth stimulator and cytochalasin as an actin perturbing drug. The Plant Journal **17,** 141-154.

Misu, K., Fujimura-Kamada, K., Ueda, T., Nakano, A., Katoh, H., and Tanaka, K. (2003). Cdc50p, a conserved endosomal membrane protein, controls polarized growth in Saccharomyces cerevisiae. Mol Biol Cell **14,** 730-747.

Muday, G.K. (2000). Maintenance of asymmetric cellular localization of an auxin transport protein through interaction with the actin cytoskeleton. J Plant Growth Regul **19,** 385-396.

Muday, G.K., Hu, S., and Brady, S.R. (2000). The actin cytoskeleton may control the polar distribution of an auxin transport protein. Gravit Space Biol Bull **13,** 75-83.

Nielsen, E., Severin, F., Backer, J.M., Hyman, A.A., and Zerial, M. (1999). Rab5 regulates motility of early endosomes on microtubules. Nat Cell Biol **1,** 376-382.

Nishimura, T., Yokota, E., Wada, T., Shimmen, T., and Okada, K. (2003). An Arabidopsis ACT2 dominant-negative mutation, which disturbs F-actin polymerization, reveals its distinctive function in root development. Plant Cell Physiol **44,** 1131-1140.

Oparka, K.J., Prior, D.A., Santa Cruz, S., Padgett, H.S., and Beachy, R.N. (1997). Gating of epidermal plasmodesmata is restricted to the leading edge of expanding infection sites of tobacco mosaic virus (TMV). Plant J **12,** 781-789.

Ovecka, M., Lang, I., Baluska, F., Ismail, A., Illes, P., and Lichtscheidl, I.K. (2005). Endocytosis and vesicle trafficking during tip growth of root hairs. Protoplasma **226,** 39-54.

Pelham, R.J., Jr., and Chang, F. (2001). Role of actin polymerization and actin cables in actin-patch movement in Schizosaccharomyces pombe. Nat Cell Biol **3,** 235-244.

Poskanzer, K.E., Marek, K.W., Sweeney, S.T., and Davis, G.W. (2003). Synaptotagmin I is necessary for compensatory synaptic vesicle endocytosis in vivo. Nature **426,** 559-563.

Pratelli, R., Sutter, J.U., and Blatt, M.R. (2004). A new catch in the SNARE. Trends Plant Sci **9,** 187-195.

Pruyne, D., and Bretscher, A. (2000). Polarization of cell growth in yeast. J Cell Sci **113,** 571-585.

Ramachandran, R., Christensen, H.E.M., Ishimaru, Y., Dong, C.-H., Chao-Ming, W., Cleary, A.L., and Chua, N.-H. (2000). Profilin Plays a Role in Cell Elongation, Cell Shape Maintenance, and Flowering in Arabidopsis. Plant Physiology **124,** 1637-1647.

Reichel, C., Mathur, J., Eckes, P., Langenkemper, K., Koncz, C., Schell, J., Reiss, B., and Maas, C. (1996). Enhanced green fluorescence by the expression of an *Aequorea victoria* green fluorescent protein mutant in mono- and dicotyledonous plant cells. Proceedings of the National Acadamy of Sciences of the USA **93,** 5888-5893.

Ringli, C., Baumberger, N., Diet, A., Frey, B., and Keller, B. (2002). ACTIN2 Is Essential for Bulge Site Selection and Tip Growth during Root Hair Development of Arabidopsis. Plant Physiol **129,** 1464-1472.

Rochlin, M.W., Dailey, M.E., and Bridgman, P.C. (1999). Polymerizing microtubules activate site-directed F-actin assembly in nerve growth cones. Mol Biol Cell **10,** 2309-2327.

Samaj, J., Baluska, F., and Hirt, H. (2004). From signal to cell polarity: mitogen-activated protein kinases as sensors and effectors of cytoskeleton dynamicity. J Exp Bot **55,** 189-198.

Samaj, J., Baluska, F., and Menzel, D. (2004). New signalling molecules regulating root hair tip growth. Trends Plant Sci **9,** 217-220.

Samaj, J., Peters, M., Volkmann, D., and Baluska, F. (2000). Effects of myosin ATPase inhibitor 2,3-butanedione 2-monoxime on distributions of myosins, F-actin, microtubules, and cortical endoplasmic reticulum in maize root apices. Plant Cell Physiol **41,** 571-582.

Samaj, J., Read, N.D., Volkmann, D., Menzel, D., and Baluska, F. (2005). The endocytic network in plants. Trends Cell Biol **15,** 425-433.

Samaj, J., Baluska, F., Voigt, B., Schlicht, M., Volkmann, D., and Menzel, D. (2004). Endocytosis, actin cytoskeleton, and signaling. Plant Physiol **135,** 1150-1161.

Samaj, J., Ovecka, M., Hlavacka, A., Lecourieux, F., Meskiene, I., Lichtscheidl, I., Lenart, P., Salaj, J., Volkmann, D., Bogre, L., Baluska, F., and Hirt, H. (2002). Involvement of the mitogen-activated protein kinase SIMK in regulation of root hair tip growth. Embo Journal **21,** 3296-3306.

Sambrook, J., Fritsch, E.F., and Maniatis, T. (1989). Molecular cloning: a laboratory manual. (New York: Cold Spring Harbour Laboratory).

Sawitzky, H., Liebe, S., Willingale-Theune, J., and Menzel, D. (1999). The anti-proliferative agent jasplakinolide rearranges the actin cytoskeleton of plant cells. European Journal of Cell Biology **78,** 424-433.

Scott, G., Leopardi, S., Printup, S., and Madden, B.C. (2002). Filopodia are conduits for melanosome transfer to keratinocytes. J Cell Sci **115,** 1441-1451.

Sheahan, M.B., Rose, R.J., and McCurdy, D.W. (2004). Organelle inheritance in plant cell division: the actin cytoskeleton is required for unbiased inheritance of chloroplasts, mitochondria and endoplasmic reticulum in dividing protoplasts. Plant J **37,** 379-390.

Sieburth, L.E., and Meyerowitz, E.M. (1997). Molecular dissection of the AGAMOUS control region shows that cis elements for spatial regulation are located intragenically. Plant Cell **9,** 355-365.

Smith, M.G., Swamy, S.R., and Pon, L.A. (2001). The life cycle of actin patches in mating yeast. J Cell Sci **114,** 1505-1513.

Sohn, E.J., Kim, E.S., Zhao, M., Kim, S.J., Kim, H., Kim, Y.W., Lee, Y.J., Hillmer, S., Sohn, U., Jiang, L., and Hwang, I. (2003). Rha1, an Arabidopsis Rab5 homolog,

plays a critical role in the vacuolar trafficking of soluble cargo proteins. Plant Cell **15,** 1057-1070.

Sorkin, A., and Von Zastrow, M. (2002). Signal transduction and endocytosis: close encounters of many kinds. Nat Rev Mol Cell Biol **3,** 600-614.

Sudhof, T.C. (2002). Synaptotagmins: why so many? J Biol Chem **277,** 7629-7632.

Sun, H., Basu, S., Brady, S.R., Luciano, R.L., and Muday, G.K. (2004). Interactions between auxin transport and the actin cytoskeleton in developmental polarity of Fucus distichus embryos in response to light and gravity. Plant Physiol **135,** 266-278.

Sutter, J.U., Sieben, C., Hartel, A., Eisenach, C., Thiel, G., and Blatt, M.R. (2007). Abscisic acid triggers the endocytosis of the arabidopsis KAT1 K+ channel and its recycling to the plasma membrane. Curr Biol **17,** 1396-1402.

Swarbreck, D., Wilks, C., Lamesch, P., Berardini, T.Z., Garcia-Hernandez, M., Foerster, H., Li, D., Meyer, T., Muller, R., Ploetz, L., Radenbaugh, A., Singh, S., Swing, V., Tissier, C., Zhang, P., and Huala, E. (2007). The Arabidopsis Information Resource (TAIR): gene structure and function annotation. Nucleic Acids Res. E-pub.

Tang, J., Maximov, A., Shin, O.H., Dai, H., Rizo, J., and Sudhof, T.C. (2006). A complexin/synaptotagmin 1 switch controls fast synaptic vesicle exocytosis. Cell **126,** 1175-1187.

Taunton, J. (2001). Actin filament nucleation by endosomes, lysosomes and secretory vesicles. Curr Opin Cell Biol **13,** 85-91.

Timmers, A.C., Niebel, A., Balague, C., and Dagkesamanskaya, A. (2002). Differential localisation of GFP fusions to cytoskeleton-binding proteins in animal, plant, and yeast cells. Protoplasma **220,** 69-78.

Topping, J.F., Wei, W., and Lindsey, K. (1991). Functional tagging of regulatory elements in the plant genome. Development **112,** 1009-1019.

Tyrrell, M., Campanoni, P., Sutter, J.U., Pratelli, R., Paneque, M., Sokolovski, S., and Blatt, M.R. (2007). Selective targeting of plasma membrane and tonoplast traffic by inhibitory (dominant-negative) SNARE fragments. Plant J **51,** 1099-1115.

Ueda, T., Yamaguchi, M., Uchimiya, H., and Nakano, A. (2001). Ara6, a plant-unique novel type Rab GTPase, functions in the endocytic pathway of Arabidopsis thaliana. Embo J **20,** 4730-4741.

Uemura, T., Ueda, T., Ohniwa, R.L., Nakano, A., Takeyasu, K., and Sato, M.H. (2004). Systematic analysis of SNARE molecules in Arabidopsis: dissection of the post-Golgi network in plant cells. Cell Struct Funct **29,** 49-65.

Van Gestel, K., Slegers, H., Von Witsch, M., Samaj, J., Baluska, F., and Verbelen, J.P. (2003). Immunological evidence for the presence of plant homologues of the actin-related protein Arp3 in tobacco and maize: subcellular localization to actin-enriched pit fields and emerging root hairs. Protoplasma **222,** 45-52.

Vantard, M., and Blanchoin, L. (2002). Actin polymerization processes in plant cells. Curr Opin Plant Biol **5,** 502.

Vidali, L., McKenna, S.T., and Hepler, P.K. (2001). Actin polymerization is essential for pollen tube growth. Mol Biol Cell **12,** 2534-2545.

Volkmann, D., and Baluska, F. (1999). Actin Cytoskeleton in Plants: From Transport Networks to Signaling Networks. Microscopy Research and Technique **47,** 135-154.

Walther, A., and Wendland, J. (2004). Apical localization of actin patches and vacuolar dynamics in Ashbya gossypii depend on the WASP homolog Wal1p. J Cell Sci **14**.

Wang, Y.S., Motes, C.M., Mohamalawari, D.R., and Blancaflor, E.B. (2004). Green fluorescent protein fusions to Arabidopsis fimbrin 1 for spatio-temporal imaging of F-actin dynamics in roots. Cell Motil Cytoskeleton **59,** 79-93.

Wedlich-Soldner, R., Bolker, M., Kahmann, R., and Steinberg, G. (2000). A putative endosomal t-SNARE links exo- and endocytosis in the phytopathogenic fungus Ustilago maydis. Embo J **19,** 1974-1986.

Wedlich-Soldner, R., Straube, A., Friedrich, M.W., and Steinberg, G. (2002). A balance of KIF1A-like kinesin and dynein organizes early endosomes in the fungus Ustilago maydis. Embo J **21,** 2946-2957.

Weiner, O.D., Servant, G., Welch, M.D., Mitchison, T.J., Sedat, J.W., and Bourne, H.R. (1999). Spatial control of actin polymerization during neutrophil chemotaxis. Nat Cell Biol **1,** 75-81.

Willemsen, V., Friml, J., Grebe, M., Van Den Toorn, A., Palme, K., and Scheres, B. (2003). Cell Polarity and PIN Protein Positioning in Arabidopsis Require STEROL METHYLTRANSFERASE1 Function. Plant Cell **15,** 612-625.

Xiang, C., Han, P., Lutziger, I., Wang, K., and Oliver, D.J. (1999). A mini binary vector series for plant transformation. Plant Molecular Biology **40,** 711-717.

Zerial, M., and McBride, H. (2001). Rab proteins as membrane organizers. Nat Rev Mol Cell Biol **2,** 107-117.

Zimmermann, P., Hirsch-Hoffmann, M., Hennig, L., and Gruissem, W. (2004). GENEVESTIGATOR. Arabidopsis microarray database and analysis toolbox. Plant Physiol **136,** 2621-2632.

Publikationen

Ketelaar, T., Allwood, E.G., Anthony, R., **Voigt, B.**, Menzel, D., Hussey, P.J. (2004). The actin interacting protein AIP1 is essential for actin organization and plant development. Curr Biol. 14(2):145-149.

Samaj, J., Baluska, F., **Voigt, B.**, Schlicht, M., Volkmann, D., Menzel, D. (2004). Endocytosis, actin cytoskeleton, and signaling. Plant Physiol. 135(3):1150-1161.

Voigt, B., Timmers, A.C.J., Samaj, J., Müller, J., Baluska, F., Menzel, D. (2005). GFP-FABD2 Fusion Construct Allows *In Vivo* Visualization of the Dynamic Actin Cytoskeleton in all cells of *Arabidopsis* seedlings. EJCB 84(6): 595-608.

Voigt, B., Timmers, A.C.J., Samaj, J., Hlavacka, A., Ueda, T., Preuss, M., Nielsen, E., Mathur, J., Emans, N., Stenmark, H., Nakano, A., Baluska, F., Menzel, D. (2005). Actin-based motility of endosomes is linked to the polar tip growth of root hairs. EJCB 84(6): 609-621.

Wilsen, K.L., Lovy-Wheeler, A., **Voigt, B.**, Menzel, D., Kunkel, J.G., Hepler, P.K. (2006). Imaging the Actin Cytoskeleton in Growing Pollen Tubes. Sex Plant Reprod 19(2): 51-62.

Dubrovsky, J.G., Guttenberger, M., Saralegui, A., Napsucialy-Mendivil, S., **Voigt, B.**, Baluska, F., Menzel, D. (2006). Neutral Red as a Probe for Confocal Laser Scanning Microscopy Studies of Plant Roots. Ann Bot 97(6): 1127-1138.

Muller, T., Benjdia, M., Avolio, M., **Voigt, B.**, Menzel, D., Pardo, A., Frommer, W.B., Wipf, D. (2006). Functional expression of the green fluorescent protein in the ectomycorrhizal model fungus Hebeloma cylindrosporum. Mycorrhiza 16: 437-442.

Feechan, A., **Voigt, B.**, Nielsen, M.E., Baluska, F., Thordal-Christensen, H. (2007). Endosomes accomplish endosomal secretion essential for SYP121-dependent penetration resistance against powdery mildew fungal ingress. In preparation.

Schapire, A.L. and **Voigt, B.**, Jasik, J., Rosado, A., Lopez-Cobollo, R., Salinas, J., Menzel, D., Mancuso, S., Valpuesta, V., Baluska, F., Botella, M.A. (2007). Arabidopsis Synaptotagmin-Like Protein 1 is Essential for Plasma Membrane Viability and Survival under Abiotic Stress. Submitted to Plant Cell.

Tagungsbeiträge

Voigt, B.: Fimbrin-GFP construct for visualization of the actin cytoskeleton in plants. 11. Cytoskeletal Club, Vranovska Ves 2003 (Vortrag)

Voigt, B., Timmers, A.C.J., Menzel, D.: Comparison of tissue-specific labelling with four different GFP-markers for the actin-cytoskeleton in plant root cells. CellBiD, Bonn 2003, EJCB 82, Suppl. 53 (2003, March)

Voigt, B., Baluska, F., Menzel, D.: In vivo imaging of the actin cytoskeleton in cells of the transition zone of *Arabidopsis* roots. SEB Meeting, Edinburgh 2004 (Vortrag)

Voigt, B., Samaj, J., Baluska, F., Menzel, D.: *In Vivo* visualization of the actin cytoskeleton in diverse cell types of *Arabidopsis thaliana*. FEBS Special Meeting on Cytoskeletal Dynamics, 2004, Helsinki, Finland

Voigt, B., Timmers, A.C.J., Samaj, J., Mathur, J., Nielsen, E., Stenmark, H., Ueda, T., Baluska, F., Menzel, D.: Actin-propelled endosomes accumulate at sites of actin-driven polar growth of root hairs. DGZ, 2004, Berlin, Germany

Voigt, B., Hlavacka, A., Craxton, M., Davletov, B., Menzel, D., Baluska, F.: Plant Synaptotagmins: effectors of calcium-regulated endocytosis and exocytosis in plants? DGZ, Heidelberg 2005, EJCB 84, Suppl. 55 (2005, March)

Voigt, B., Craxton, M., Davletov, B., Hussey, P.J., Menzel, D., Baluska, F.: Expression and localization of *Arabidopsis* synaptotagmins. First Symposium on Plant Neurobiology, May 17-20, 2005 Florence, Italy

Voigt, B., Craxton, M., Hussey, P.J., Menzel, D., Baluska, F.: Expression and localization of *Arabidopsis* synaptotagmins. 17. International Botanical Congress, July 17-23, 2005 Vienna, Austria

Voigt, B., Thordal-Christensen, H., Mancuso, S., Menzel, D., Baluska, F.: The *Arabidosis thaliana* SNARE protein PEN1 localizes to endosomes and at sites of polarized endosomal secretion in root cells. Second Symposium on Plant Nerobiology, May 21-26, 2006 Beijing, China (Vortrag)

Voigt, B., Schapire, A.L., Botella, M.A., Mancuso, S., Baluska, F.: Arabidopsis synaptotagmin A is enriched at cortical ER domains and is implicated in salt stress tolerance. Third Symposium on Plant Neurobiology, May 14-18, 2007 Strebske Pleso, Slovakia

Erklärung

Ich versichere hiermit, dass ich die vorliegende Arbeit in allen Teilen selbst und ohne jede unerlaubte Hilfe angefertigt habe. Diese oder eine ähnliche Arbeit ist noch keiner anderen Stelle als Dissertation eingereicht worden. Die Arbeit ist an nachstehend aufgeführten Stellen auszugsweise veröffentlicht worden:

Voigt, B., Timmers, A.C.J., Samaj, J., Müller, J., Baluska, F., Menzel, D. (2005). GFP-FABD2 Fusion Construct Allows *In Vivo* Visualization of the Dynamic Actin Cytoskeleton in all cells of *Arabidopsis* seedlings. EJCB 84(6): 595-608.

Voigt, B.**,** Timmers, A.C.J., Samaj, J., Hlavacka, A., Ueda, T., Preuss, M., Nielsen, E., Mathur, J., Emans, N., Stenmark, H., Nakano, A., Baluska, F., Menzel, D. (2005). Actin-based motility of endosomes is linked to the polar tip growth of root hairs. EJCB 84(6): 609-621.

Ich habe früher noch keinen Promotionsversuch unternommen.

Bonn, den